AD-A046 565 AIR FORCE INST OF TECH WRIGHT-PATTERSON AFB OHIO F/G 13/6
A COMPARATIVE STUDY OF THE RIDE QUALITY OF TRACV SUSPENSION ALT--ETC(U)
SEP 77 R A LUHRS

UNCLASSIFIED AFIT-CI-78-2 NL

1 OF 2
AD A046565

UNCLASSIFIED
SECURITY CLASSIFICATION OF THIS PAGE (When Data Entered)

(1)

REPORT DOCUMENTATION PAGE

READ INSTRUCTIONS BEFORE COMPLETING FORM

1. REPORT NUMBER: CI 78-2
2. GOVT ACCESSION NO.
3. RECIPIENT'S CATALOG NUMBER (9)
4. TITLE (and Subtitle) (6): A Comparative Study of the Ride Quality of TRACV Suspension Alternatives.
5. TYPE OF REPORT & PERIOD COVERED: Master's Thesis
6. PERFORMING ORG. REPORT NUMBER
7. AUTHOR(s) (10): 2d Lt Richard A. Luhrs USAF
8. CONTRACT OR GRANT NUMBER(s)
9. PERFORMING ORGANIZATION NAME AND ADDRESS: AFIT Student at Princeton University, Princeton NJ
10. PROGRAM ELEMENT, PROJECT, TASK AREA & WORK UNIT NUMBERS
11. CONTROLLING OFFICE NAME AND ADDRESS: AFIT/CI, WPAFB OH 45433
12. REPORT DATE (11): Sep[illegible] 1977
13. NUMBER OF PAGES: 112 Pages
14. MONITORING AGENCY NAME & ADDRESS (if different from Controlling Office) (14): AFIT-CI-78-2 (12) 125p.
15. SECURITY CLASS. (of this report): Unclassified
15a. DECLASSIFICATION/DOWNGRADING SCHEDULE
16. DISTRIBUTION STATEMENT (of this Report): Approved for Public Release; Distribution Unlimited

DDC RECEIVED NOV 21 1977 B

17. DISTRIBUTION STATEMENT (of the abstract entered in Block 20, if different from Report)
18. SUPPLEMENTARY NOTES: JERRAL F. GUESS, Captain, USAF, Director of Information, AFIT

APPROVED FOR PUBLIC RELEASE AFR 190-17.

19. KEY WORDS (Continue on reverse side if necessary and identify by block number)
20. ABSTRACT (Continue on reverse side if necessary and identify by block number)

012 200 1B

DD FORM 1 JAN 73 1473 EDITION OF 1 NOV 65 IS OBSOLETE

UNCLASSIFIED
SECURITY CLASSIFICATION OF THIS PAGE (When Data Entered)

A COMPARATIVE STUDY OF THE RIDE QUALITY OF TRACV SUSPENSION ALTERNATIVES

by

Richard A. Luhrs

Princeton University
School of Engineering and Applied Science
Aerospace and Mechanical Sciences Department

Submitted in partial fulfillment of the requirements for the degree of Master of Science in Engineering from Princeton University, 1977.

Prepared by:

Richard A. Luhrs
Richard A. Luhrs

Approved by:

H. C. Curtiss, Jr.
Professor H. C. Curtiss, Jr.

Larry M. Sweet
Professor L. M. Sweet

September 1977

ABSTRACT

A linear, unconstrained perturbation model for the Tracked Ram Air Cushion Vehicle is developed. This model is the result of theoretical expressions for the TRACV which have been verified by wind tunnel and towed model tests. This model is varied to allow for passively suspended, two-degree-of-freedom winglets and for processor-controlled actuators on the same winglets. Optimization of the springs and dampers in the passive suspension is performed according to a performance index based on acceleration, winglet gap variation, and control power. Linear optimal control is applied to the active suspension to determine the optimal feedback gains using a similar performance index. The basic, passively suspended, and actively suspended vehicles are analyzed to determine root mean squared values for the following: 1) vertical acceleration in the foremost and rearmost seats in the passenger cabin, 2) gap variation at the front and rear winglet areas, and 3) control deflection. The acceleration spectral density of each of the vehicle types is compared to the Urban Tracked Ram Cusion Vehicle standard. The active control system is analyzed to see if a reduced set of sensors may achieve acceptable ride quality based on the above measures.

ACKNOWLEDGEMENTS

The culmination of my year at Princeton and this thesis is the result of the help, encouragement, and dedication of those around me, many of whom played no small part. I owe a debt of gratitude to the Daniel and Florence Guggenheim Foundation and the Department of the Air Force who co-sponsored me with a tuition grant and without which my Princeton enrollment would never have come to pass. I thank my advisor, Professor H. C. Curtiss, Jr. for the many hours he spent with me teaching, advising, and helping. Throughout my time at Princeton I never knew him to put my questions off, and often found him willing to discuss matters far removed from academia. With him as a source of advice was Professor Larry M. Sweet, whose hours spent with me prevented much wasted time and many false starts. The fact that these two guided me through the course of my research without ever giving opposing suggestions even when there was no opportunity for coordination bespeaks their complimentary abilities and professionalism. I thank both for help in research and writing.

I also acknowledge the U. S. Department of Transportation who provided the inspiration for the research on the TRACV as well as the funds, and my opportunity to take part therein.

Thanks also go to Bette Snedeker, whose conscientiousness as a technical typist far outstripped mine as a technical writer. Her patience and effort have not gone unnoticed, as she well knows. In addition, Betty Brost provided a smaller hand with the typing, but played a large role as a sympathetic ear which was often needed.

This work I dedicate to my father who was always the first to say, "That's not good enough!" and always the first to say "Well done!"

This thesis carries the number 1348-T in the records of the Department of Aerospace and Mechanical Sciences.

TABLE OF CONTENTS

ABSTRACT

A linear, unconstrained perturbation model for the Tracked Ram Air Cushion Vehicle is developed. This model is the result of theoretical expressions for the TRACV which have been verified by wind tunnel and towed model tests. This model is varied to allow for passively suspended, two-degree-of-freedom winglets and for processor-controlled actuators on the same winglets. Optimization of the springs and dampers in the passive suspension is performed according to a performance index based on acceleration, winglet gap variation, and control power. Linear optimal control is applied to the active suspension to determine the optimal feedback gains using a similar performance index. The basic, passively suspended, and actively suspended vehicles are analyzed to determine root mean squared values for the following: 1) vertical acceleration in the foremost and rearmost seats in the passenger cabin, 2) gap variation at the front and rear winglet areas, and 3) control deflection. The acceleration spectral density of each of the vehicle types is compared to the Urban Tracked Ram Cusion Vehicle standard. The active control system is analyzed to see if a reduced set of sensors may achieve acceptable ride quality based on the above measures.

LIST OF FIGURES

LIST OF TABLES

NOMENCLATURE

A	system state matrix; time non-dimensionalization constant, $A = 1.456$ sec.; guideway roughness parameters, $A = 1.27\pi \times 10^{-6}$ ft.; (when subscripted) area
B	system control matrix; linear damper constant
C	system disturbance matrix
c	vehicle chord length, $c = 150$ ft.
C_L	lift coefficient, $C_L = \frac{L}{\frac{\rho u^2}{2} Wc}$
C_M	moment coefficient, $C_M = \frac{M}{\frac{\rho u^2}{2} Wc^2}$
g	gravitational acceleration, $g = 32.2$ ft/sec.^{2}
h	height above a reference in feet, positive up
$\bar{h}$	non-dimensional height, $\bar{h} = \frac{h}{c}$
HM	hinge moment on winglet around axis parallel to longitudinal axis, positive tips up
$\tilde{HM}$	hinge moment on winglet around axis perpendicular to longitudinal axis, positive leading edge up
K	linear spring constant; feedback gain matrix
k_y	radius of gyration about axis perpendicular to longitudinal axis
L	lift; vehicle length, $L = 150$ ft.
M	moment about c.g., positive nose up; performance index transformation matrix
m	vehicle mass
P	underside surface pressure
R	solution of steady-state matrix Ricatti equation

r_o	area ratio of winglet gap to intake area less exit area
r_1	area ratio change due to winglet pitch
S	vehicle surface area, S = Wc
s	Laplace operator
t	time
U	vehicle forward velocity, U = 300 fps
u	control vector
W	vehicle width including winglets, W = 15 ft.
w	noise vector
x	state variable vector; distance along vehicle from front in feet
$\bar{x}$	distance along vehicle from front as a decimal portion of chord, $\bar{x} = \frac{x}{c}$
Z	diagonal matrix of weighting factors
α	bottom slope of vehicle, $\alpha = \theta + \alpha_o$
α_o	level vehicle bottom slope, α_o = 0.028 rad.
$\bar{\alpha}$	area ratio of intake less exit area to exit area
δ_{w_1}	winglet deflection around axis parallel to longitudinal axis in radians
δ_{w_2}	winglet deflection around axis perpendicular to longitudinal axis
η	Gaussian white noise function

θ	pitch angle in radians from horizontal, positive nose up
λ	guideway disturbance wavelength in feet
ξ	dummy state variable
ρ	density of air, $\rho = 0.00238$ slugs/ft^3
τ	non-dimensional time, $\tau = \frac{t}{A}$

Subscripts

c.p.	center of pressure
E	of the exit or tailing edge region
g	of the guideway
L.E.	leading edge
n	variable index
r	of the vehicle with respect to the guideway
T.E.	trailing edge
v	of the vehicle with respect to the inertial frame
w	of the winglet
o	initial value; steady-state value

Superscripts

$\bar{}$	trial index
$\cdot$	derivative with respect to real time
$'$	derivative with respect to non-dimensional time

CHAPTER I

INTRODUCTION

Reliable and inexpensive high-speed intercity transportation is receiving increasing attention as the cost of operating automobiles continues to soar. Present modes, however, face time and convenience problems which the car does not. Aircraft are capable of cruising at great speed, but the time lost on the ground getting into and out of airports can be thrice the enroute time on short and medium distance runs. In addition, due to space requirements, airports usually cannot be located in or near the center of cities. Trains do not face the same requirements; their stations are often in the heart of the business district of town. But while trains have terminal convenience, they often have as little as one-tenth the cruise speed of aircraft.

The most convenient form of mass transit would combine the better half of each of these, giving both high speed and terminal convenience to the vehicle. High speed ground transportation can provide this combination once the dangers to public safety and construction problems are removed. Several schemes have been advanced and the most likely fall into three major categories: high-speed rail, magnetic levitation (mag-lev), and air cushion vehicles. Each of the classes has varying subtypes with advantages and drawbacks.

The high-speed rail concept utilizes an improved rail with welded joints and modified existing equipment and technology. On the other hand

high-speed increases the consequence of the ever-present derailment threat, and road maintenance is particularly costly if freight must also move on the high quality rails. Magnetically levitated vehicles of either the attractive or repulsive type are less susceptible to derailment and use non-contact suspension, but some are statically unstable and all face the cost and weight of cryogenic coil cooling. In addition unavoidable electrical discontinuity in guideway joints causes field interruptions.

Air cushion vehicles do not pose such problems. They are statically stable and may use ordinary, locally rough, non-conducting guideway materials such as concrete. Derailment is not a problem a tracked air cusion vehicle is likely to face. Low loading on the guideway decreases maintenance costs. Static cushion vehicles, however, suffer from high captation drag, induced by turning incoming air downward. Even this problem, though, is absent in a Tracked Ram Air Cushion Vehicle (TRACV). Such a vehicle uses dynamic air pressure to generate lift, and virtually flies in ground effect down its guideway. Its non-contact suspension is not as noise-transmitting as a train, and the presence of the ground gives it far better lift/drag characteristics than aircraft.

This study investigates t[illegible]e quality of a particular TRACV configuration. As a passenger vehi[illegible]ossibility, the TRACV's ride quality as measured by accelerations and suspension travel is important. A linear pitch-heave model of the vehicle has been developed and the longitudinal dynamics are analyzed to determine the vertical accelerations felt by the passengers and likelihood of vehicle-guideway contact. Three configurations

are considered: 1) an all-rigid vehicle, 2) a vehicle with moveable control surfaces suspended by springs and dampers, and 3) a vehicle with moveable control surfaces controlled by actuators subject to active feedback. The basic tradeoff for all three types is between minimizing vertical accelerations and maintaining adequate clearance between the vehicle and the guideway without unwieldy control power requirements.

PREVIOUS WORK

Since the TRACV is a fairly recent concept, literature discussing its dynamics is not abundant. Dynamics analyses have been performed, but a pitch-heave analysis which accounts for the considerable coupling has not been done. Some of the work on static air cushion suspensions is indirectly applicable, but the dynamics are considerably different and results do not necessarily correspond.

T. M. Barrows and S. E. Widnall (1970) presented a paper which laid out the aerodynamics for the "ram wing". This paper discusses ride quality of the heave-only constrained vehicle after developing expressions for heave and pitch forces due to ground disturbances.

W. E. Fraize and T. M. Barrows (1973) performed a system definition study which hypothesized a 154-foot vehicle with a one hundred passenger capacity. This extensive study defined all aspects of a full-scale system and studied feasibility and basic dynamics. Appendix C of this reference discusses a TRACV suspended on one-degree-of-freedom winglets for heave control and performs a body heave-winglet dynamics analysis which was later found to contain some errors. Earlier that same year, Barrows presented a paper which shows that almost any body natural frequency and damping ratio can be

achieved in a suspended TRACV and discusses some active control concepts in TRACV suspension.

P. V. Aidala (1974) studied the lateral stability of the TRACV and determined stability derivatives. His report also compares longitudinal forces with the numerical predictions of a one-dimensional flow mass conservation theory given by Boccardoro, and shows that lateral and longitudinal forces may be considered independent.

H. C. Curtiss, Jr., and W. F. Putman (1977) present a simplified theory for lift and moment characteristics and show good agreement between this theory and wind tunnel and towed model tests. Their report presents equations for lift and moment stability derivatives and describes pitch and heave static stability, but there is no discussion of coupled pitch-heave dynamics.

THE VEHICLE

The vehicle model used in this study is a full-scale TRACV with a linear sloping bottom surface and haveing the cross-section of the upper half of an NACA 0021 airfoil. It is 150 feet long and 15 feet wide with 2.5-foot winglets. The guideway is 12 feet wide and about 7 feet deep, with winglet running lips placed at a 45 degree angle to horizontal. The size of the vehicle (but not the shape) is similar to that of the Mitre Corp. Study (Fraize and Barrows, 1973). Figure 1 shows the front and side views of the vehicle. The bottom slope is .028 rad (about 1.5°) and the bottom surface clearance at the trailing edge is three feet. These values were

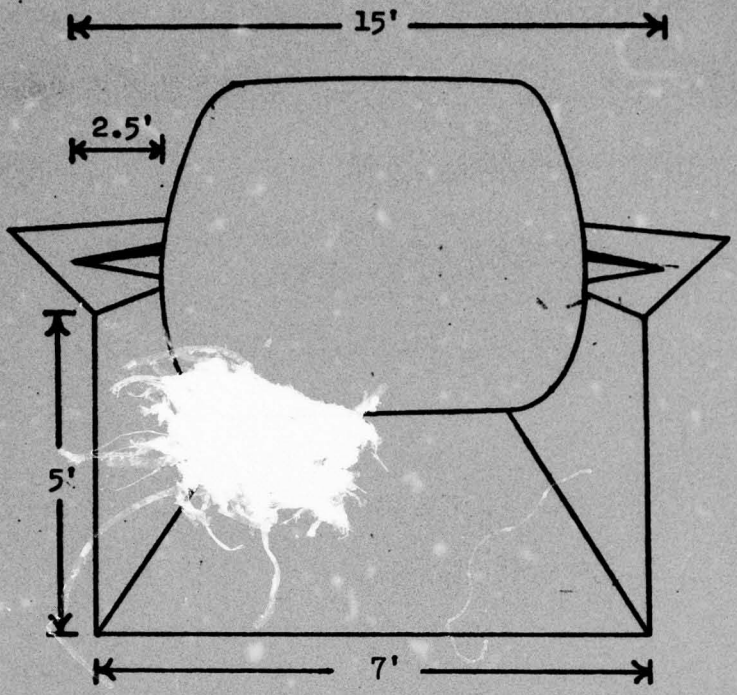

a. Front View

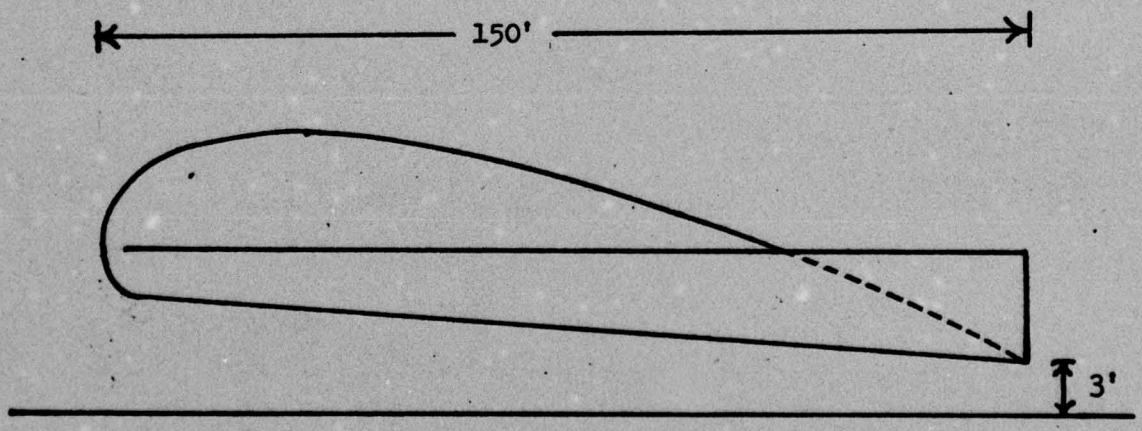

b. Side View

Figure 1. Dimensions of TRACV

derived from $\bar{\alpha} = 1.4$, which experiment showed to give good L/D characteristics and good correlation between theory and experiment. The vehicle is constrained to a constant forward velocity of 300 fps or 205 mph.

The winglets ride in very close proximity to the guideway lips, having a nominal 1.07 inch clearance. With the vehicle length of 150 feet, this close clearance will necessitate very good control of pitch displacements; and gap variations at the forward and trailing corners of the winglets will prove to be the limiting values. The reason for such close clearance is that the winglets essentially act as a pressure seal to keep up the underside pressure. Because of this fact, the lift variation with height change is strongly dependent upon gap variation; the stability derivatives support this conclusion.

OVERVIEW OF ANALYSIS

This thesis first reviews the various terms and ratios used to develop the stability derivatives. The latter part of Chapter II derives the control surface derivatives and presents the basic model. It then describes the guideway roughness modelling process and describes the effect of size of the vehicle on short-wavelength guideway disturbances.

Chapter III discusses the dynamics of the rigid vehicle with its immoveable winglets. The acceleration spectral density is compared to the Urban Tracked Air Cushion Vehicle (UTACV) standard, and rms values of acceleration and winglet gap variation are presented. These are the measures by

which this study determines ride quality and Chapters III, IV, and V follow similar formats.

Chapter IV develops the passively suspended vehicle using massless winglets. Linear torsional springs and dampers are attached to the winglets and the values for these are optimized according to a criterion based on acceleration, gap variation, and winglet deflection. This optimization procedure is a four-variable gradient search performed by a digital computer.

Chapter V presents the model for the active suspension. Linear optimal control is applied to find the optimal feedback gains according to a performance index similar to that used in Chapter IV. Spectral densities are shown, as in all cases, for the foremost and rearmost passengers' seats. The feedback gain matrix is then altered in a simple check to find the effects of reduced sensor capability on ride quality.

CHAPTER II

MODELLING THE VEHICLE

Given that the TRACV is supported by aerodynamic forces, the mathematical model of it can be placed in a form similar in some respects to those of aircraft. Hence, the equations of motion contain coefficients of lift and moment as well as stability derivatives similar to those of aircraft. At this point, however, most of the similarities end. The parameters of interest from which these derivatives are calculated are considerably different from other vehicles. These parameters arise from the fact that the TRACV operates in ground effect and they are ones which can be measured in tests and expressed explicitly in equations of motion and derivatives. They are also useful in that they appear in non-dimensional form and may readily be applied to either scale models or full-sized vehicles. In addition, the axes are not body fixed, but are fixed in an inertial reference and translate with the vehicle, giving such that the axes are not free to rotate. In this coordinate system, the word "position" refers to the state of the vehicle in pitch and height at a given point in time.

This Chapter first discusses the motion variables which will later be used as state variables, then explains the non-dimensional ratio parameters as they appear in the work of Curtiss and Putman (1977). Finally, all these are drawn together into the various parts of the model on which the dynamics analysis is to be done. This model is developed part by part to include attitude stability derivatives, control surface

motions and guideway roughness. It is hoped that this development will give the reader a thorough understanding of all the aspects of this unique vehicle being studied.

ATTITUDE AND RATE

The two most obvious variables to present themselves are the height of the vehicle and its pitch attitude, called $\bar{h}$ and θ respectively. The height variable, $\bar{h}$, is the measure of the vehicle's height in feet above some reference, the value of which is divided by the length of the vehicle (called chord length, or c). Thus, $\bar{h}$ has no dimension. Theta (θ) is the pitch attitude of the vehicle with respect to some reference, measured in radians.

The vertical velocity, $\dot{\bar{h}}$, is the vertical velocity in feet per second non-dimensionalized by the forward speed, U. This variable is not the same as the time derivative of $\bar{h}$, but is related to it by the constant $(\frac{c}{U})$. The pitching velocity, q, is similarly related to the time derivative of θ by the same constant.

Thus, there are four variables which describe the state of the TRACV: $\bar{h}$, θ, $\dot{\bar{h}}$, q. Upward translation and nose up rotation are considered to be positive. It is also important to keep track of the relations

$$\dot{\bar{h}} = \frac{c}{U}\left[\frac{d}{dt}(\bar{h}(\right] \qquad\qquad q = \frac{c}{U}\left[\frac{d}{dt}(\theta)\right]$$

since we will eventually wish to use common variables in expressing the equations of motion. The stability derivatives will be the derivatives

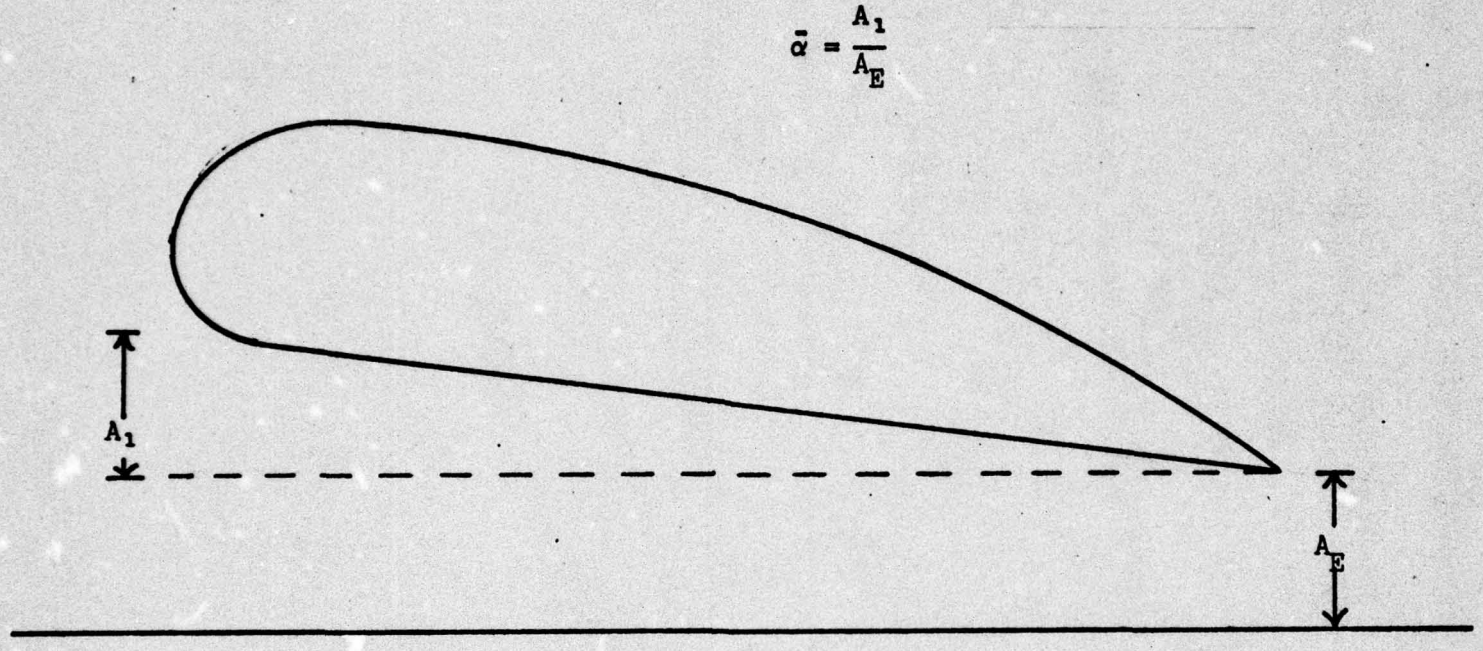

Figure 1. Geometry of $\bar{\alpha}$.

of the lift and moment coefficients with respect to each of these four.

The reference against which each of these motion variables is to be measured, as well as the specific motion being measured, is denoted by special subscripting or prescripting. For instance, the height of the vehicle center of gravity above some inertial reference is $\bar{h}_v$, whereas the relative height of the vehicle c.g. above the point directly below on the guideway surface, or relative height, is $\bar{h}_r$. A full description of various notations may be found in the Nomenclature.

RATIO PARAMETERS

In keeping with the idea of using variables which may be conveniently expressed and solved for, the development of the equations of lift and moment coefficient are functions of three parameters: $\bar{\alpha}$, r_o, r_1. These three are ratios of different areas and arise from the fact that the lift and moment equations are based on the continuity equation for the control volume which is the airspace between the vehicle and the guideway. Air enters the frontal area and escapes beneath the winglets and out the trailing edge area at free stream pressure. A detailed description of the theory is discussed in Curtiss and Putman (1977). Thus, the most convenient way to express lift and moment coefficients are as a function of the ratios of entrance and exit areas.

The first ratio is $\bar{\alpha}$, which is defined as the ratio of the frontal area less the exit area to the exit area. This ratio is depicted in Figure 1 as $\frac{A_1}{A_\ell}$. The defining relationship is

$$\bar{\alpha} = \frac{Wc\alpha}{A_\ell}$$

where A_ε is the trailing edge exit area, W is vehicle width, c is chord length, and α is the slope of the bottom surface with respect to the guideway expressed in radians. Note that for small angles $\sin \alpha \doteq \alpha$, so $h_1 \doteq c\alpha$. In Figure 1, the width is the dimension out of the page. The bottom slopes upward toward the front, giving the vehicle positive angle-of-attack.

The second parameter, r_o, is a ratio of winglet gap area to area A_1 as defined in Figure 1 when the winglets are parallel to the guideway lip. Its defining relation is

$$r_o = \frac{2\,\delta_o c}{W\,\alpha\,c}$$

The term δ_o is the size of the gap between the winglet tip and guideway lip (see Figure 2a) and the factor of two accounts for both winglets. Hence, r_o includes the <u>total</u> winglet gap area, not just that for one side.

Finally, the third parameter is r_1, which expresses the change in winglet gap area as the winglets take on nonzero angles with respect to the guideway lip. It is given by

$$r_1 = \frac{-2\,c\,\theta\,c}{W\,\alpha\,c}$$

and represents the difference in winglet gap area between a non-parallel winglet and a parallel one divided through by area A_1 of Figure 1. Theta is the angle the winglets make with respect to the guideway, or simply the body pitch angle perturbation.

CONTROL SURFACE DISPLACEMENTS

Like other aerodynamic vehicles, the TRACV may require surfaces of some sort which exert controllable forces on the vehicle. Since the motion variables of interest are pitch and heave and their rates of change with time, surfaces which control each of these motion separately are most desirable from a control standpoint. Although several types are possible, the form which appears to be feasible, realizeable, and giving uncoupled $\bar{h}$ and $\bar{\theta}$ control is a two-degree-of-freedom winglet rotation. The first motion is rotation about an axis parallel to the vehicle longitudinal axis and is designated δ_{w_1}; the second is a rotation about an axis perpendicular to the longitudinal axis of the vehicle located at about a forty percent chord position, designated δ_{w_2}. These motions are depicted in Figures 2a and 2b respectively.

STABILITY DERIVATIVES

In order to arrive at a reasonably complete and yet workable model, we must make a few assumptions. The first of these is that we are interested in small perturbations from the steady-state only. Since large motions while cruising necessarily mean poor ride quality, they must be prevented in the first place by a tight feedback control or a suspension. The second, a direct result of the first, is that the lift and moment may be described by a Taylor series truncated after the first order terms, since second order and higher terms are vanishingly small in a small perturbation analysis.

As can be seen in Appendix A, the steady-state and perturbation parts of the problem may be separated. The equations of motion are then expressed

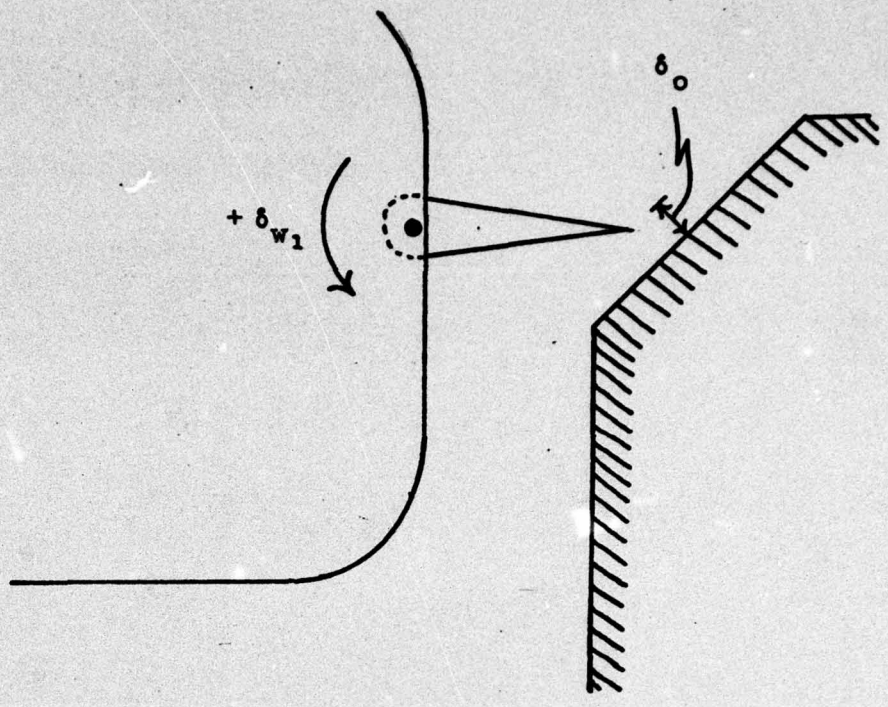

a. Front View Closeup Showing Winglet Gap and δ_{w_1}.

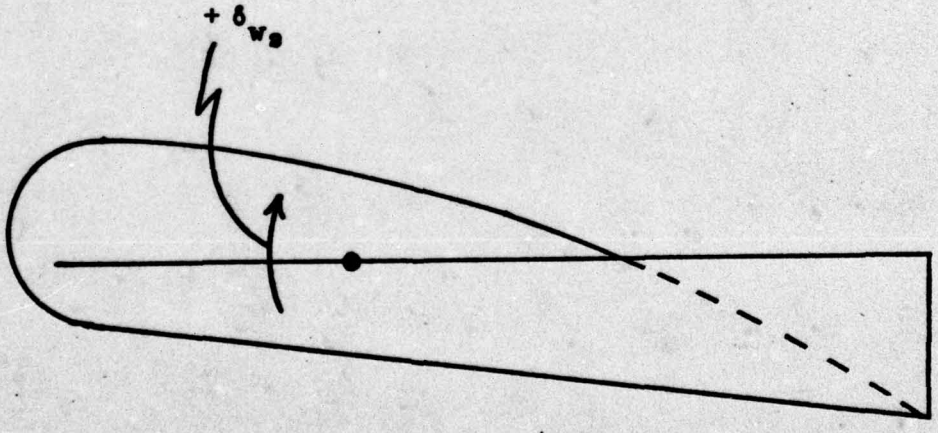

b. Side View Showing δ_{w_2} Convention.

Figure 2. Winglet Gap and Motions.

as the products of derivatives and corresponding attitude perturbations. These derivatives are expressed as a series of partial derivatives with respect to each of the three area ratio parameters. For instance, the change in lift with variation in height is expressed as

$$\frac{\partial C_L}{\partial \bar{h}} = \frac{\partial C_L}{\partial \bar{\alpha}} \cdot \frac{\partial \bar{\alpha}}{\partial \bar{h}} + \frac{\partial C_L}{\partial r_o} \cdot \frac{\partial r_o}{\partial \bar{h}} + \frac{\partial C_L}{\partial r_1} \cdot \frac{\partial r_1}{\partial \bar{h}}$$

and in similar fashion for the remaining three motion quantities, θ, $\dot{\bar{h}}$, and q. Each of these partials may be found using equations found in Appendix B.

In addition to the derivatives with respect to each of the motion variables, we must consider the effects of change in control surface position on lift and moment. There are four such terms: lift and moment derivatives with respect to each of the two winglet motions, δ_{w_1} and δ_{w_2}. As before, these are expressed as a series of partial derivatives with respect to the three ratio parameters; for example:

$$\frac{\partial C_L}{\partial \delta_{w_1}} = \frac{\partial C_L}{\partial \bar{\alpha}} \cdot \frac{\partial \bar{\alpha}}{\partial \delta_{w_1}} + \frac{\partial C_L}{\partial r_o} \cdot \frac{\partial r_o}{\partial \delta_{w_1}} + \frac{\partial C_L}{\partial r_1} \cdot \frac{\partial r_1}{\partial \delta_{w_1}}$$

A full development of these is also found in Appendix B. We now state the third assumption: the effect of winglet motion rate ($\dot{\delta}_{w_1}$ and $\dot{\delta}_{w_2}$) on vehicle dynamics is negligible. This assumption simplifies the model and seems reasonable since the damping effects of winglet rate is probably small with respect to steady-state forces.

The result is a coupled pair of fourth order equations in the variables $\dot{\bar{h}}$, q, $\bar{h}$, and θ with the control variables δ_{w_1} and δ_{w_2}. The accelerations

of the vehicle are strictly dependent upon the relative attitude and velocity of the vehicle with respect to the guideway. The perturbation equations of motion appear in the following form:

$$\frac{m}{\frac{1}{2}\rho U^2 S}\ddot{h}_v = \frac{\partial C_L}{\partial \dot{h}}\Delta\dot{h} + \frac{\partial C_L}{\partial q}\Delta q + \frac{\partial C_L}{\partial \bar{h}}\Delta\bar{h} + \frac{\partial C_L}{\partial \theta}\Delta\theta + \frac{\partial C_L}{\partial \delta_{w_1}}\Delta\delta_{w_1} + \frac{\partial C_L}{\partial \delta_{w_2}}\Delta\delta_{w_2}$$

$$\frac{I_y}{\frac{1}{2}\rho U^2 Sc}\ddot{\theta}_v = \frac{\partial C_M}{\partial \dot{h}}\Delta\dot{h} + \frac{\partial C_M}{\partial q}\Delta q + \frac{\partial C_M}{\partial \bar{h}}\Delta\bar{h} + \frac{\partial C_M}{\partial \theta}\Delta\theta + \frac{\partial C_M}{\partial \delta_{w_1}}\Delta\delta_{w_1} + \frac{\partial C_M}{\partial \delta_{w_2}}\Delta\delta_{w_2}$$

These equations are further refined in Appendix A.

MODELLING THE GUIDEWAY

Considering that this is a ride quality study, the effect of the guideway roughness on vehicle motions is a necessary part of the overall model. Any control design or suspension must account for the spectrum of the disturbances; the values for acceleration and suspension displacement will be largely dependent upon the type of surface over which the vehicle will travel. As the entire model so far is linear, some linear model of guideway roughness is desirable.

A search of the literature shows that a commonly used model for roadway surfaces has a power spectral density given by

$$\Phi_g(s) = -\frac{AU}{s^2}$$

where U is the forward velocity and A is a surface roughness parameter (Hedrick, Billington and Dreesbach, 1974). For a smooth highway, A = 1.27 $\pi \times 10^{-6}$ ft. is a typical value; this seems a likely value for a guideway constructed for the TRACV and not one which, as a design specification, would require strict construction tolerances, driving the construction cost out of practical limits. The above relationship can also be expressed as $\Phi_g = |h_g(s)|^2$. It then follows that if we let $h_g(s) = \frac{\sqrt{AU}}{s}$ (ignoring phase relationships) then, once again involving the small angle assumption ($\sin\theta \doteq \theta$) then we can say

$$\frac{d}{dt}\left(\frac{h_g}{U}\right) = \theta_g \rightarrow \theta_g(s) = \frac{s}{U}\left(\frac{\sqrt{AU}}{s}\right) = \sqrt{\frac{A}{U}}\ \text{rad-sec}^{\frac{1}{2}}$$

Thus, it seems that the guideway appears as white noise filtered by an integrator in height and simply held at a constant value over all frequencies in pitch. Using white noise as an input for the overall model simplifies the analysis and control problem since it has an even spectrum and does not affect closed loop characteristic modes of motion. Standard methods for control such as found in Bryson and Ho (1969) may be directly applied.

FINITE PAD LENGTH EFFECT

The above guideway model is incomplete, however. It has a drawback in that such a definition seems to say that at any instant of time and regardless of frequency, the entire segment of guideway under the vehicle has a uniform height and pitch. For instance, a stairstep in the guideway would not appear to the vehicle as an obstacle to climb, but as a step change (in the guideway model) in the height of the entire guideway. If the vehicle had a point contact suspension this would work, but in a model which is of finite length and attitude and rate dependent, the

result is infinite rms accelerations in the vehicle. This cannot be, but there is a correction for this error known as the finite pad length effect.

If we assume that that which primarily affects the vehicle is the average of each of the guideway variables over the length of the vehicle, then the very short wavelength disturbances seem to be filtered out by the size of the vehicle, as one might reasonably expect. This assumption is not an attempt to model the unsteady aerodynamics of the TRACV which are assumed to be unimportant, and is made by way of analogy to other levitated vehicles. The result given is thoroughly developed in Appendix C (Riblich, Captain, and Richardson; 1967).

The effect of taking the average of guideway variables is to seemingly attenuate the guideway spectrum by the function $\left|\frac{\sin x}{x}\right|$. This attenuation can be closely approximated by the magnitude function of a second order filter, such as the one depicted in Figure 3. A second order filter was chosen because it had sufficient dropoff to insure that there were no infinite acceleration in the total model (as would have been the case with a first order model) although it slightly overestimates the attenuation of the $\left|\frac{\sin x}{x}\right|$ function. This filter has the transfer function (in real time)

$$G_f(s) = \frac{45.3}{(s + 5.5)(s + 8.24)}$$

The linear model of the guideway as it appears to the vehicle, then, is white noise filtered by an integrator and further filtered by a second order finite pad length approximation for height disturbances, and the

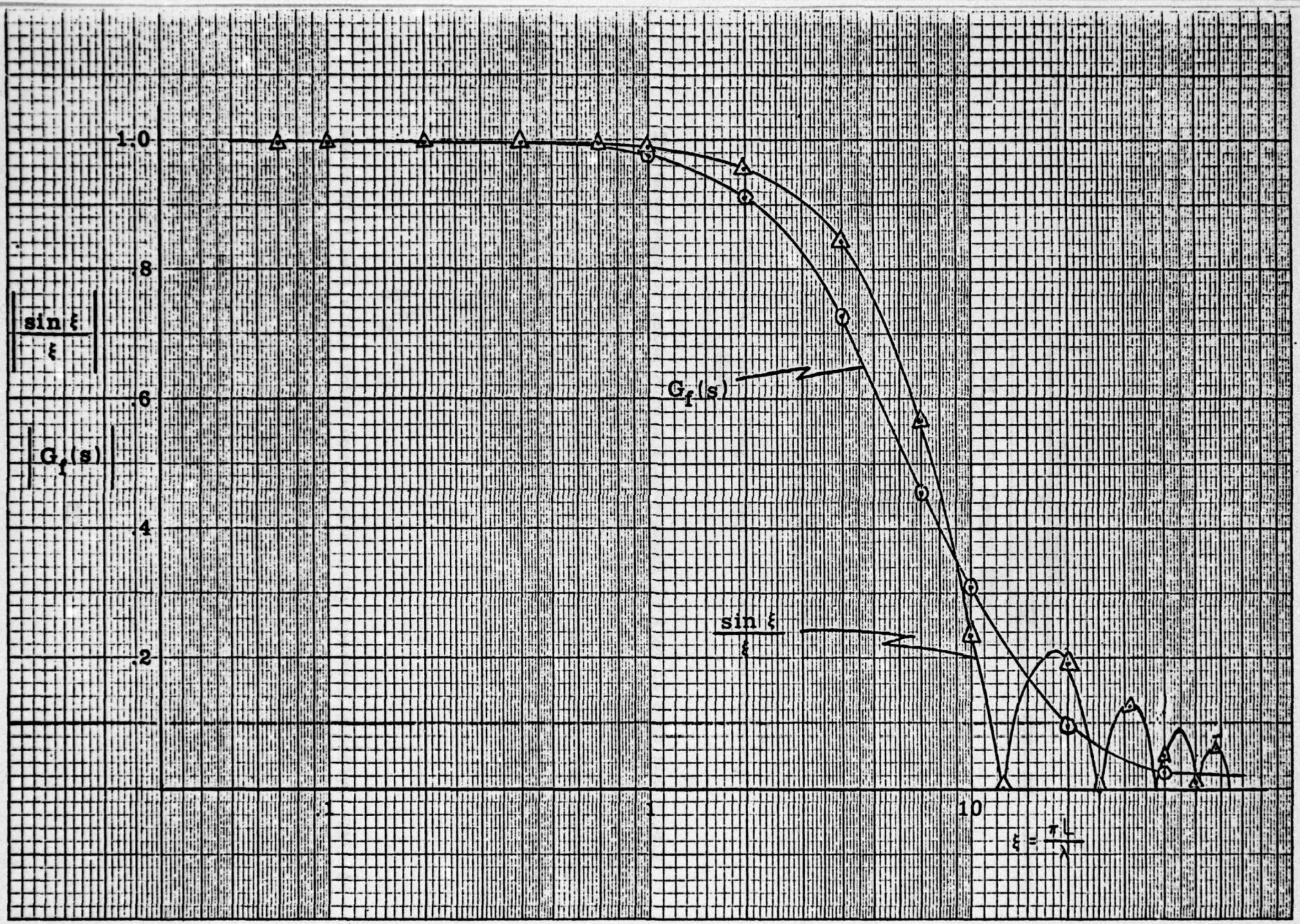

Figure 3. Approximation of the Finite Pad Length Effect.

time derivative of the same for pitch disturbances. The relationship is illustrated in block diagram form in Figure 4.

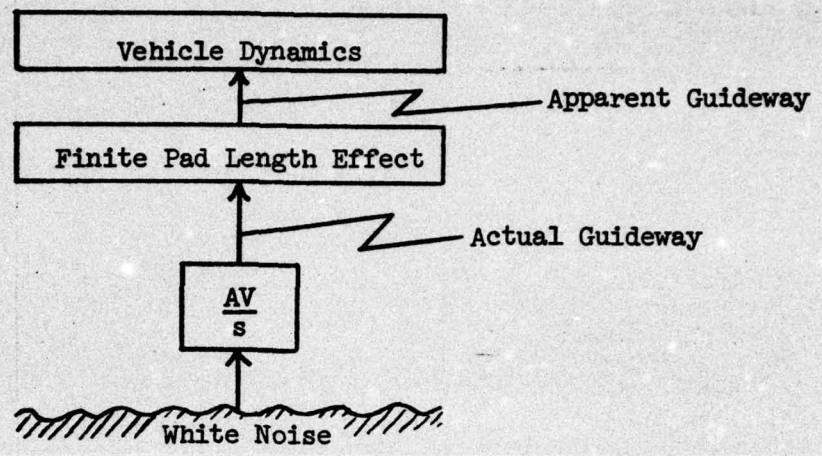

Figure 4. Block Diagram Representation of Guideway Model.

The advantage of using such a linear model is that it does not unduly complicate the understanding of vehicle dynamics and it does not affect a Gaussian process (white noise) other than in magnitude. The guideway spectra may then be expressed by the following differential equations.

$$\ddot{\theta}_g + 13.7\,\dot{\theta}_g + 45.3\,\theta_g = \sqrt{\frac{A}{U}}\,\eta(t)$$

$$\frac{c}{U}\,\ddot{h}_g = \dot{\theta}_g$$

where $\eta(t)$ is a white noise source with unity spectral density. This is a third order set of equations which completely describes the guideway variations as seen by the vehicle traversing over it.

TOTAL MODEL

The total model is a fourther order set of vehicle equations controlled by two inputs and disturbed by a third order white noise filter which models the guideway. It is expressed in state variable form as $\dot{x} = Ax + Bu + Cw$ where A, B, and C are matrices and x, u, w are vectors. These are presented in Appendix D. The stability derivatives are derived from lift and moment coefficients and a first order Taylor series assumption. Since we are interested only in small perturbations about some steady-state, we can eliminate the steady-state terms from the equations of motion. The guideway is assumed to have the spectrum of a typical smooth highway and the effect of vehicle size on small bumps has been approximated by assuming that the average value of the guideway under the vehicle which is of interst.

The complete model as presented does have its drawbacks. The linearity of the system will not predict the changes in lift coefficient derivatives, for instance, when the gap is altered drastically in violation of the small perturbation assumption. However, the theory shows that the derivatives remain approximately constant over gap height change. For example, the steady-state gap of one inch presently used corresponds to $r_o = 0.5$. Varying r_o as much as $\pm$ 0.475 changed none of the lift derivatives by more than three persent. All the derivatives were within a fifteen percent tolerance except for $\frac{\partial C_M}{\partial \bar{h}}$ which varied by thirty-five percent. This seems to say that a linear assumption is reasonably good. Also, there is no provision for air turbulence; the model assumes a

stationary air mass in the guideway. Though this last assumption is not likely to be the case, it does provide a good starting point for the TRACV dynamic analysis and will yield a good impression of what the dominant modes of motion are likely to be.

CHAPTER III
RIGID VEHICLE DYNAMICS

Having assembled a complete model, the first item of business is to explore the dynamics of the rigid vehicle, one in which the winglets are firmly fixed with respect to the body. Doing so provides an initial idea of the fundamental vehicle dynamics and whether some form of suspension is necessary. Setting up the tools for this analysis also paves the way for later more complicated analysis.

EIGENVALUES AND EIGENVECTORS

We start with a look at the eigenvalues and eigenvectors, for they describe the vehicle characteristics in detail. Table I gives these for the rigid vehicle. From these values we can see there are two oscillatory modes in the vehicle: one low frequency, very lightly damped mode and a second higher frequency, moderately damped mode. Because there are two complex pairs, only two eigenvectors need be expressed; the other two are the complex conjugates of these. The pitch attitude variable (θ) is the base for each eigenvector.

The rigid vehicle has two natural frequencies which are fairly close together, neither of which are strongly damped. The eigenvectors indicate that the height variation and pitch variation are nearly in phase for the low frequency mode. This means that the nose comes up with the rising of the c.g. in the guideway such that the front end of the vehicle has the largest excursions. One might infer that the winglet gap at the front will have the greatest variation, since forward of the c.g., the pitch and heave oscillations add to each other. The attitude mode ratio for

TABLE 1

EIGENVECTORS AND EIGENVALUES OF RIGID VEHICLE

Eigenvalues
-8
-5.5
0
-2.08 + i 9.01
-2.08 - i 9.01
-.4717 + i 6.03
-.4717 - i 6.03

Eigenvalues in units of sec^{-1}

Eigenvectors

High Frequency

$$\begin{bmatrix} \bar{h}_r' \\ \theta_r' \\ \bar{h}_r \\ \theta_r \end{bmatrix} = \begin{bmatrix} 44.5\, e^{i\,162^\circ} \\ 13.7\, e^{i\,101^\circ} \\ 3.31\, e^{i\,59.2^\circ} \\ 1.0\, e^{i^\circ} \end{bmatrix}$$

Low Frequency

$$\begin{bmatrix} \bar{h}_r' \\ \theta_r' \\ \bar{h}_r \\ \theta_r \end{bmatrix} = \begin{bmatrix} 4.74\, e^{i\,91.1^\circ} \\ 8.80\, e^{i\,94.5^\circ} \\ .539\, e^{i-3.37^\circ} \\ 1.0\, e^{i\,^\circ} \end{bmatrix}$$

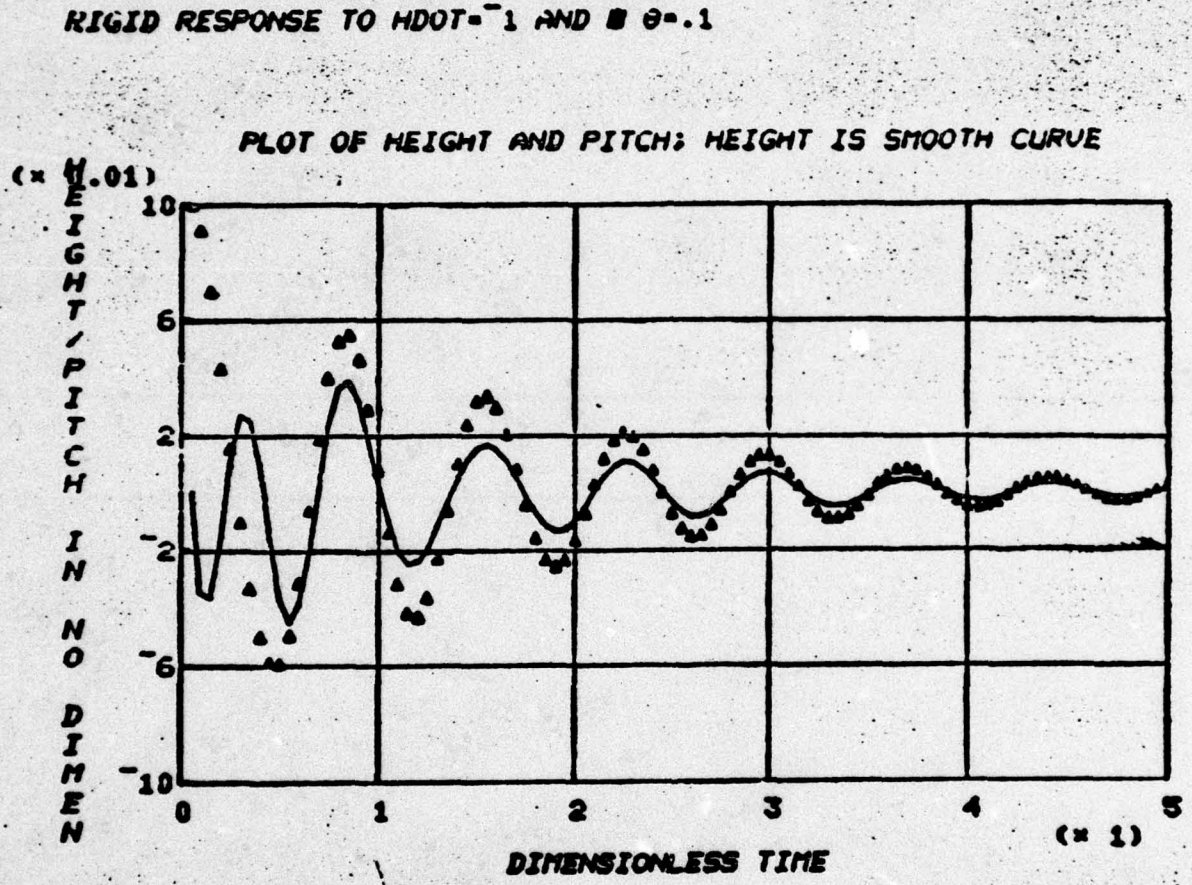

Figure 1. Transient Response of Rigid Vehicle.

the low frequency eigenvector is $\frac{\bar{h}}{\theta} = 0.54$, indicating that a 0.1 radian pitch variation coincides with an 8.1 foot variation in c.g. height. For the 150 foot-long vehicle, this motion appears as a rotation about an effective center at about the 94 percent chord position, almost at the tail end. Figure 1, a time-domain step response, shows this in-phase relationship. Having an effective center of rotation at .94c suggests that the forward-most seat in the cabin will experience the worst accelerations, having the longest moment arm.

On the other hand, the high frequency mode is sixty degrees out of phase and has a mode ratio $\frac{\bar{h}}{\theta}$ which is six times greater than that of the low frequency. This will mean that this frequency appears as nearly all heave and the small pitch component does not add as much vertical acceleration to any vehicle location as does the low frequency mode. This effect is apparent in the spectral density plots which follow, particularly if one remembers that part of the high frequency reduction at .90c is due to the reduced reinforcement of the nearby low frequency mode.

SPECTRAL DENSITY AND RIDE QUALITY

Table II shows the A and C matrices for the rigid vehicle. Since there are no control motions (winglet movements), the B matrix is of no concern. Using these matrices and Cramer's rule, the transfer functions may be found for the various state variables with respect to the noise vector which has been normalized to one. The magnitude squared of this function plotted against frequency is the spectral density. For vehicle

TABLE 2.

GENERALIZED MATRIX FORM OF RIGID VEHICLE STATE EQUATIONS

$$\dot{x} = Ax + Cw$$

$$A = \begin{bmatrix} \frac{c}{UA} C_{L_{\dot{h}}} & \frac{c}{UA} C_{L_q} & C_{L_h} & C_{L_\theta} & \frac{-c}{UA} C_{L_{\dot{h}}} & \frac{-c}{UA} C_{L_q} & 0 \\ \frac{c}{UA} C_{M_{\dot{h}}} & \frac{c}{UA} C_{M_q} & C_{M_h} & C_{M_\theta} & \frac{-c}{UA} C_{M_{\dot{h}}} & \frac{-c}{UA} C_{M_q} & 0 \\ 1 & 0 & 0 & 0 & -1 & 0 & 0 \\ 0 & 1 & 0 & 0 & 0 & -1 & 0 \\ 0 & 0 & 0 & 0 & 0 & \frac{u}{c} & 0 \\ 0 & 0 & 0 & 0 & 0 & -20 & -96 \\ 0 & 0 & 0 & 0 & 0 & 1 & 0 \end{bmatrix}$$

$$C = \begin{bmatrix} 0 \\ 0 \\ 0 \\ 0 \\ 0 \\ 96\sqrt{\frac{A}{U}} \\ 0 \end{bmatrix}$$

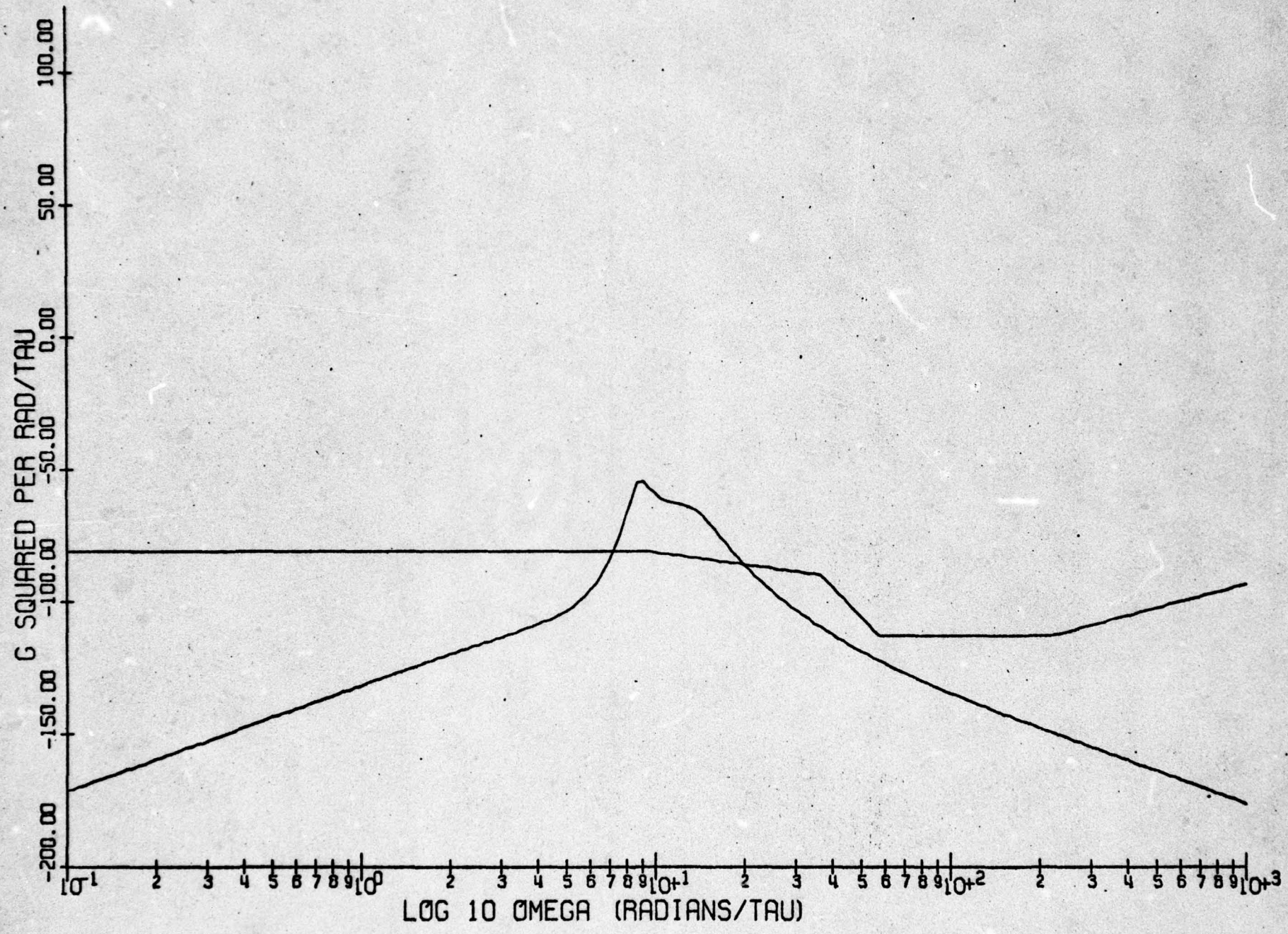

Figure 2. Rigid Vehicle Acceleration Spectral Density at .40c (c.g.).

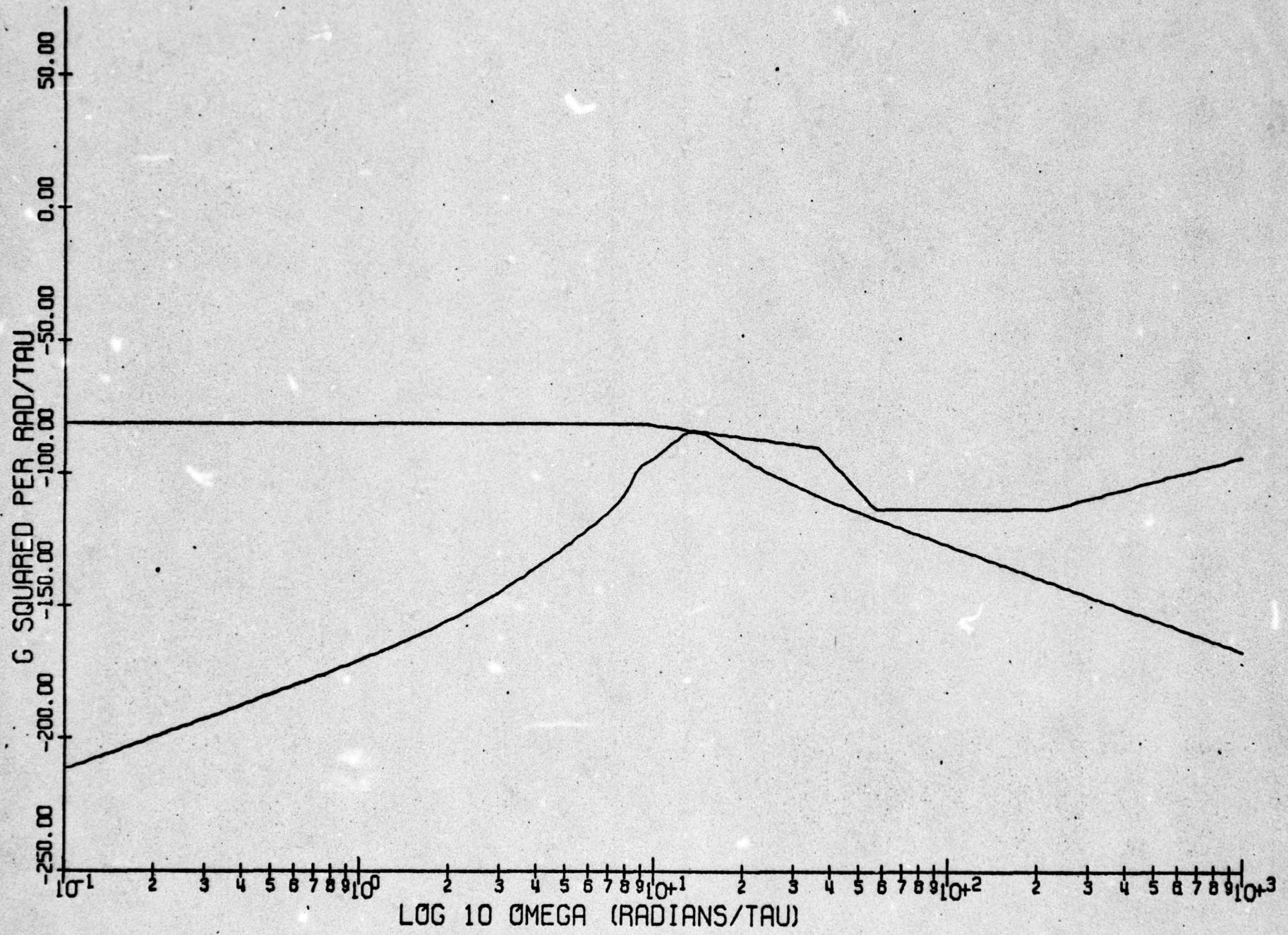

Figure 3. Rigid Vehicle Acceleration Spectral Density at .90c.

accelerations, we use $|s\ \bar{h}_v'|^2$ as our c.g. spectral density, and a linear combination of $\bar{h}_v'$ and θ_v' will give the acceleration transfer function at other vehicle locations. These spectral densities may be plotted against a ride quality standard which will show at what frequencies the accelerations are unacceptable.

One such standard is the Urban Tracked Air Cushion Vehicle (UTACV) standard (DOT Specification, 1972) which sets an upper limit on the magnitude of the spectral density plot. Figure 2 shows the spectral density of accelerations at the c.g. as compared to the UTACV limit. It shows that the accelerations in the range from 0.764 - 2.24 Hz are unacceptable. At the rearmost seat, near the apparent low frequency mode center of rotation, we would expect that the spectral density plot would show a diminished low frequency peak and overall reduced acceleration according to the prediction of the eigenvectors. Figure 3 shows this to be the case, although the standard is scarcely met. These figures and similar ones in later paragraphs are in non-dimensional frequency. The defining relationship is 1 Hz = 9.15 rad/τ. The vertical axis has units of db (20 log $\left|\frac{g^2}{\text{rad}/\tau}\right|$).

RMS ACCELERATION AND GAP VARIATION

In addition to spectral density comparisons, an important indicator of ride quality is the root mean squared (RMS) acceleration. Whereas the spectral density plot shows acceleration level at a frequency, the rms value gives the overall acceleration felt by the passenger. Both indicators are necessary for a complete picture. If G(s) is the transfer function of

interest, then the mean squared value is given by

$$E(x^2) = \frac{1}{j\pi} \int_{-\infty}^{\infty} G(s)\, G(-s)\, ds; \quad s = j\omega$$

This integral has been solved in closed form and tabulated for systems up to tenth order (Newton, Gould, and Kaiser; 1957). At the c.g., the rms acceleration was found to be 0.121 g, a fairly rough ride. The rearmost seat, at .90c, proved to be far better as predicted, having rms acceleration of 0.0055 g.

Not only are we interested in the rms value of the accelerations, but the rms variation in the gap at each end will give an idea of frequency of contact with the guideway. Once again, the Gaussian white noise assumption is useful, because the gap variation is Gaussian as well, a direct result of having a linear gap to white noise transfer function. The rms value is related to the standard deviation of the Gaussian distribution, so a knowledge of the steady-state gap size and the rms variation will indicate what percentage of the time the winglets are in contact with the guideway.

The rigid vehicle leading edge rms gap variation is 14.7 inches and the trailing edge rms gap variation is 6.07 inches as compared to a steady-state value of about one inch. Since the vehicle can not appear below the guideway, these values tell us that the vehicle is likely to spend much of its time in contact with the guideway, or simply put, it will "bottom out" frequently, particularly at the front, primarily because of the influence of the very lightly damped low frequency mode. The reader should remember that these numbers are the result of an unconstrained linear model and while they are quite good as estimates of

what will occur, they cannot exactly describe the actual nonlinear problem of guideway contact.

The conclusion to be drawn from this rigid case analysis is that from all measures the ride quality of the rigid vehicle is unacceptable. There are frequencies in all positions of seats where the accelerations are uncomfortable. The overall ride is rough, and the vehicle tends frequently to bottom out. The vehicle has one oscillatory mode which is very lightly damped at about 1 Hz which is in large measure the cause of these problems, only to be aided by another mode of light damping nearby at 1.5 Hz. It is readily apparent that some form of suspension or control is necessary if the TRACV is to be implemented. The Chapters that follow explore this possibility in both the passive and active sense and compare those cases to this one to determine what degree of improvement can be made.

CHAPTER IV

THE PASSIVE SUSPENSION

Since it is clear that the rigid vehicle is unacceptable, the ways in which the ride quality can be made acceptable become important. If the winglets are given freedom to move about, then they can be used to control winglet gap and thus vehicle motions, since the theory of lift and moment indicates that the forces are very strongly a function of the winglet gap. The motions of the winglets as described in Chapter II can be controlled by two means: passive suspension and active control. In this chapter the former case is considered; a model is developed and the ride quality of this model is examined. Since the passive suspension is much less expensive to implement than active control, if their performances can be made nearly equal, then passive suspension is preferable.

THE REVISED MODEL

The passively suspended model can be considered an uncontrollable dynamic system as opposed to a system with control surfaces, with the winglets restrained by springs and dampers. We assume massless winglets for simplicity because they will be very small in mass compared to the vehicle and their natural frequencies will be so high that for the present purpose they are infinitely fast. There are then two first order equations which are added to the equations of the rigid case, one for each degree-of-freedom of the winglets. The motions of the winglets $\Delta\delta_{w_1}$ and $\Delta\delta_{w_2}$ are considered state variables and the coefficients become part of the A

matrix. After finding values of spring and damper constants which give the best performance, the analysis of such performance parallels that of Chapter III.

We start by writing a force balance equation for each winglet motion. Once again, only perturbations are of present concern. The hinge moment on the winglet for each mode of motion is related to the pressure distribution under the vehicle and is a function of the motion and control variables.

$$B_1 \Delta\dot{\delta}_{w_1} + K_1 \Delta\delta_{w_1} = HM\ (\dot{\bar{h}},\ q,\ \bar{h},\ \theta,\ \delta_{w_1},\ \delta_{w_2})$$

$$B_2 \Delta\dot{\delta}_{w_2} + K_2 \Delta\delta_{w_2} = \tilde{HM}\ (\dot{\bar{h}},\ q,\ \bar{h},\ \theta,\ \delta_{w_1},\ \delta_{w_2})$$

In the above equations, HM and $\tilde{HM}$ refer to the hinge moment around the first and second winglet axes, respectively. For the first of these two, the hinge moment is related to the lift since the pressure generating lift places a moment on the winglet.

$$HM = x_{cp} \frac{A_w}{2} P$$

$$HM = x_{cp} \frac{A_w}{2} \frac{L}{S}$$

$$HM = \frac{x_{cp}}{2} \frac{A_w}{S} L$$

$$HM = \left[\frac{x_{cp} A_w}{2S}\right] \frac{1}{2} \rho U^2 S\, C_L$$

$$HM = \left[\frac{x_{cp} A_w}{2S} \frac{1}{2} \rho U^2 S\right] C_L$$

$$\frac{\partial HM}{\partial \xi} = P\, C_{L_\xi} \; ; \qquad P = \frac{x_{cp} A_w \rho U^2}{4}$$

We note that x_{cp} is the distance from the axis to the center of pressure on the winglet in feet and A_w is the total area of the winglets (including the area of both winglets). Since the theory assumes that the pressure at the gap is that of free stream and the pressure near the root of the winglet is that under the vehicle, there must be some gradient of pressure along the width of the winglet. Assuming a linear gradient, as approximation the center of pressure is at $\frac{W_w}{3}$, or 0.833 feet. This value yields P = 33440 ft.-lbs.

The second type of hinge moment is also related to previous lift and moment coefficients, but in a different way.

$$\tilde{HM} = (\bar{x}_{c.r.} - \bar{x}_o)\, C \frac{A_w}{2} \frac{L}{S} + \frac{A_w}{2} \frac{M}{S}$$

In the above equation, the first term describes the pressure at the c.g. due to lift acting on the winglet, the second relates the effect of the lengthwise pressure distribution which causes the aerodynamic moment on the vehicle. Again calling on the assumption that $\bar{x}_{c.r.} = \bar{x}_o$, the first term drops out and we get

$$\tilde{HM} = \frac{A_w}{2S} M$$

$$\tilde{HM} = \frac{A_w}{2S} \frac{1}{2} \rho U^2 \, Sc \, C_M$$

$$\tilde{HM} = \frac{A_w \rho U^2 c}{4} C_M$$

$$\frac{\partial \tilde{HM}}{\partial \xi} = \frac{A_w \rho U^2 c}{4} \frac{\partial C_M}{\partial \xi}$$

$$\frac{\partial \tilde{HM}}{\partial \xi} = R\, C_{M_\xi} \qquad R = \frac{A_w \rho U^2 c}{4} \left(\frac{k_y}{c}\right)^2$$

Because of our earlier notation $C_{M_\xi} = \frac{c^2}{K_y^2} \frac{\partial C_M}{\partial \xi}$, the radius of gyration term must be carefully reinserted to insure consistency. This development yields R = 3753 ft.-lbs.

The basic equations of motion in state variable form appear as $\dot{x} = Ax + Cw$ where A, instead of being a seventh order matrix, is a ninth order matrix. The eighth and ninth rows come from the equations below which are once again written in non-dimensional time.

$$\tilde{B}_1 \Delta\delta_{w_1}' = \frac{Pc}{UA} C_{L_{\dot{\bar{h}}}} \Delta\bar{h}' + \frac{Pc}{UA} C_{L_q} \Delta\theta' + P\, C_{L_{\bar{h}}} \Delta\bar{h} + P\, C_{L_\theta} \Delta\theta$$

$$+ (P\, C_{L_{\delta_{w_1}}} - K_1) \Delta\delta_{w_1} + P\, C_{L_{\delta_{w_2}}} \Delta\delta_{w_2}$$

$$\tilde{B}_2 \Delta\delta_{w_2}' = \frac{Rc}{UA} C_{M_{\dot{\bar{h}}}} \Delta\bar{h}' + \frac{Rc}{UA} C_{M_q} \Delta\theta' + R\, C_{M_{\bar{h}}} \Delta\bar{h} + R\, C_{M_\theta} \Delta\theta$$

$$+ R\, C_{M_{\delta_{w_1}}} \Delta\delta_{w_1} + (R\, C_{M_{\delta_{w_2}}} - K_2) \Delta\delta_{w_2}$$

Notice the change in notation to the new damping constants, $\tilde{B}_1$ and $\tilde{B}_2$. This is to indicate that these two have also been shifted to non-dimensional time. The full state matrix form with the two added equations may be found in Appendix D.

OPTIMIZING THE PASSIVE SUSPENSION

The ride quality of the passively suspended TRACV is dependent on the four spring and damper constants; K_1, K_2, B_1, and B_2. The values which give the best possible ride quality must be determined, but the process involved is not very simple because of a ninth-order model and a ride quality which is a function of four variables. The most obvious method of solution is a gradient search on a computer, since the analytical method would involve multiple determinants of a ninth order system and as a result the likelihood of multiple algebraic errors. A gradient search which simply looks for the direction of largest improvement in a cost function and adjusts the four variables accordingly would be fast and relatively simple to program.

The routine which was used was the simplest gradient method possible, based on the procedure

$$x_n^{k+1} = x_n^k - \epsilon_n \left(\frac{J^k - J^{k-1}}{x_n^k - x_n^{k-1}}\right)$$

Where x_n is the particular variable being incremented, k is the iteration counter, ϵ_n in the step size constant for x_n, and J is the cost function. The procedure is to find the partial derivative of the cost function with respect to each of the four variables, adjust by the corresponding ϵ_n, and use the result as the stepsize for each variable.

The cost function which was used placed a cost on six values. These values are the rms acceleration in heave and pitch, rms gap variation fore and aft, and rms winglet deflection for both motions. These were

found for a given A matrix by using Cramer's rule to find the transfer function of each with respect to unity white noise and calculating the mean squared error integral of that transfer function. The value of x_n^{k-1} was taken as five percent larger than x_n^k rather than the actual previous value to insure that a large previous step does not adversely influence the derivatives at the present point. Computationally, using old values would have been less expensive, but the cost margin was deemed small. The cost function used is described by

$$J = \frac{1}{2}\int_0^\infty x^T Z x \; dt$$

where x is a vector of the state variables and Z is a diagonal matrix of weighting constants. The values of Z were set by

$$Z(n,n) = \left|\frac{1}{x_{n_{max}}}\right|^2$$

which is the inverse of the desired maximum value of each of the respective state variables. The values chosen were h''^2_{max} .01g, Δh_{Gap} = 0.33 inches. and no weighting on control deflections or pitching accelerations. These values were actually the result of first having solved the active optimal control problem and finding out what set of weighting coefficients worked best.

Using this cost function, an algorithm for the optimization of the spring and damper constants was developed. Figure 1 gives a flow diagram for the algorithm. When implemented on the IBM 370 computer using APL, the method converged in approximately twenty steps. The cost function

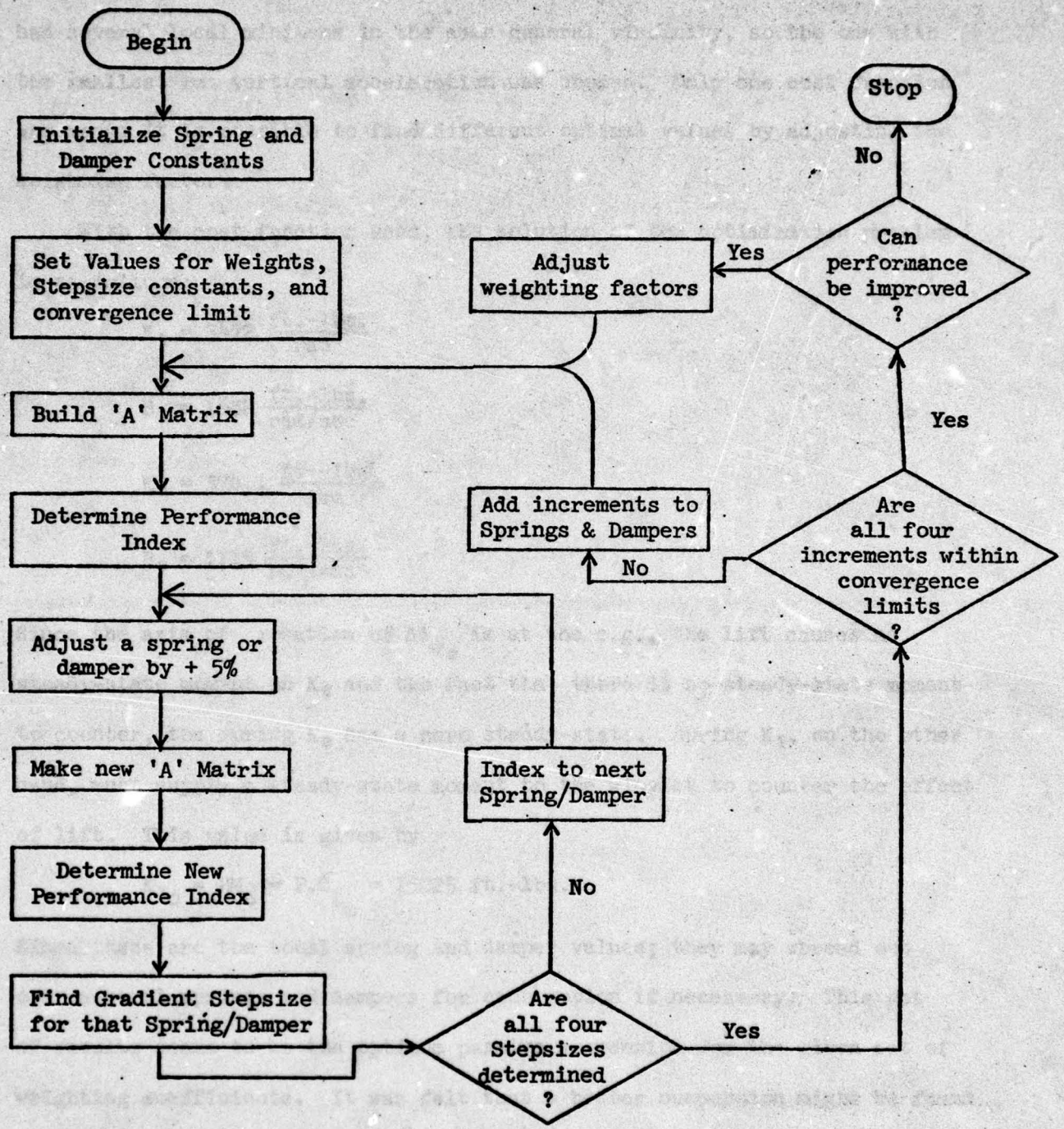

Figure 1. Passive Suspension Optimization Technique.

had several local minimums in the same general vincinity, so the one with the smallest rms vertical acceleration was chosen. Only one cost function was used; it is possible to find different optimal values by adjusting the weighting factors.

With the cost function used, the solution of the optimization problem is as follows:

$$K_1 = 3472 \frac{\text{ft.-lbs.}}{\text{rad}}$$

$$B_1 = 1652 \frac{\text{ft.-lbs.}}{\text{rad/sec}}$$

$$K_2 = 374.1 \frac{\text{ft.-lbs.}}{\text{rad}}$$

$$B_2 = 1115 \frac{\text{ft.-lbs.}}{\text{rad/sec}}$$

Since the axis of rotation of $\Delta\delta_{w_2}$ is at the c.g., the lift causes no steady-state moment on K_2 and the fact that there is no steady-state moment to counter, the spring K_2 has a zero steady-state. Spring K_1, on the other hand, must supply a steady-state moment to the winglet to counter the effect of lift. This value is given by

$$K_{1_o} = HM_o = P.C_{L_o} = 15225 \text{ ft.-lbs.}$$

Since these are the total spring and damper values; they may spread out over several springs and dampers for each motion if necessary. This set of results seems to be the optimum passive suspension for the given set of weighting coefficients. It was felt that a better suspension might be found by repeating the entire process with several sets of weighting parameters. Rather than grind away numerically at considerable costs, however, a

local search around this optimum was made by using educated guessing, and no better tradeoff between vertical acceleration and gap variation could be found.

With the spring and damper constants determined, the overall model is easily described in state variable form with two more variables than in the rigid case; $\Delta\delta_{w_2}$ and $\Delta\dot{\delta}_{w_2}$ are becoming state variables. We now have a ninth order system which may be evaluated using the same criteria as used in Chapter III.

EIGENVALUES AND EIGENVECTORS

Once again we start with a study of the eigenvalues and eigenvectors. For the passive suspension they differ greatly from the rigid case, as shown in Table I. The eigenvalues show a marked change from very low damping to moderate damping and drastic lowering of natural frequencies. For the rigid vehicles, the two frequencies occurred at two and three hertz; in the passive case they occur at 0.036 and 0.325 Hz, so that they are not only lower, but they are relatively further apart. Spreading them apart and increasing the damping means that, on the whole, the acceleration will be much lower and more nearly uniform over the range of frequencies.

The eigenvectors also show a marked change. The mode ratios of heave to pitch for the two frequencies are much larger, indicating that the degree of coupling is drastically reduced. The high frequency mode has a $\frac{\bar{h}}{\theta}$ mode ratio which is sixty-four times greater than the ratio for the rigid case, implying that the high frequency mode is nearly all heave.

TABLE 1

EIGENVALUES AND EIGENVECTORS OF PASSIVE SUSPENSION

Eigenvalues

-8
-5.5
0
-.967 + i 1.79
-.967 - i 1.79
-.077 + i .215
-.077 - i .215
-128.3
- 37.2

Winglet Modes

Eigenvalues in units of sec^{-1}

Eigenvectors

High Frequency

$$\begin{bmatrix} \bar{h}_r' \\ \theta_r' \\ \bar{h}_r \\ \theta_r \end{bmatrix} = \begin{bmatrix} 628\, e^{i\,226^\circ} \\ 4.38\, e^{i\,151^\circ} \\ 212\, e^{i\,108^\circ} \\ 1.0\, e^{i\,0^\circ} \end{bmatrix}$$

Low Frequency

$$\begin{bmatrix} \bar{h}_r' \\ \theta_r' \\ \bar{h}_r \\ \theta_r \end{bmatrix} = \begin{bmatrix} .0173\, e^{i\,110^\circ} \\ .349\, e^{i\,111^\circ} \\ .0522\, e^{i\,.043^\circ} \\ 1.0\, e^{i\,0^\circ} \end{bmatrix}$$

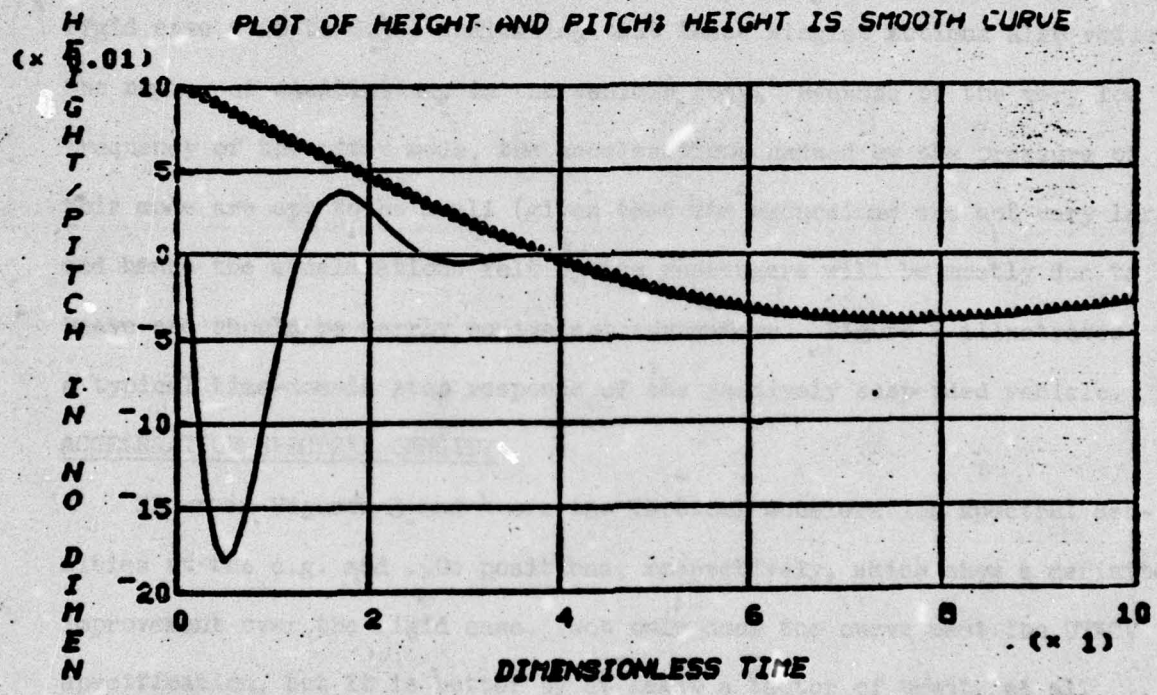

Figure 2. Transient Response of Passively Suspended Vehicle.

For the low frequency mode, the opposite is true, the $\frac{\theta}{h}$ mode ratio for the passive case is over ten times greater than that of the rigid case and the low frequency mode is nearly all pitch motion.

These values suggest that the motions of $\Delta\delta_{w_1}$ act so as to decouple almost entirely the two modes of motion of the body while they move to track variations in the guideway, keeping the vehicle body as motionless as possible. The high frequency damping ratio has increased from the rigid case value of 0.23 to 0.48 and the low frequency ratio has improved from the rigid case 0.08 to 0.34, indicating that these winglet motions also reduce the number of oscillations in the vehicle body. Because of the very low frequency of the pitch mode, the accelerations caused by the pressure of this mode are apt to be small (given that the excursions are not very large) and hence the accelerations felt by the passengers will be mostly due to heave and should be nearly equivalent everywhere. Figure 2 illustrates a typical time-domain step response of the passively suspended vehicle.

ACCELERATION SPECTRAL DENSITY

Shown in Figures 3 and 4 are the vertical acceleration spectral densities at the c.g. and .90c positions, respectively, which show a definite improvement over the rigid case. Not only does the curve meet the UTACV specification, but it is better by at least a factor of twenty at all frequencies. There are no sharp peaks, indicating that the damping is improved as well. These figures would suggest a very acceptable ride quality as a result of the passive suspension by the low level of acceleration at all frequencies.

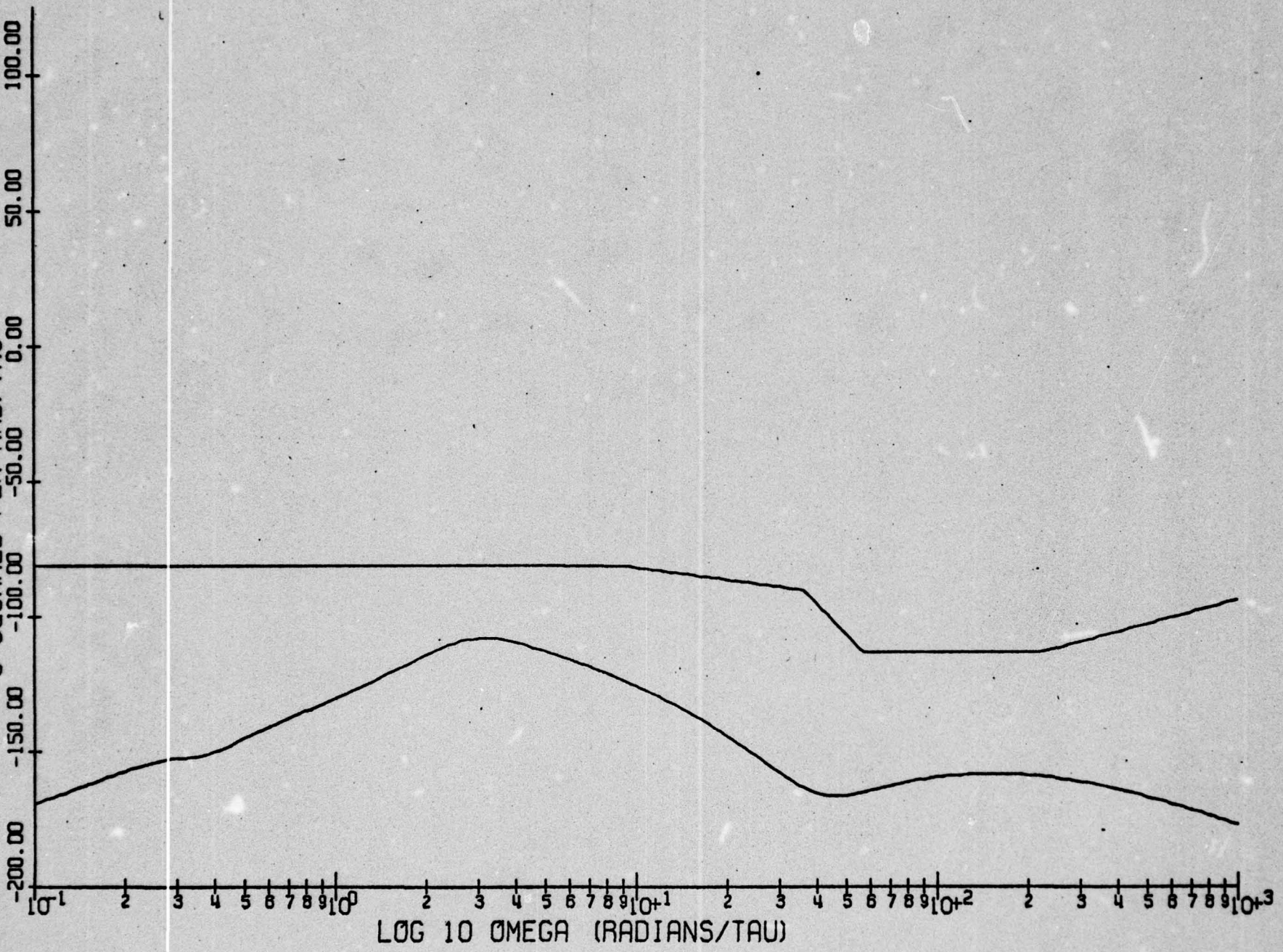

Figure 3. Passive Suspension Acceleration Spectral Density at .40c.

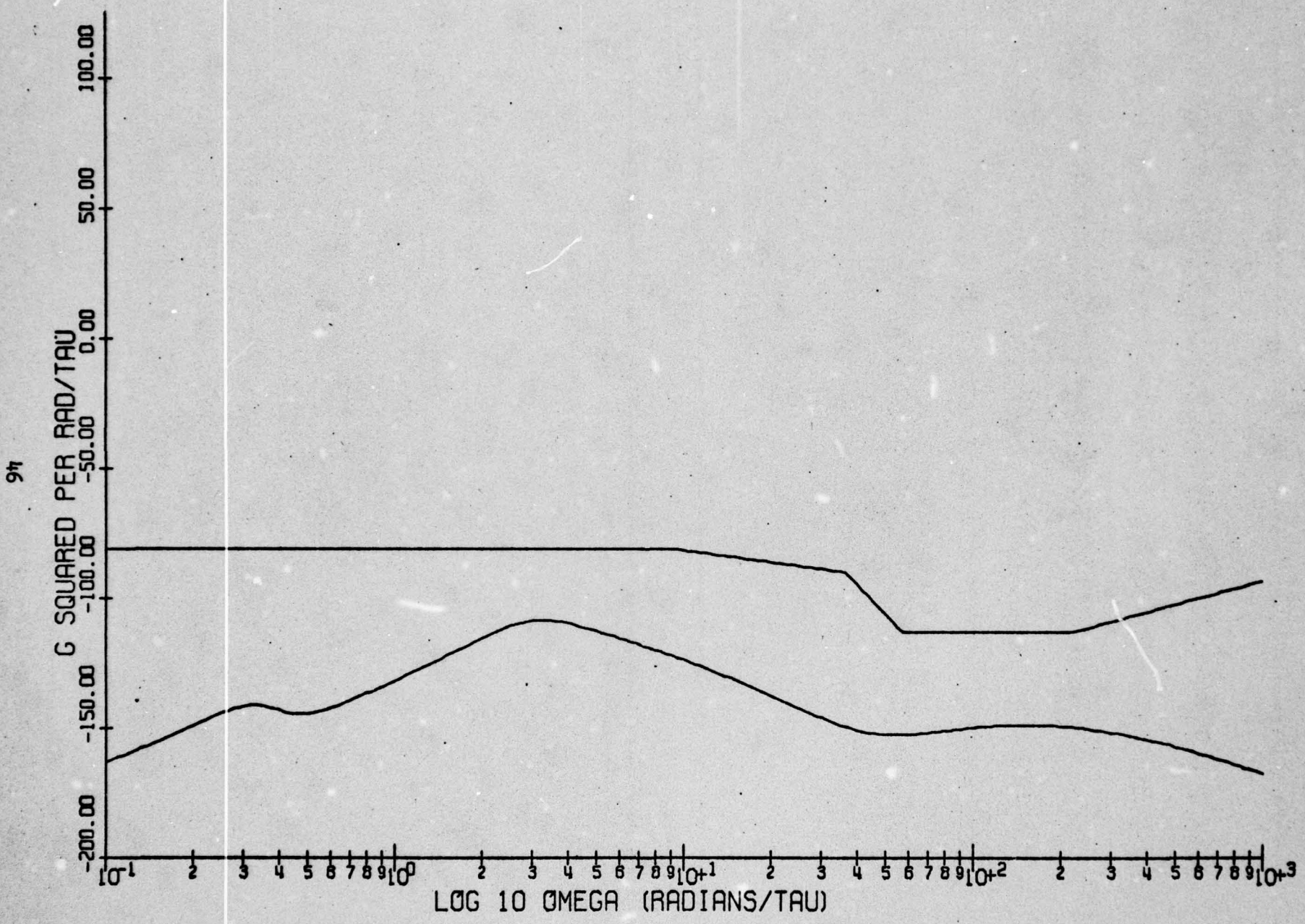

Figure 4. Passive Suspension Acceleration Spectral Density at .90c.

RMS ACCELERATION, GAP VARIATION, AND CONTROL DEFLECTION

The acceleration at the c.g. was greatly improved by the passive suspension. In the rigid vehicle the rms vertical acceleration was found to be 0.121g, while the passive suspension improved this to 0.0072g, a very smooth ride. The rearmost seat was about the same as the c.g. in the passive suspension, as predicted, experiencing 0.009g accelerations which are slightly worse than the rigid case. The very smooth .90c acceleration level for the rigid case was due to the in-phase coupling of the modes which is destroyed in the passive suspension. Hence, the slight loss of ride quality at that location is understandable.

Another significant improvement is in the gap variation. The leading edge rms gap variation is one percent of and the trailing edge value is 3.5% of the rigid case value. These new values are $\Delta h_{LE\ Gap} = .143$ inches and $\Delta h_{TE\ Gap} = .224$ inches. Since the steady-state gap is slightly over one inch, one can safely say that the winglets rarely touch the guideway. In fact, it seems that there is some margin in these values, and that adjusting the cost function to weight accelerations more heavily might result in some set of springs and dampers which enlarge this variation slightly and yielded still lower acceleration levels. It is interesting that the trailing edge has the larger variation, which is not true of the rigid vehicle. It is clear from the above values, however, that the difference is smaller, as a result of mode decoupling. The decoupling and phasing of $\bar{h}$ and θ motions is further illustrated by this fact.

There is one other result of interest, and that is the rms deflection of the two winglet modes. These values are found in the same way as the others and give an idea of the typical size of the control surface displacements. For the passive suspension, rms $\Delta\delta_{w_1}$ is 0.0154 rad. and rms $\Delta\delta_{w_2}$ is 0.000534 rad. The typical heave control is small, varying through a typical $\pm 1^{\circ}$. A deflection of one degree represents a change of gap on the order of one-half inch, however, and that is significant. This seems to tell us that the motions of the winglet are such that the heave in the guideway is countered by similar motions of the winglet so that the gap remains constant along with the c.g. while the winglet and guideway move together. The typical pitch deflection is also quite small, for we find that the value of 0.000534 rad. corresponds to $.03^{\circ}$, and a gap change at the vehicle rear of about 0.6 inches. Once again, the winglet deflection is larger than the gap variation, indicating that the second mode of motion is also probably necessary to keep the vehicle body unaccelerated and to prevent winglet-guideway contact.

To summarize, we have built a passive suspension by allowing the winglets two-degrees-of-freedom but restraining each mode with a spring and a damper. The effect of this configuration (if one finds optimal springs and dampers) is to lower the frequencies of both modes while spreading them apart, increasing damping, and decoupling the modes of motion. In terms of the ride quality, the new configuration is very good and a tremendous improvement over the rigid vehicle. The overall acceleration level is quite low and there are no particular "bone-jarring" frequencies.

The rate of winglet contact goes from almost continuous to almost never, and the size of springs and dampers required is reasonable and permit only very small control deflections, so that the passive suspension does not attempt to violate the assumptions from which the model arose. All in all, the general outlook is very good for this form of control.

CHAPTER V

ACTIVE SUSPENSION

The active suspension is one in which the winglets are controlled by actuators which receive signals from feedback circuits originating at vehicle position and rate sensors. In this chapter the linear optimal control problem is solved using a performance index very similar to the one in the previous chapter. The form of the equations is varied slightly to accommodate the solution technique in that the winglet motion equations are dropped as a result of assuming that the winglet-servo response to control inputs is of sufficient bandwidth to be considered infinitely fast. The method of solution involves the solution of the matrix Ricatti equation and using this to find the feedback gains. Solving this problem will give some idea of the best which this particular vehicle can possibly do, and provides an index against which other types of suspensions may be compared. Having found the optimal feedbacks, we will proceed to analyze the ride quality along the lines of previous chapters.

ACTIVE SUSPENSION MODEL

This model assumes a controllable dynamic system with white noise disturbance. The state equations written as matrices have the form $\dot{x} = Ax + Bu + Cw$ where the A and C matrices are identical to those of the rigid vehicle model, and the B matrix is the set of derivatives of lift and moment coefficient with respect to each of the two control motions. The result is a seventh order system with two control inputs and one disturbance input.

Since there are seven state variables, this formulation assumes seven sensors from which the feedback signals originate. This may not always be feasible, so a comparison is done later with a system in which some of the sensors are turned off. The seven states are vehicle heave rate and pitch rate, relative heave and pitch, and guideway heave rate, pitch rate, and pitch. The first two may easily be sensed with on-board accelerometers, the output of which is integrated. The second pair could be sensed by measuring capacitance, using small feelers, or even by carefully measuring under-vehicle pressure at several points and deriving attitude from the lift and moment relationships. Of these possibilities, use of feelers is the least desirable since the feelers create noise and would continually require replacement because of wear.

Infrared ranging of the relative distance is difficult because the track is subject to differential heating which would throw measurements off. A laser ranger would be a distinct possibility, but such devices are expensive. No matter what the type of sensing, a reliable knowledge of height above the guideway at two different chord positions would be all that is required for height and pitch determination. If relative and vehicle rates and displacements are known, then the guideway rates and displacements are but an algebraic sum of these and easy to generate. However, some thought must still be given to means of sensing the vehicle and guideway states.

THE LINEAR OPTIMAL CONTROL PROBLEM

The straightforward optimal control problem involves finding the

coefficients of the feedback matrix which yield collectively the lowest cost function value when the cost function is a function of the states and the control inputs. The desired cost function, however, is not in these terms. Instead, the items weighted are vertical acceleration, gap variation, and control deflections. Some transformation must be made to rewrite the performance index as a function of actual state variables and control inputs. Letting $\tilde{x}$ be the vector of variables to be weighted and x be the actual state variables, then the following linear transformation may be made:

$$\tilde{x} = M\begin{bmatrix} x \\ u \end{bmatrix}$$

which says simply that the desired variables are merely linear combinations of the state variables.

Since $\tilde{x}$ is a vector of six variables and x has seven and u has two, M is a six by nine matrix of constants. Letting Z be a diagonal matrix of weighting factors as previously used, we develop the following cost function:

$$J = \frac{1}{2}\int_{t_o}^{\infty} \tilde{x}^T Z \tilde{x}\, dt$$

$$J = \frac{1}{2}\int_{t_o}^{\infty} ([x^T\ u^T]\ M^T)\ Z\ (M\ [\tfrac{x}{u}])\, dt$$

$$J = \frac{1}{2}\int_{t_o}^{\infty} [x^T\ u^T]\ M^T \cdot Z \cdot M\ [\tfrac{x}{u}]\, dt$$

The term $(M^T \cdot Z \cdot M)$ is the matrix inner product of the transpose of M, M itself, and Z. This product gives a matrix with off-diagonal terms

and the resultant cost function expressed in standard notation is

$$J = \frac{1}{2}\int_{t_o}^{\infty} [x^T u^T] \begin{bmatrix} Q & N \\ N^T & P \end{bmatrix} \begin{bmatrix} x \\ u \end{bmatrix} dt$$

for a state system appearing as $\dot{x} = Ax + Bu$. However, it is possible to rewrite this problem (Bryson and Ho; 1969) so that the cross terms of x and u which appear in the submatrix N above become zero. We first rewrite the system equation as $\dot{x} = (A-BP^{-1}N^T)\, x + Bu$, and then the cost function becomes

$$J = \frac{1}{2}\int_{t_o}^{\infty} [x^T u^T] \begin{bmatrix} Q - NP^{-1}N^T & 0 \\ 0 & P \end{bmatrix} \begin{bmatrix} x \\ u \end{bmatrix} dt$$

The submatrices off the main diagonal are now all zero and the form is along more standard lines. For this formulation, we find that

$$K^T = P^{-1}\,(N^T + B^T R)$$

is the feedback matrix where R is the solution of the matrix Ricatti equation cited in numerous references (Schultz and Melsa; 1967).

The procedure to be followed starts with determining the linear transformation matrix M and then selecting the values of Z, the weighting factors. Then the matrix multiplication must be performed and the submatrices Z, N and P. determined. The modified A matrix $\tilde{A} = A - BP^{-1}N^T$ is calculated as well as the modified Q matrix $\tilde{Q} = Q - NP^{-1}N^T$. These are substituted into the matrix Ricatti equation which now appears as

$$\tilde{A}^T R + R\tilde{A} - RBP^{-1}B^T R + \tilde{Q} = 0$$

This particular form is used since we are interested in a terminal time

at infinity where $\dot{R}$ is zero. Several methods of solving for R are available, but the most convenient way is to integrate backward in time from the terminal condition $R(\infty) = 0$, until R is constant to within some limit. The optimal feedback matrix K^T is found and we rewrite the system as a white-noise-disturbed regulator:

$$\dot{x} = (A - BK^T)\, x + Cu$$

This description of the system is that of which we will analyze the ride quality according to the pattern of the previous chapters.

This entire process was programmed in APL because of that language's ability to handle matrices with ease. The reader will find in Appendix E the source codes for the entire routine as it was programmed for this problem, along with the appropriate logic flow diagram of the overall solution technique. The entire routine required several cost function variations before an optimal control form was discovered, but the cost of solving this problem was less than that for the passive suspension owing to the greater efficiency of this technique. The initial values of the weighting factors was found by exactly the same means as that described in the previous chapter: the inverse square magnitude of the maximum permissible value.

THE OPTIMAL CONTROLLER AND VARIATIONS

After several trials, the set of weighting parameters which produced the best results were the inverse magnitudes squared of the following maximum permissible values

$$\ddot{z} = 0.01g$$

$$\theta'' = \infty$$

$$h_{\text{TE Gap}} = 0.33 \text{ in.}$$

$h_{LE\ Gap} = 0.33$ in.

$\Delta\delta_{w_1} = \infty$

$\Delta\delta_{w_2} = \infty$

It is interesting to note that there was no weighting necessary upon the control surfaces or the pitching accelerations. The control deflection terms were free because the gap control had an influence upon how large the control deflections were and would not permit large deflections which result in large gap variations. The controller would not permit high pitching accelerations because over the ninety feet from c.g. to the tail these would necessarily mean substantial gap variations.

In Table I are listed the values of the feedback gain matrix. None of the values are so large as to be unwieldy; in fact, most are quite small. The controller's response to a guideway pitch change of + 10° is to add in a $\Delta\delta_{w_2}$ of + 11.6° and a $\Delta\delta_{w_1}$ of - 28.3° (-14.8 inches at the winglet tip). The pitch control to such a situation is moderate and nearly exactly tracking the guideway. The heave control seems to be leading the approaching grade by beginning to lift the vehicle earlier and spreading out the upward acceleration over a longer period of time. On the other hand, if the vehicle were to have a one foot per second rise rate, the controller would move the winglet tips down by 0.1 inch and pitch the winglets nose up by 0.015° which corresponds to dropping the trailing edges by 0.29 inch and raising the leading edges by 0.19 inch

in an effort to induce a negative moment to pitch the body nose down and check the vertical rise. This second set of motions seems small by comparison to the response to attitude changes and one might guess that ignoring the rate inputs, while deteriorating performance, might still produce an acceptable vehicle. This possibility and the results of doing it are discussed later.

EIGENVALUES AND EIGENVECTORS

We now begin the system evaluation of the actively controlled vehicle and proceed in the usual fashion. This configuration may serve as a standard against which any other type of suspension may be compared, since for the given set of weighting parameters, this is the optimal solution. Table I displays the eigenvalues and eigenvectors for the three cases. Once again, as compared to the rigid vehicle, the actively controlled vehicle shows a distinctly improved performance. The natural frequencies are considerably lower and the damping ratio for both modes is around 0.7. This damping is somewhat better than the passive suspension, and much greater than the rigid case.

The eigenvectors show that the low frequency $\frac{\theta}{\bar{h}}$ mode ratio is altered similarly to the passive so that this mode is primarily pitch in nature and contains considerably less heave content than the rigid case. The high frequency $\frac{\bar{h}}{\theta}$ mode ratio is almost unaltered from the rigid case. Whereas the passive case high frequency mode is all heave, the active case contains a small amount of pitch, but this is still so small that the high frequency mode, as in the rigid case, may be considered nearly all heave. Figure 1 shows a typical time domain response of the active

TABLE 1

EIGENVALUES AND EIGENVECTORS OF ACTIVE SYSTEM

Eigenvalues	Eigenvectors
-8	High Frequency:
-5.5	$\begin{bmatrix} \bar{h}_r' \\ \theta_r' \\ \bar{h}_r \\ \theta_r \end{bmatrix}$ $\begin{bmatrix} 7.48\, e^{i\,214^\circ} \\ 2.36\, e^{i\,126^\circ} \\ 3.65\, e^{i\,79.9^\circ} \\ 1\ \ e^{i0^\circ} \end{bmatrix}$
0	
.976 + i 1.014	
.976 - i 1.014	
.408 + i .412	
.408 - i .412	

Low Frequency:

$\begin{bmatrix} \bar{h}_r' \\ \theta_r' \\ \bar{h}_r \\ \theta_r \end{bmatrix}$ $\begin{bmatrix} .0712\, e^{i\,129^\circ} \\ .844\ e^{i\,133^\circ} \\ .0844\, e^{i\,-3.84^\circ} \\ 1\ \ e^{i0^\circ} \end{bmatrix}$

The following are the feedback gains for the controller:

	$\Delta\delta_{w_1}$	$\Delta\delta_{w_2}$	Units
$\Delta\bar{h}_r'$	- .00474	.000266	$\frac{\text{rad}}{\text{fps}}$
$\Delta\theta_r'$	.338	- .0319	$\frac{\text{rad}}{\text{rad/sec}}$
$\Delta\bar{h}_r$	-.565	.000847	$\frac{\text{rad}}{\text{ft}}$
$\Delta\theta_r$	4.52	- 1.16	$\frac{\text{rad}}{\text{rad}}$
$\Delta\bar{h}_g'$	.00474	.0584	$\frac{\text{rad}}{\text{fps}}$
$\Delta\theta_g'$	.0885	-.00477	$\frac{\text{rad}}{\text{rad/sec}}$
$\Delta\theta_g$	1.69	.000266	$\frac{\text{rad}}{\text{rad}}$

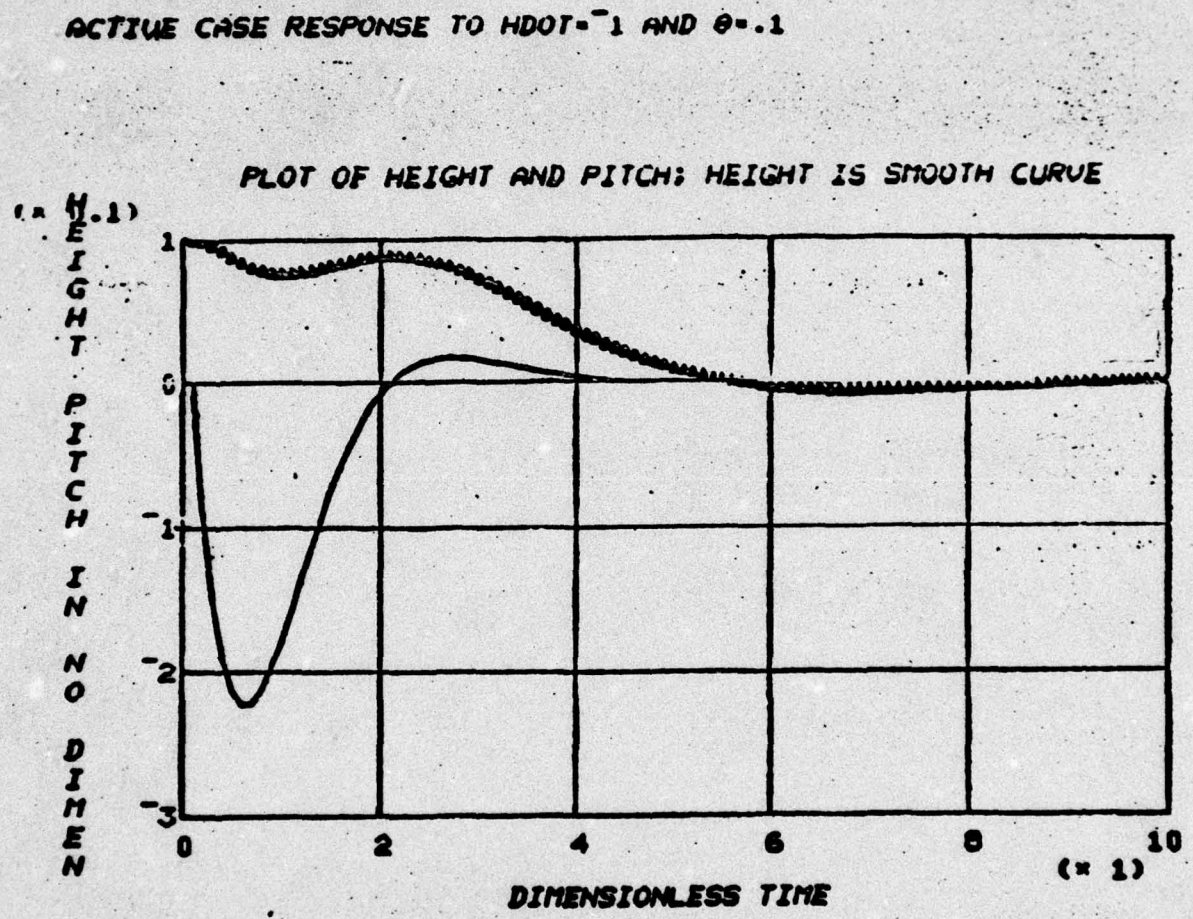

Figure 1. Transient Response of Actively Suspended Vehicle.

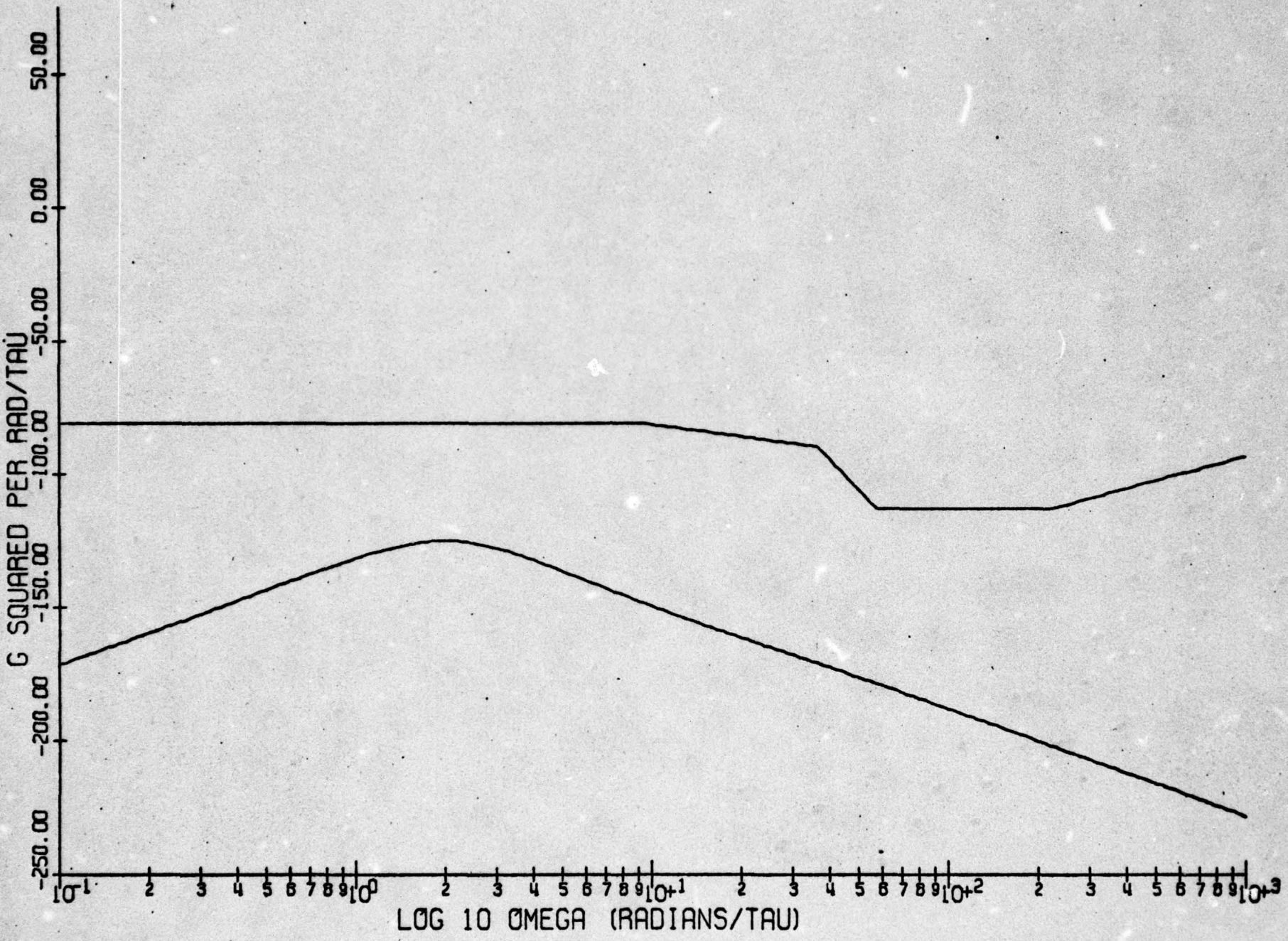

Figure 2. Active Suspension Acceleration Spectral Density at .40c.

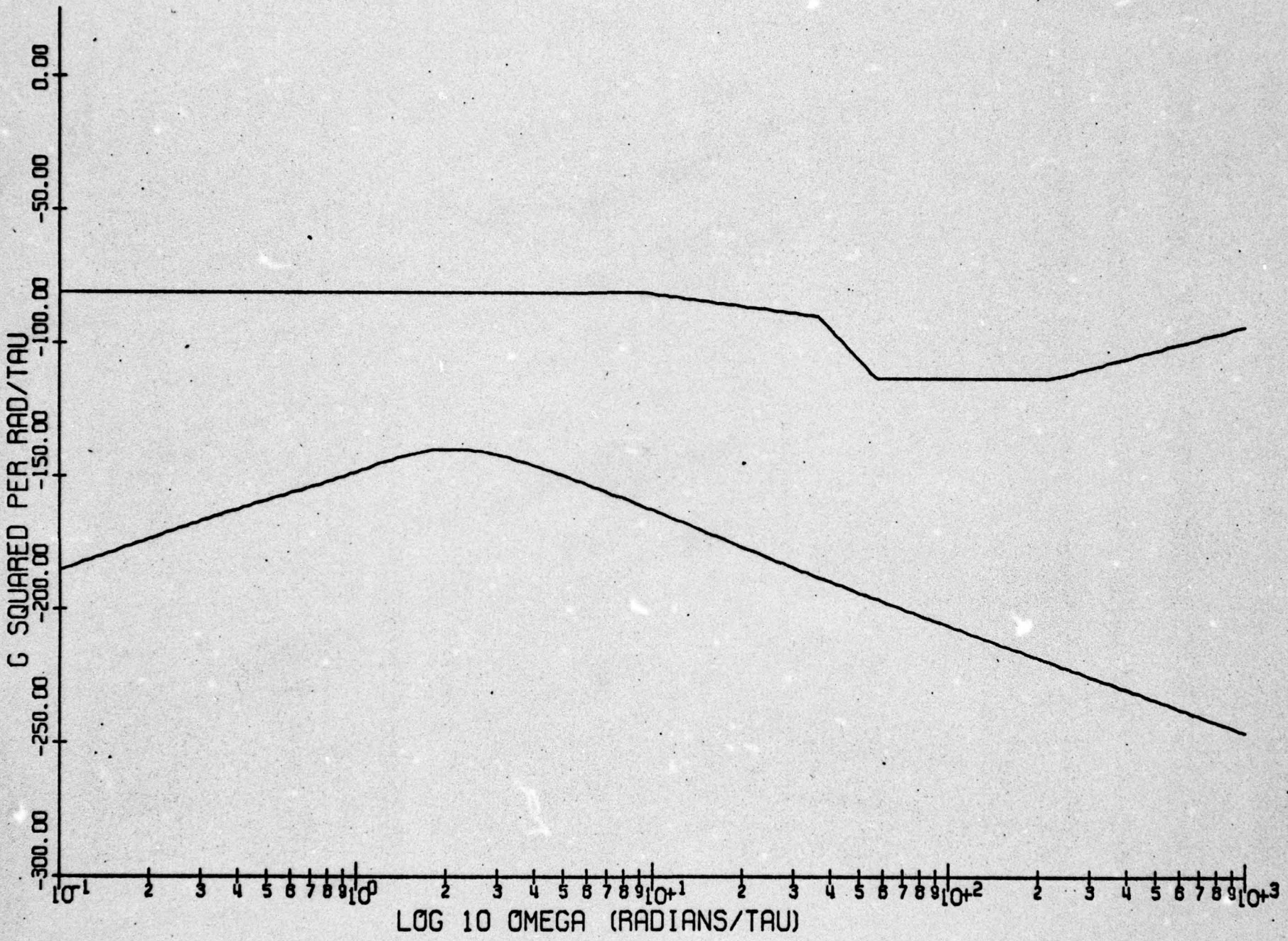

Figure 3. Active Suspension Acceleration Spectral Density at .90c.

case, in which the virtual separation of the modes (decoupling $\bar{h}$ and θ) can be seen.

ACCELERATION SPECTRAL DENSITY

In Figures 2 and 3 are shown the acceleration spectral densities of the .40c and .90c positions in the vehicle. The curves show a very smooth transition from low to high frequencies and agreement with the specification at all frequencies with room to spare. There are no sharp peaks or valleys, only a very gentle rounded peak indicating the combined effect of the two modes. When compared against the corresponding figures of the other two cases, the active case proves to have the lowest vertical acceleration at any given frequency, as one might expect. Once again the reader's attention is called to the vertical axis labelling, which is $20 \log_{10} \left| \frac{g^2}{\text{rad}/\tau} \right|$ format. The conversion to hertz is 9.15 rad/τ = 1 Hz.

RMS ACCELERATION, GAP VARIATION, AND CONTROL DEFLECTION

The accelerations at the c.g. are greatly improved over the rigid vehicle (0.121g) and somewhat better than the passive suspension (0.0071g) having a rms value of 0.00212g. This could be considered a very smooth and comfortable ride. The rearmost seat proved even smoother, being on the order of 0.001g. The seats in between will have values ranging between these two, so that the overall level of vertical accelerations is very low indeed.

The rms gap variation is on the order of one-third inch, that being the criterion against which the cost function was altered. There is a tradeoff between gap variation and accelerations, and the cost function

was adjusted until this level of gap variation was met but not exceeded. Hence the values of 0.218 inch at the leading edge and 0.327 at the trailing edge are not so much a result as they are a design condition for the active controller. These values mean that the steady-state gap is more than three standard deviations out on the normal distribution, implying that contact is rare. As with the passive suspension, there is a reversal from the rigid case in the relative size of leading and trailing edge gap variation.

The typical winglet motions are slightly larger for the active controller; the rms $\Delta\delta_{w_1}$ is 0.025 rad. which corresponds to 0.75 inch at the tip, and rms $\Delta\delta_{w_2}$ is 0.00055 rad. corresponding to a trailing edge gap variation of 0.594 inch. These are both significant motions with regard to the size of the gap, but they are small enough on the vehicle level to imply that the power required for the winglets is likely to be relatively small as compared to total vehicle energy consumption. The seemingly small feedback gains yield a fairly tight, or fast-responding, control system, resulting in a smooth ride for the passenger. As with the passive case, the dominant mode of winglet motion is as a guideway follower so that both gap and vehicle height remain nearly constant. With the active controller, however, there seems an additional leading of the guideway by the vehicle which tends to spread the accelerations over a longer time period, helping to smooth out the ride in a way that the passive suspension could not do.

THE "PARTIALLY BLIND" CONTROLLER

In the process of designing for cost, one might be led to ask, "Is there any way to reduce the number of sensors and feedback circuits and

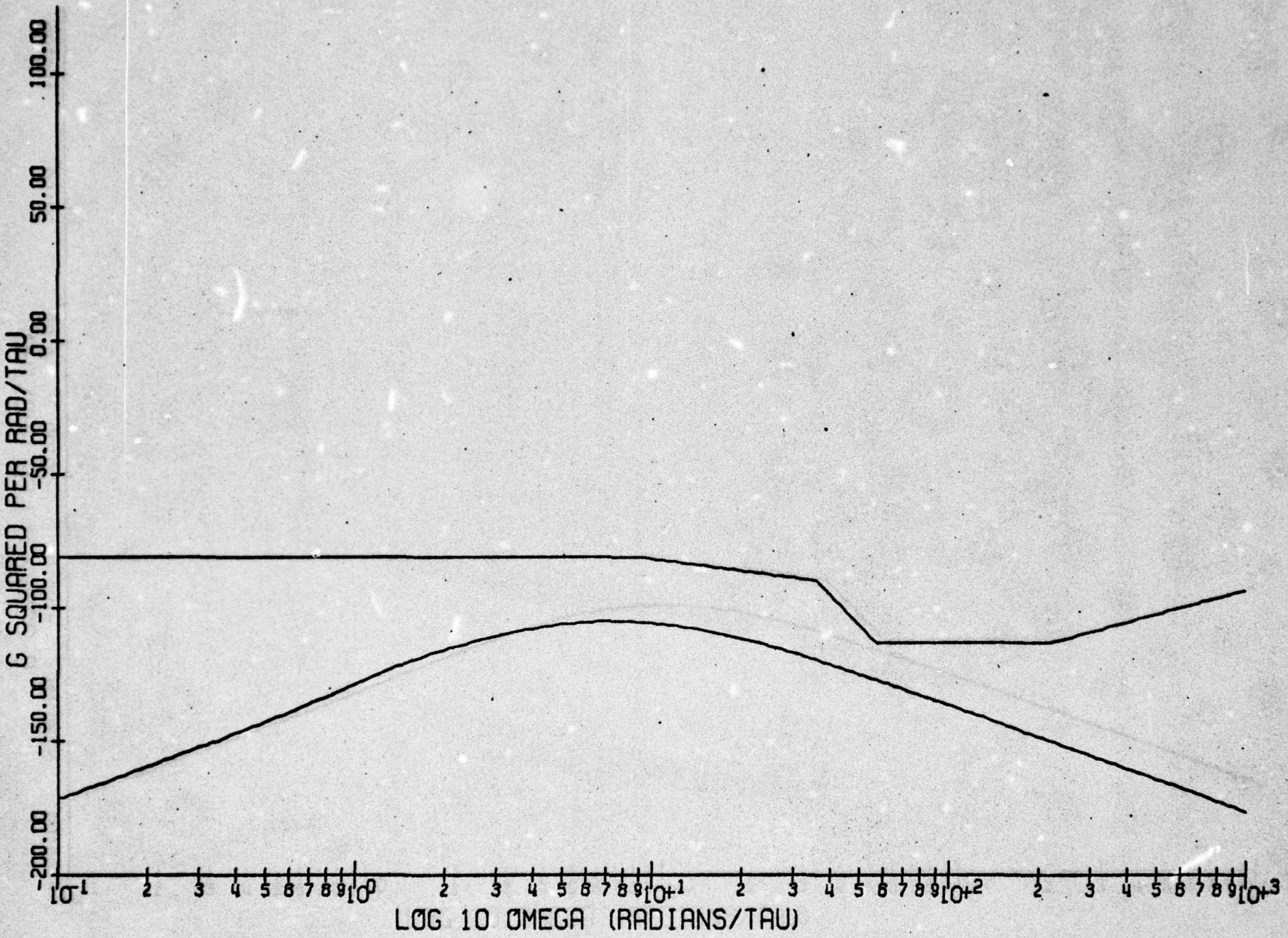

Figure 4. Partially Sensing Active Suspension Acceleration Spectral Density at .40c.

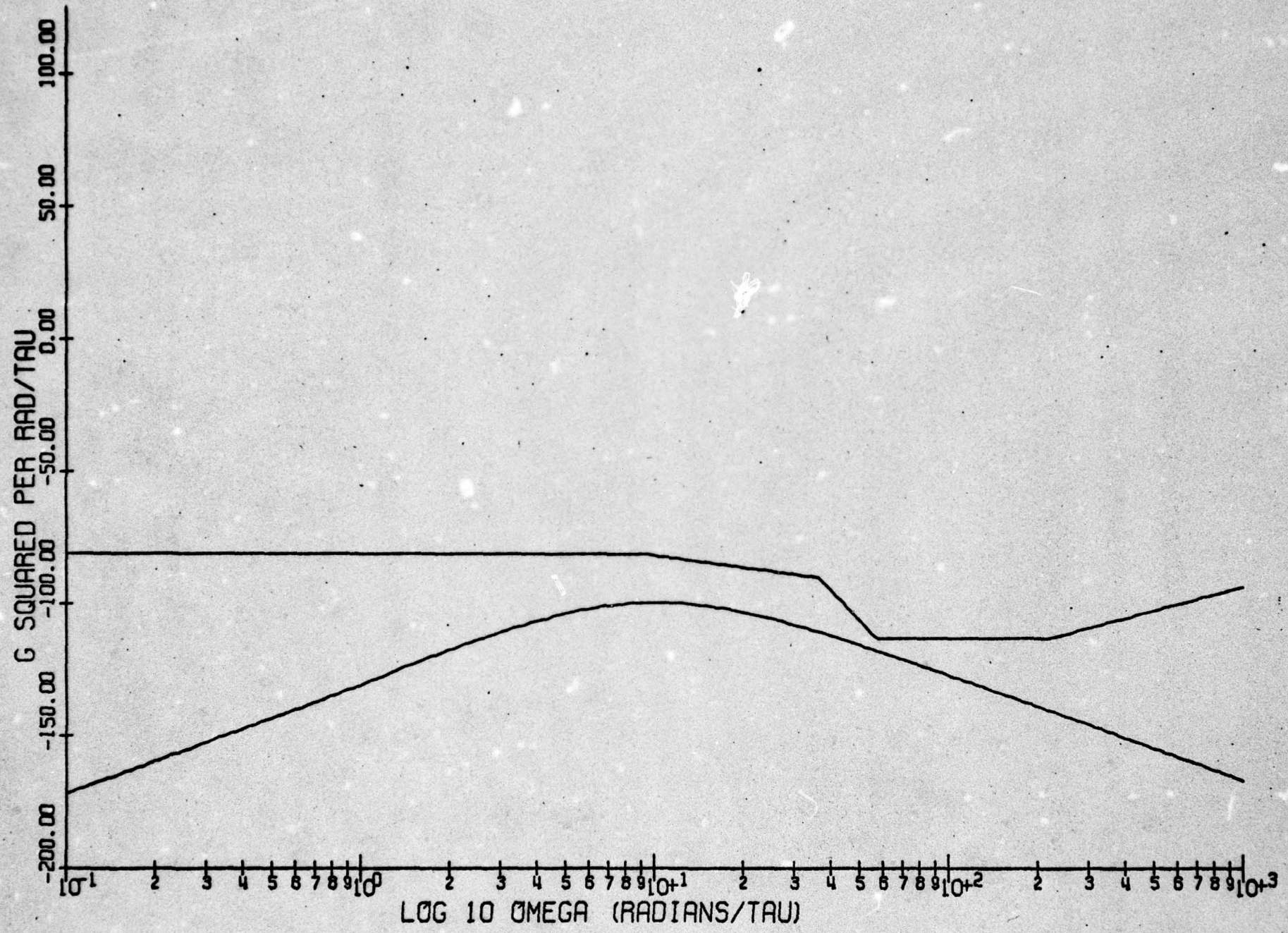

Figure 5. Partially Sensing Active Suspension Acceleration Spectral Density at .90c.

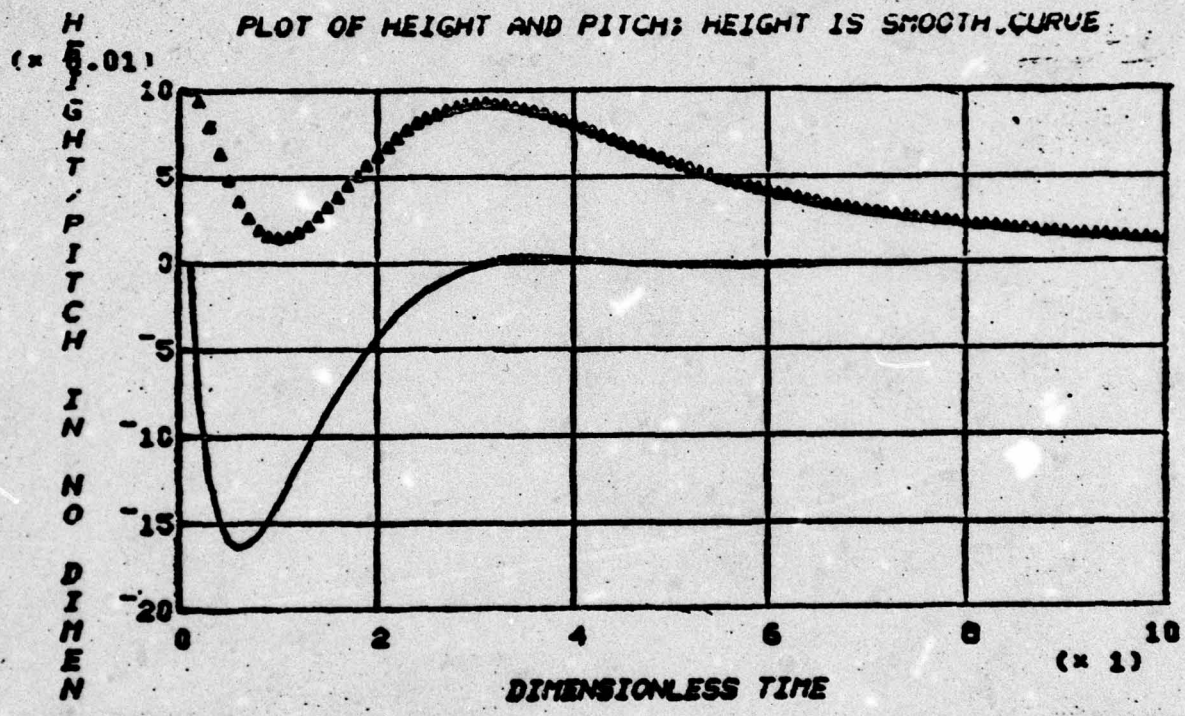

Figure 6. Transient Response of "Partially Blind" Vehicle.

still achieve reasonable performance?" The answer seems to be yes. By zeroing elements of the feedback matrix, one effectively shuts down sensors and "blinds" the controller to those inputs. Doing so and performing a ride quality analysis yields interesting results. Eliminating all sensing of the guideway motions with respect to the earth (the last three states) produces no noticeable change in vehicle performance. With only vehicle velocities and relative displacements, the performance is almost exactly the same as full sensing, the difference being less than one percent by any measure. It seems that these three of the seven sensors may be eliminated out of hand.

The feedback of relative displacements is crucial to performance and provides most of the improvement noted above. Eliminating the velocity feedbacks does degrade performance noticeably, but not so far as to be intolerable. With only the relative height and pitch displacement feedbacks, we find that the rms accelerations increase to 0.017g at the c.g. and 0.026g at .90c. While these are not exactly considered a smooth ride, they are quite tolerable. The respective spectral densities are shown in Figures 4 and 5. Figure 6 shows the time response of this system to the same set of initial conditions as used before and one may see from this plot that some of the pitch damping is gone, but that the overall response is similar. The indication is that attitude feedback is most critical, while rate feedback fine tunes the response and adds some degree of smoothness. Guideway position and rate feedback is unnecessary.

Overall, the active control does an extremely effective job of smoothing

out the ride and maintaining a reasonable gap clearance. The acceleration levels are somewhat improved over the passive suspension, though there might be reasonable doubt that the improvement is worth the extra cost of the active system over the passive. The active controller does, however, yield accelerations of the order of 0.002g or less (depending on position inside the passenger compartment), requires very small control deflections and hence small control power, and allows us to virtually select what levels of gap variation the vehicle should have. The feedbacks are quite small and therefore easily realized. In addition, even if the active system is not to be realized, it does provide some insight to the limits of vehicle performance. It seems that, as a result of this analysis, the performance of the TRACV at its best seems to be very promising indeed.

CHAPTER VI

CONCLUSION

In examining the Tracked Ram Air Cushion Vehicle, one finds himself confronted with a high degree of heave-pitch coupling. This strong coupling means that for longitudinal studies, one cannot ignore one when studying the other. In addition, any control system or suspension must be able to avoid this coupling as well as changing the frequency and damping of the dominant modes. Using this criterion for a choice in suspension methods will lead toward the ability to positively control ride quality.

Since the TRACV is intended as high-speed ground transportation for passengers, the ride quality of the passenger compartment in terms of noise and accelerations is of paramount importance. The vertical accelerations experienced in the passenger compartment are the subject of this study; the test subjects are the basic vehicle and two types of vehicle control (passive element and active) using two-degrees-of-freedom winglets. The ride quality of these three configurations over a surface having the roughness of smooth highway is the design criterion and the outcome is briefly described below.

CONCLUSIONS

Using a linear, unconstrained model of the vehicle dynamics, the following conclusions may be drawn about TRACV performance:

1. The basic vehicle with no control surfaces is unacceptable. In almost all positions in the passenger compartment, the

TABLE 1

SUSPENSIONS COMPARISON

	Rigid Vehicle	Passive Suspensions	Active Suspensions
RMS Accel. at .4c (g)	0.121	0.0072	0.00212
RMS Accel. at .9c (g)	0.0055	0.0091	0.00092
RMS L.E. Gap Variation (in.)	14.7	0.143	0.218
RMS T.E. Gap Variation (in.)	6.07	0.224	0.327
RMS $\Delta\delta_{w_1}$ (rad.)	--	0.0154	0.025
RMS $\Delta\delta_{w_2}$ (rad.)	--	0.00053	0.00055
High Frequency Mode (Hz)	1.47	0.324	0.224
Low Frequency Mode (Hz)	0.962	0.036	0.134
High Frequency Damping	0.226	0.475	0.692
Low Frequency Damping	0.078	0.337	0.704

acceleration spectral density exceeds the UTACV standard in the 1 - 2 Hz range. In addition, potentially destructive winglet-guideway contact frequently occurs.

2. A two-degree-of-freedom winglet suspended by springs and dampers smooths out most of the accelerations of the rigid vehicle. Guideway contact is rare, the accelerations meet the specifications, and the modes of motion are almost completely decoupled in addition to the lowering of vehicle natural frequencies and increasing damping by allowing the winglets to become guideway followers.
3. The active control of the two-degree-of-freedom winglets further improves the performance. The accelerations reach a level approaching the threshold of sensitivity while not requiring large amounts of power to do so. This configuration, however, gives only moderate performance improvement over the passive suspension (which is quite acceptable) in return for substantial construction and maintenance cost increases.
4. If the active controller is to be used, the sensing of the guideway motions is irrelevant to ride quality. Rate sensing, while not strictly necessary, does give substantial improvement at levels where improvement is needed.

DIRECTIONS FOR FURTHER INVESTIGATION

One point of this study subject to question is the guideway approximation.

The average of guideway pitch and height is a fine descriptor for wavelengths much smaller or much larger than the length of the vehicle. In the transition region near where the length of the vehicle is about one-half the guideway wavelength, the effects not accounted for in the second order linear approximation may be of importance, particularly with regard to the effect on moment forces of such a bump as it traverses the length of the vehicle; these bear further study.

Different schemes for control also seem to be a likely prospect for study. Mechanization of a two-degree-of-freedom winglet may be no small task, and there might be alternatives. One such possibility is pitch control by way of a trailing edge flap. This possibility requires study of the dynamics of a two-segment bottom slope. Another possibility is that given the pitch control, $\Delta\delta_{w_2}$, is very small, allowing the winglet only $\Delta\delta_{w_1}$ freedom and warping the winglet to obtain $\Delta\delta_{w_2}$ effects may be a distinct possibility. This prospect, however, requires close study of stress and fatigue factors.

Finally, vehicle dimensions will play a strong role in the dynamics. A vehicle fifty feet long is as likely as one one hundred fifty feet long. Top surface lift will have an effect on moment equations. The flat, sloping bottom surface is an important part of the present model as well as aspect ratio and weight. Since all of these factors will significantly affect the dynamics, it is important that a practicable vehicle be laid out before any further detailed work on longitudinal ride quality is undertaken.

LIST OF REFERENCES

1. Aidala, P. V.: "Lateral Stability of a Ram Air Cushion Vehicle", MIT Report No. FRA-ORD&D-75-6, August 1974.

2. Barrows, T. M.: "Ram Air Cushion Advanced Fluid Suspension for Tracked Levitated Vehicles", Trans. ASME Paper No. 73-ICT-14.

3. Barrows, T. M., and S. E. Widnall: "The Aerodynamics of Ram Wing Vehicles for Application to High Speed Ground Transportation", AIAA Paper No. 70-142, Meeting January 19-21, 1970.

4. Bryson, A. E., Jr., and Yu-Chi Ho: APPLIED OPTIMAL CONTROL, McGraw-Hill Publishing Company, New York, 1967.

5. Curtiss, H. C. Jr., and W. F. Putman: "Experimental Investigation of Aerodynamic Characteristics of a Tracked Ram Air Cushion Vehicle", Princeton University AMS Report 1318 and DOT Report in preparation, 1977.

6. Fraize, W. E., and T. M. Barrows: "The Tracked Ram Air Cusion Vehicle (TRACV): A System Definition Study", Mitre Corporation Report No. MTR-6554, November 1973.

7. Hedrick, J. K., G. F. Billington, and D. A. Dreesbach: "Analysis, Design and Optimization of High Speed Vehicle Suspensions Using State Variable Techniques", TRANS. ASME Paper No. 74-Aut.-K, January 3, 1974.

8. Kuester, J. L., and J. Mize: OPTIMIZATION TECHNIQUES WITH FORTRAN, McGraw-Hill Publishing Company, New York, 1973.

9. Newland, D. G.: RANDOM VIBRATIONS AND SPECTRAL ANALYSIS, Longman, New York, 1975.

10. Newton, G. C., L. A. Gould, and J. F. Kaiser: ANALYTICAL DESIGN OF LINEAR FEEDBACK CONTROLS, Wiley Publishing Company, New York, 1957.

11. Anon: Performance Specification and Engineering Design Requirements for the UTACV, DOT Specification, 1972.

12. Riblich, W. A., K. M. Captain, and H. H. Richardson: "An Analysis of the Effects of Finite Fluid-Suspension Pad Length on the Dynamics of a Vehicle on an Irregular Guideway", MIT Engineering Projects Laboratory Report No. DSR-76110-6, September 1967.

13. Schultz, D. G., and J. L. Melsa: STATE FUNCTIONS AND LINEAR CONTROL SYSTEMS, McGraw-Hill Publishing Company, New York, 1967.

APPENDIX A

EQUATIONS OF MOTION

The model of the TRACV used in this thesis is a two-degree-of-freedom aerodynamic mode with freedom in heave and pitch. It assumes that the lateral and longitudinal aspects may be considered separately, and the present concern is on longitudinal motions only. Other assumptions include constant forward velocity, constant mass, and fixed center of gravity. The lift and moment may be described by Taylor series:

$$L = L_o + \frac{\partial L}{\partial \dot{\bar{h}}} \Delta\dot{\bar{h}} + \frac{\partial L}{\partial q} \Delta q + \frac{\partial L}{\partial \bar{h}} \Delta\bar{h} + \frac{\partial L}{\partial \theta} \Delta\theta + (\text{higher-order terms})$$

$$M = M_o + \frac{\partial M}{\partial \dot{\bar{h}}} \Delta\dot{\bar{h}} + \frac{\partial M}{\partial q} \Delta q + \frac{\partial M}{\partial \bar{h}} \Delta\bar{h} + \frac{\partial L}{\partial \theta} \Delta\theta + (\text{higher-order terms})$$

This expression of the lift and motion reflects the basic vehicle dynamics. Assuming small perturbations of the motion quantities only around some steady-state, the higher order terms may be neglected. In steady-state, $M = 0$, $L = mg$, and there are no perturbations, so we may write:

$$mg = L = L_o \qquad 0 = M = M_o$$

The sum of all the steady-state terms is zero and they may be dropped along with the higher-order terms. In addition, if the winglets are allowed to move, then the lift and moment have derivatives with respect to the control motions. In final form the equations are:

$$\Delta L = \frac{\partial L}{\partial \dot{\bar{h}}} \Delta\dot{\bar{h}} + \frac{\partial L}{\partial q} \Delta q + \frac{\partial L}{\partial \bar{h}} \Delta\bar{h} + \frac{\partial L}{\partial \theta} \Delta\theta + \frac{\partial L}{\partial \delta_{w_1}} \Delta\delta_{w_1} + \frac{\partial L}{\partial \delta_{w_2}} \Delta\delta_{w_2} \qquad \text{(A-1)}$$

$$\Delta M = \frac{\partial M}{\partial \dot{\bar{h}}} \Delta \dot{\bar{h}} + \frac{\partial M}{\partial q} \Delta q + \frac{\partial M}{\partial \bar{h}} \Delta \bar{h} + \frac{\partial M}{\partial \theta} \Delta \theta + \frac{\partial M}{\partial \delta_{w_1}} \Delta \delta_{w_1} + \frac{\partial M}{\partial \delta_{w_2}} \Delta \delta_{w_2} \qquad \text{(A-2)}$$

It should be noted that the motion variables above are all of the vehicle relative to the guideway.

Having expressed the change in lift and moment, we may now write relations concerning vehicle accelerations:

$$m\ddot{\bar{h}}_v = \Delta L$$

$$mc\ddot{\bar{h}}_v = \frac{1}{2} \rho U^2 S \Delta C_L$$

$$\frac{mc}{\frac{1}{2} \rho U^2 S} \ddot{\bar{h}}_v = \Delta C_L$$

$$\frac{c C_{L_o}}{g} \ddot{\bar{h}}_v = \Delta C_L \qquad \text{(A-3)}$$

The term $\frac{cC_L}{g}$ has the units sec^2 so that one convenient way to obsorb it is to change to non-dimensional time. Such a conversion is convenient in that if, during the scaling process, the term $\frac{c}{UA}$ is kept constant (A defined below), the dynamics will be unchanged except for frequency. We then write:

$$A = \sqrt{\frac{cC_L}{g}} \text{ seconds}$$

$$\tau = \frac{t}{A} \qquad \text{(A-4)}$$

In making this conversion, one must be careful that any time related terms be adjusted. All the time derivatives must be rewritten as is $\ddot{\bar{h}}$ below:

$$\ddot{\bar{h}} = \frac{d^2}{dt}\bar{h} = \frac{d^2}{d(A\tau)^2}\bar{h} = \frac{1}{A^2}\bar{h}''$$

and equation (A-3) can be rewritten:

$$\frac{cC_{L_o}}{g}\left(\frac{1}{A^2}\ddot{\bar{h}}\right) = A^2\left(\frac{1}{A^2}\bar{h}''\right) = \bar{h}'' = \Delta C_L$$

Remembering from Chapter II the relationships

$$\dot{\bar{h}} = \frac{c}{U}\dot{\bar{h}} \qquad\qquad q = \frac{c}{U}\dot{\theta}$$

we are able to express equation (A-1) in the following forms:

$$\bar{h}'' = \frac{c}{UA}C_{L_{\dot{\bar{h}}}}\Delta\bar{h}' + \frac{c}{UA}C_{L_q}\Delta\theta' + C_{L_{\bar{h}}}\Delta\bar{h} + C_{L_\theta}\Delta\theta$$

$$+ C_{L_{\delta_{w_1}}}\Delta\delta_{w_1} + C_{L_{\delta_{w_2}}}\Delta\delta_{w_2} \qquad \text{(A-5)}$$

The compact notation $C_{L_{\bar{h}}}$ means $\frac{\partial C_L}{\partial \bar{h}}$ and so on.

Following a similar argument yields a moment equation:

$$\theta_v'' = \frac{c}{UA}C_{M_{\dot{\bar{h}}}}\Delta\bar{h}' + \frac{c}{UA}C_{M_q}\Delta\theta' + C_{M_{\bar{h}}}\Delta\bar{h} + C_{M_\theta}\Delta\theta$$

$$+ C_{M_{\delta_{w_1}}}\Delta\delta_{w_1} + C_{M_{\delta_{w_2}}}\Delta\delta_{w_2}\Delta\delta_{w_2} \qquad \text{(A-6)}$$

In the development of (A-6) however, the term $\left(\frac{k_y}{c}\right)^2$ comes up, where k_y is the vehicle radius of gyration. We define $C_{M_{\bar{h}}}$ to be $\frac{c^2}{k_y^2}\frac{\partial C_M}{\partial \bar{h}}$ and so forth to absorb it. In the present model, k_y was taken to be the value of the gyration radius of a uniform rigid bar of vehicle proportions. Adding the two relationships $\bar{h}' = \frac{d}{d\tau}\bar{h}$ and $\theta' = \frac{d}{d\tau}\theta$ to (A-5) and (A-6)

gives us our fourth order pitch-heave model.

The steady-state lift coefficient is $C_{L_o} = .455$, a value found to be typical of those found in towed model tests at the Princeton University Dynamic Model Track. With an assumed forward velocity of 300 fps, the vehicle weight for equilibrium is 110,000 lbs., agreeing fairly closely with the Mitre vehicle (Fraize and Barrows, 1973). Also the present model implies A = 1.456 sec. It should be noted that this theory assumes no upper surface contributions to either lift or moment. In actuality, the shape described adds a $\Delta C_L \cong .25$, which will slightly alter moment characteristics and allow a heavier vehicle.

APPENDIX B

STABILITY DERIVATIVES

Presented below are the equations for the attitude stability derivatives as they were theoretically developed in (Curtiss and Putman; 1977). The rate derivatives are the result of a quasi-static theory developed by Professor H. C. Curtiss, Jr. of Princeton University, and are based on the under-vehicle pressure which assumes a level pitch attitude ($\theta = 0$) and incompressible flow. The effect of vehicle rates is as an increment to the lift and moment coefficients.

$$\frac{\partial C_L}{\partial \bar{h}} = \frac{-\bar{\alpha}^2}{\alpha_o} \frac{\partial C_L}{\partial \bar{\alpha}} + \frac{2c}{\alpha_o W} \frac{\partial C_L}{\partial r_o}$$

$$\frac{\partial C_L}{\partial \theta} = \frac{1}{\alpha_o} \{[\bar{\alpha} + \bar{\alpha}^2 (1 - \bar{x}_o)] \frac{\partial C_L}{\partial \bar{\alpha}} - r_o \frac{\partial C_L}{\partial r_o} - \frac{2c}{W} \frac{\partial C_L}{\partial r_1}\}$$

$$\frac{\partial C_M}{\partial \bar{h}} = \frac{-\bar{\alpha}^2}{\alpha_o} \frac{\partial C_M}{\partial \bar{\alpha}} + \frac{2c}{\alpha_o W} \frac{\partial C_M}{\partial r_o}$$

$$\frac{\partial C_M}{\partial \theta} = \frac{1}{\alpha_o} \{[\bar{\alpha} + \bar{\alpha}^2 (1 - \bar{x}_o)] \frac{\partial C_M}{\partial \bar{\alpha}} - r_o \frac{\partial C_M}{\partial r_o} - \frac{2c}{W} \frac{\partial C_M}{\partial r_1}\}$$

$$\frac{\partial C_L}{\partial \dot{h}} = \frac{2Wc}{A_E \bar{\alpha}^2} [\ln \frac{1}{1 + \bar{\alpha}} + \frac{\bar{\alpha}}{1 + \bar{\alpha}}]$$

$$\frac{\partial C_L}{\partial q} = \frac{-Wc}{A_E \bar{\alpha}^2} [2 (1 + \frac{1}{\bar{\alpha}} - \bar{x}_o)(\ln \frac{1}{1 + \bar{\alpha}} + \frac{\bar{\alpha}}{\bar{\alpha} + 1}) + \frac{\bar{\alpha}}{1 + \bar{\alpha}}]$$

$$\frac{\partial C_M}{\partial \dot{\bar{h}}} = \left(\bar{x}_o - \frac{\bar{\alpha} + 1}{\bar{\alpha}}\right) \frac{\partial C_L}{\partial \dot{\bar{h}}} - \frac{2Wc}{A_E \bar{\alpha}^3} \left(\bar{\alpha} + \ell n \frac{1}{1 + \bar{\alpha}}\right)$$

$$\frac{\partial C_M}{\partial q} = \left(\bar{x}_o - \frac{\bar{\alpha} + 1}{\bar{\alpha}}\right) \frac{\partial C_L}{\partial q} + \frac{Wc}{A_E \bar{\alpha}^3} \left[2 \left(1 + \frac{1}{\bar{\alpha}} - \bar{x}_o\right)\left(\bar{\alpha} + \ell n \frac{1}{1 + \bar{\alpha}}\right)\right.$$

$$\left. - \frac{1}{\bar{\alpha}} \left\{\frac{1}{2} \left([1 + \bar{\alpha}]^2 - 1\right) + \ell n \frac{1}{1 + \bar{\alpha}}\right\}\right]$$

The various partial derivatives with respect to the ratio parameters may be found in the cited reference and were computed by the FORTRAN program at the end of this Appendix.

To find the derivatives of lift and moment derivatives with respect to the control surface deflections, we express them as effects on the dimensionless parameters. We find that δ_{w_1} affects only r_o, and δ_{w_2} affects only r_1. Figure B-1 illustrates a perturbed winglet proximate to a guide-way lip. Examination of this geometry shows that, assuming a guideway lip cant of forty-five degrees and anominally level winglet, on can write

$$\Delta\delta_o = .707\ W_w \cdot \Delta\delta_{w_1}$$

and, incorporating the definition of r_o, one can express the lift coefficient and moment coefficient derivatives as follows:

$$\frac{\partial C_L}{\partial \delta_{w_1}} = \frac{\partial C_L}{\partial r_o} \cdot \frac{\partial r_o}{\partial \delta_{w_1}} = \frac{\partial C_L}{\partial r_o} \cdot \frac{.707\ W_w}{W\ \alpha}$$

$$\frac{\partial C_M}{\partial \delta_{w_1}} = \frac{\partial C_M}{\partial r_o} \cdot \frac{\partial r_o}{\partial \delta_{w_1}} = \frac{\partial C_M}{\partial r_o} \cdot \frac{.707\ W_w}{W\ \alpha}$$

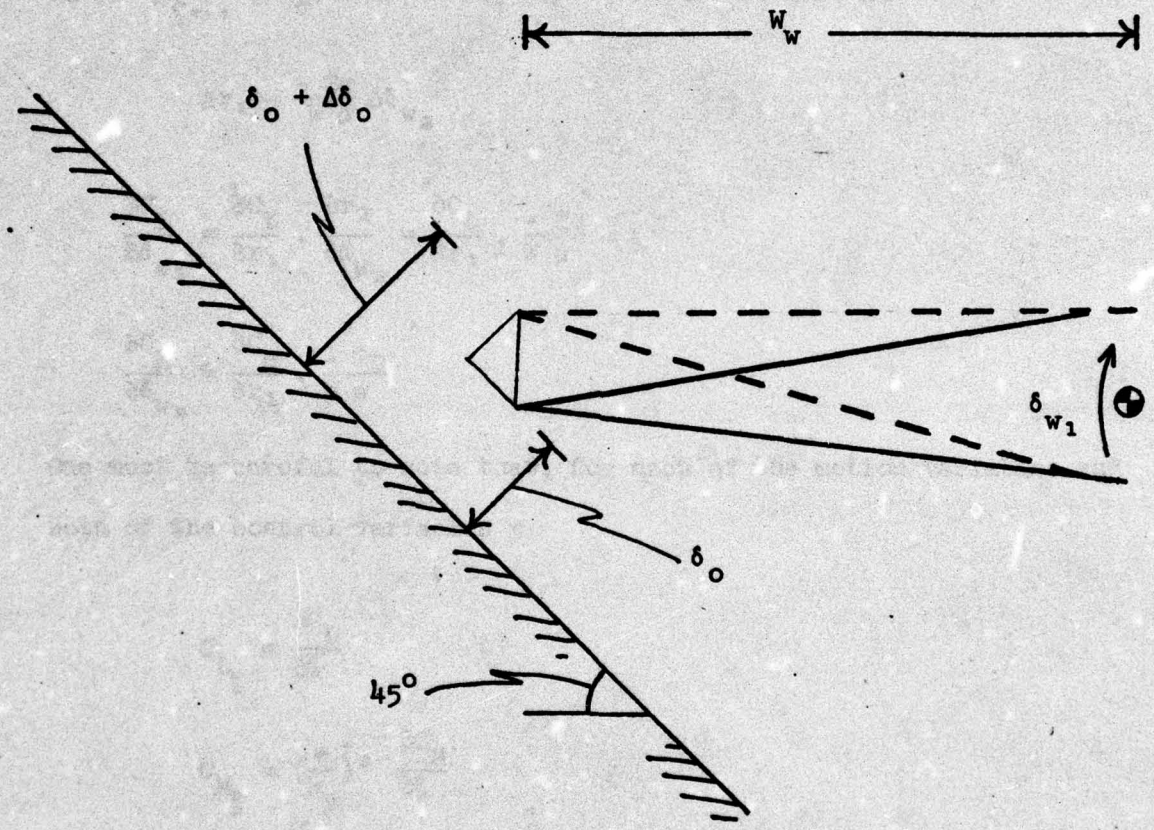

Figure B-1. Geometry of the Perturbed Winglet.

Assuming that the center of rotation for δ_{w_2} is at the c.g., δ_{w_2} affects only r_1. Violating this assumption forces us to include the relationship

$$\Delta r_o = \frac{2c}{W\alpha} (\bar{x}_{c.r.} - \bar{x}_o) \Delta\delta_{w_2}$$

but if $\bar{x}_{c.r.} = \bar{x}_o$, then we may ignore it and we can write

$$\Delta r_1 = \frac{-2c}{W\alpha} \Delta\delta_{w_2}$$

$$\frac{\partial C_L}{\partial \delta_{w_2}} = \frac{\partial C_L}{\partial r_1} \cdot \frac{\partial r_1}{\partial \delta_{w_2}} = \frac{\partial C_L}{\partial r_1} \cdot \frac{-2c}{W\alpha}$$

$$\frac{\partial C_M}{\partial \delta_{w_2}} = \frac{\partial C_M}{\partial r_1} \cdot \frac{-2c}{W\alpha}$$

One must be careful to note that, for each of the motion variables and both of the control variables

$$C_{L_{\bar{\xi}}} = \frac{\partial C_L}{\partial \bar{\xi}}$$

$$C_{M_{\bar{\xi}}} = \left(\frac{c}{k_y}\right)^2 \frac{\partial C_M}{\partial \bar{\xi}}$$

```
    $JCE          B5704.DOTTRAIN,TIME=59,PAGES=260,C=0
ARNING**  MIS-PUNCHED JOB OPTION. C=0    IS INVALID
      C
      C        THIS PROGRAM CALCULATES THE CHARACTERISTICS OF A RAM-AIR
      C     CUSHION VEHICLE BY DETERMINING THE CHARACTERISTIC EQUATION
      C     COEFFICIENTS, THE ROOTS, AND THE STABILITY DERIVITIVES.
      C     THESE ARE CALAULATED ON FOUR INPUT CARDS.
      C        THE FIRST CARD SHOULD BE INITIAL PITCH ANGLE AND INITIAL
      C     R SUB ZERO IN 2F10.5 FORMAT.  THE SECOND CARD SHOULD BE CHORD AND
      C     WIDTH IN 2F10.5 FORMAT.  THE THIRD CARD SHOULD BE BOTTOM SLOPE AND
      C     ALPHA BAR.
      C        ALL ANGLES ARE IN RADIANS, DISTANCES IN FEET AND TIME IN SECONDS
      C        IT IS POSSIBLE TO ITERATE MORE THAN CG POSITION.  THIS IS DONE
      C     BY PLACING VALUES FOR FLAG,LIMIT, AND STEPSIZE ON THE FOURTH INPUT
      C     CARD IN I1,F10.5,F10.5 FORMAT.  THESE SHOULD BE INPUT AS ZEROES
      C     IF NO ITERATION IS DESIRED.   CODES FOR THE FLAG ARE:
      C                "1" = ALPHA BAR
      C                "2" = BOTTOM SLOPE
      C                "3" = CHORD
      C                "4" = INITIAL PITCH ANGLE
      C                "5" =R SUB ZERO
      C                "6" = WIDTH
      C     INITIAL VALUE FOR THE ITERATION IS THE VALUE IN THE RESPECTIVE OF THE
      C     FIRST THREE CARDS.  FINAL VALUE IS SET BY  THE LIMIT VALUE.  THIS
      C     ITERATIVE PROCEDURE STEPS ONLY UPWARD.
      C
      C     THIS SEGMENT GIVES THE STABILITY DERIVATIVES AND THE CHAR. EQN.
      C        "TA" MEANS THETA (PITCH ANGLE)
      C        "BOTTOM" MEANS ALPHA SUB ZERO
      C     EXCEPT IN "BOTTOM", ANY "C" CHARACTERS ARE ZEROES.
      C     INPUT DATA ARE:   CHORD (FEET),  THETA0 (RADIANS),
      C                       WIDTH (FEET),  RC, BOTTOM,
      C                       ALFBAR,        X0.
      C
  1           IMPLICIT REAL*8 (A-H,O-$)
  2           EXTERNAL F1,F2
  3           COMPLEX*16 ROOT1,ROOT2,CDSQRT,ROOTA,ROOTB,ROOTC,ROOTD
  4           REAL LIMIT
  5           INTEGER FLAG
  6           REAL RC,K,THETA0,BOTTOM
  7           ALOG(X)=DLOG(X)
  8           ATAN(X)=DATAN(X)
  9           SQRT(X)=DSQRT(X)
 10           READ(5,150)C,W
 11           READ(5,150)BOTTOM,ALFBAR
 12    150    FORMAT(2F10.5)
 13           READ(5,151)FLAG,LIMIT,STPSIZ
 14    151    FORMAT(I1,F10.5,F10.5)
 15           THETA0=0
 16           HTE=3.
 17           DELC=HTE-2.916
 18           ALFBAR=C/HTE*(THETA0+BOTTOM)
 19           RC=2*DELO/(W*(THETA0+BOTTOM))
 20           R1=-2*C*THETA0/(W*(THETA0+BOTTOM))
 21           ALFCFG=ALFBAR
 22           BOTCFG=BOTTOM
 23           WCFG=W
 24           CCFG=C
 25           RCCFG=RC
 26           THECFG=THETA0
```

```
27          ELAMDA=SQRT((1.0+ALFBAR)**2-1.0)
28          F2L=-2.0*ELAMDA/SQRT(ELAMDA**2+1.0)
           1+ATAN(ELAMDA)/SQRT(ELAMDA**2+1.0)
           2 +ALOG(ELAMDA+SQRT(ELAMDA**2+1.0))
29          F3L=ELAMDA-2.0*ATAN(ELAMDA)+ALOG(ELAMDA+SQRT(ELAMDA**2+1.0))
           1    /SQRT(ELAMDA**2+1.0)
30          F2M=ELAMDA-ATAN(ELAMDA)-ENTGRL(0.0D00,ELAMDA,F1,.001D00)
31          F3M=ELAMDA*SQRT(ELAMDA**2+1.0)*.5
           1 -.5*ALOG(ELAMDA+SQRT(ELAMDA**2+1.0))
           2 -ENTGRL(0.0D00,ELAMDA,F2,.001D00)
32          EL2=2.0*F2L/ALFBAR
33          EL3=(F3L-2.0*F2L)/ALFBAR**2
34          EM2=2.0*F2M/ALFBAR**2
35          EM3=(F3M-2.0*F2M)/ALFBAR**3
36          DLDA=(1.0+ALFBAR)*((1.0+ALFBAR)**2-1.0)**(-.5)
37          F2L1=(1./SQRT(ELAMDA*ELAMDA+1.)*(-2.0)+ELAMDA*ELAMDA*2.0
           1*(ELAMDA*ELAMDA+1.)**(-1.5))*DLDA
38          F2L2=(1.0/(ELAMDA*ELAMDA+1.)**.5*1.0/(ELAMDA*ELAMDA+1.0)+
           1 ATAN(ELAMDA)*(-1.0)*(ELAMDA**2+1.0)**(-1.5)*ELAMDA)*DLDA
39          F2L3=((1.0+ELAMDA*(ELAMDA**2+1.0)**(- .5))/(ELAMDA+(ELAMDA**2+1.0)
           1    **(.5)))*DLDA
40          DF2L=F2L1+F2L2+F2L3
41          F3L1=1.0*DLDA
42          F3L2=-2.0/(ELAMDA**2+1.0)*DLDA
43          F3L3=(1.0/(ELAMDA**2+1.0)**(.5)*(1.0+ELAMDA*(ELAMDA**2+1.0)
           1  **(-.5))/(ELAMDA+(ELAMDA**2+1.0)**(.5))
           2+ALOG(ELAMDA+(ELAMDA**2+1.0)**(.5))*(-1.0)*(ELAMDA*(ELAMDA**2+1.0)
           3**  (-1.5)))*DLDA
44          DF3L =F3L1+F3L2+F3L3
45          F2M1=DLDA
46          F2M2=-1.0/(ELAMDA**2+1.0)*DLDA
47          F2M3=(-ELAMDA*ATAN(ELAMDA)/(ELAMDA**2+1.0))*DLDA
48          DF2M=F2M1+F2M2+F2M3
49          F3M1=(.5*(ELAMDA**2+1.0)**(.5)+.5*ELAMDA**2*(ELAMDA**2+1.0)**(-.5)
           1    )*DLDA
50          F3M2=-.5*(1.0+ELAMDA*(ELAMDA**2+1.0)**(-.5))/(ELAMDA+(ELAMDA**2+1.
           1)**(.5))*DLDA
51          F3M3=-(ELAMDA*ALOG(ELAMDA+(ELAMDA**2+1.0)**(.5))/(ELAMDA**2+1.0))
           1 *DLDA
52          DF3M=F3M1+F3M2+F3M3
53          DL2DA=2.0*(1.0/ALFBAR*DF2L -1.0/ALFBAR**2*F2L)
54          DL3DA=1.0/ALFBAR**2*(DF3L-2.0*DF2L)+(-2.0/ALFBAR**3)*(F3L-
           1 2.0*F2L)
55          DM2DA=2.0*(1.0/ALFBAR**2*DF2M-2.0/ALFBAR**3*F2M)
56          DM3DA=1.0/ALFBAR**3*(DF3M-2.0*DF2M)
           1 -3.0/ALFBAR**4*(F3M-2.0*F2M)
57          X0=0.402
58    2     CONTINUE
59          AR=W/C
60          R1=-2.*C*THETA0/(W*(THETAC+BOTTOM))
61          DCLDA=1./(1.+ALFBAR)**2-RC*DL2DA
C
62          DM1DA=-1./ALFBAR**2+2.*(1./ALFBAR**3*ALOG(1.+ALFBAR))-1./ALFBAR**2
           1/(ALFBAR+1.)
63          DCLDR=-ALFBAR**2*DCLDA-2./AR*EL2
64          CLC=ALFBAR/(1.+ALFBAR)-R0*EL2+R1*(X0-1.)*EL2+R1*EL3
C
65          DCLDR1=(X0-1.)*EL2+EL3
66          DCLDRA=(ALFBAR+ALFBAR**2*(1.-X0))*DCLDA+R0*EL2-2./AR*DCLDR1
67          DCMLA=DM1DA-R0*DM2DA+DCLDA*(X0-(ALFBAR+1.)/ALFBAR)+CL0*ALFBAR**(-2
```

AD-A046 565 AIR FORCE INST OF TECH WRIGHT-PATTERSON AFB OHIO F/G 13/6
A COMPARATIVE STUDY OF THE RIDE QUALITY OF TRACV SUSPENSION ALT--ETC(U)
SEP 77 R A LUHRS

UNCLASSIFIED AFIT-CI-78-2 NL

2 OF 2
AD A046565

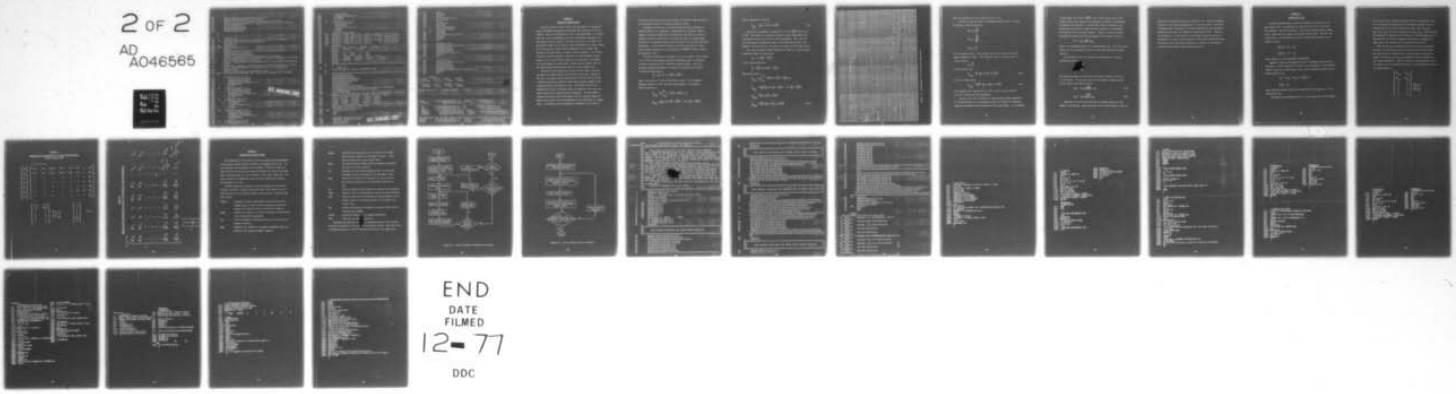

END
DATE FILMED
12-77
DDC

```
     1)
C
      DCMDP0=-EM2-EL2*(X0-(ALFBAR+1.)/ALFBAR)
      DCMDH=-ALFBAR**2*DCMDA+2./AR*DCMDRC
      DCMDP1=(X0-1.)*EM2+EM3+DCLDR1*(X0-(ALFBAR+1.)/ALFBAR)
      DCMDPA=(ALFBAR+ALFBAR**2*(1.-X0))*DCMDA-R0*DCMDP0-2./AR*DCMDR1
      DCMDH=DCMDH/BOTTOM
      DCMDPA=DCMDPA/BOTTOM
      DCLDPA=DCLDPA/BOTTOM
      DCLDH=DCLDH/BOTTOM
C
C
C
      WRITE(6,110)
  110 FORMAT(1X,T4,'DCLDH',T14,'DCLDPA',T24,'DCMDH',T34,'DCMDPA')
      WRITE(6,111)DCLDH,DCLDPA,DCMDH,DCMDPA
      WRITE(6,112)
  112 FORMAT(1X,'      ')
  111 FORMAT(1X,4E10.4)
      RAT=15
      RADGYR=((RAT**2+1.)+(X0-0.5)**2*12.*RAT**2)/(12.*RAT**2)
      DEXT=ALOG(1./(1.+ALFBAR))
      WHAT=ALFBAR/(THETA0+BOTTOM)
      DCLDHD =2.*WHAT/ALFBAR**2*(DEXT+ALFBAR/(1.+ALFBAR))
      DCLDQ=-WHAT/ALFBAR**3*(ALFBAR**2/(1.+ALFBAR)+2.*ALFBAR*(1.+1./ALFB
     1AR-X0)*(DEXT+ALFBAR/(1.+ALFBAR)))
      DCMDHD =(X0-(ALFBAR+1.)/ALFBAR)*DCLDHD -2.*WHAT/ALFBAR**3*(ALFBAR+
     1DEXT)
      DCMDQ=(X0-(ALFBAR+1.)/ALFBAR)*DCLDQ+WHAT/ALFBAR**3*(((-2.-ALFBAR)/
     12.)+1./ALFBAR*(-DEXT)+2.*(ALFBAR+DEXT)*(1.+1./ALFBAR-X0))
      WRITE(6,401)
      WRITE(6,111)DCLDHD ,DCLDQ,DCMDHD ,DCMDQ
  401 FORMAT(1X,T4,'DCLDHDT',T14,'DCLDQ',T24,'DCMDHDT',T34,'DCMDQ')
C
      IF(FIAG.NE.1)GO TO 10
         WRITE(6,117)X0,ALFBAR
         ALFBAR=ALFBAR+STPSIZ
         IF(ALFBAR.LE.LIMIT)GO TO 2
         ALFBAR=ALFORG
         GO TO 1
   10 IF(FIAG.NE.2)GO TO 11
         WRITE(6,118)X0,BOTTOM
         BOTTOM=BOTTOM+STPSIZ
         IF(BOTTOM.LE.LIMIT)GO TO 2
         BOTTOM=BOTORG
         GO TO 1
   11 IF(FIAG.NE.3)GO TO 12
         WRITE(6,119)X0,C
         C=C+STPSIZ
         IF(C.LE.LIMIT)GO TO 2
         C=CORG
         GO TO 1
   12 IF(FIAG.NE.4)GO TO 13
         WRITE(6,120)X0,THETA0
         THETA0=THETA0+STPSIZ
         IF(THETA0.LE.LIMIT)GO TO 2
         THETA0=THEORG
         GO TO 1
   13 IF(FIAG.NE.5)GO TO 14
         WRITE(6,121)X0,R0
```

```
119           R0=R0+STPSIZ
120           IF(R0.LE.LIMIT)GO TO 2
121           R0=R0ORG
122           GO TO 1
123    14     IF(FLAG.NE.6)GO TO 9
124           WRITE(6,122)X0,W
125           W=W+STPSIZ
126           IF(W.LE.LIMIT)GO TO 2
127           W=WORG
128           GO TO 1
129    9      WRITE(6,117)X0,ALFBAR
130    117    FORMAT(/,' ABOVE RUN AT XC= ',F10.5,' ALFBAR= ',F10.5,/////)
131    118    FORMAT(/,' ABOVE RUN AT XC= ',F10.5,' BOTTOM= ',F10.5,/////)
132    119    FORMAT(/,' ABOVE RUN AT XC= ',F10.5,'      C= ',F10.5,/////)
133    120    FORMAT(/,' ABOVE RUN AT XC= ',F10.5,' THETA0= ',F10.5,/////)
134    121    FORMAT(/,' ABOVE RUN AT XC= ',F10.5,'     R0= ',F10.5,/////)
135    122    FORMAT(/,' ABOVE RUN AT XC= ',F10.5,'      W= ',F10.5,/////)
136    1      CONTINUE
137           PRINT,' HTE:  ',HTE,'   THETA0:  ',THETA0
138           PRINT,'  ALFBAR:   ',ALFBAR,'   R0:   ',R0,'   R1:   ',R1
139           PRINT,'    '
140           PRINT,'  I2=  ',EL2,'  I3=  ',EI3
141           PRINT,'  M2=  ',EM2,'  M3=  ',EM3
142           PRINT,'  DCMDA=  ',DCMDA,'  DCLDA=  ',DCLDA
143           PRINT,'  DCMDR0=  ',DCMDR0,'  DCLDR0=  ',DCLDR0
144           PRINT,'  DCMDR1=  ',DCMDR1,'  DCLDR1=  ',DCLDR1
145           PRINT,'    '
      C     ************************************************************
      C     *                                                          *
146           AFAC=.3433
      C      AFAC IS THE SQ. ROOT OF  (C*G/(U**2*CL0)
      C     *                                                          *
      C     ************************************************************
147           DCMDH=DCMDH/RADGYR
148           DCMDPA=DCMDPA/RADGYR
149           DCMDHD=DCMDHD*AFAC/RADGYR
150           DCMDQ=DCMDQ*AFAC/RADGYR
151           DCLDHD=DCLDHD*AFAC
152           DCLDQ=DCLDQ*AFAC
153           A0=DCLDH*DCMDPA-DCLDPA*DCMDH
154           A1=DCMDQ*DCLDH-DCLDQ *DCMDH+DCLDHD*DCMDPA-DCLDPA*DCMDHD
155           A2=DCMDQ*DCLDHD-DCMDHD*DCLDQ-DCLDH-DCMDPA
156           A3=-DCLDHD-DCMDQ
157           PRINT, 'THE FOLLOWING ARE NOT THE ACTUAL COEFFICIENTS, BUT RATHER
             1THEY ARE THE CORRESPONDING NUMBERS FOR THE A MATRIX.'
158           PRINT, 'DCLDHD= ',DCLDHD,'   DCLDQ= ',DCLDQ
159           PRINT, 'DCLDH= ',DCLDH,'   DCLDPA= ',DCLDPA
160           PRINT, 'DCMDHD= ',DCMDHD,'   DCMDQ= ',DCMDQ
161           PRINT, 'DCMDH= ',DCMDH,'   DCMDPA= ',DCMDPA
162           PRINT,' THE FOLLOWENG ARE THE CHARACTERISTIC POLYNOMIAL COEFFICIE
             1NTS, FROM THE HIGHEST ORDER DOWN.'
163           WRITE(6,402)A4,A3,A2,A1,A0
164    402    FORMAT(1X,5(F10.3,4X))
165           STOP
166           END

167           FUNCTION ENTGRL(LB,UB,F,DX )
168           IMPLICIT REAL*8 (A-H,O-$)
169           REAL*8 LB,UB,DX
170           NI=(UB-LB)/DX
```

```
171           A=0.C
172           FB=F(LB)
173           XB=LB
174           IF(NI.EQ.0) GO TO 2
175           DO 1 I=1,NI
176           FA=FB
177           XB=DX*I+LB
178           FB=F(XB)
179           A=A+.5*(FA+FB)*DX
      C       WRITE(6,100)FB,A
180   1       CONTINUE
181   2       CONTINUE
182           A=A+.5*(FB+F(UB))*(UB-XB)
183           ENTGRL=A
184           RETURN
185           END

186           FUNCTION F1(X)
187           IMPLICIT REAL*8 (A-H,O-$)
188           ALOG(X)=DLOG(X)
189           ATAN(X)=DATAN(X)
190           SQRT(X)=DSQRT(X)
191           F1=X*ATAN(X)/(X**2+1.0)
192           RETURN
193           END

194           FUNCTION F2(X)
195           IMPLICIT REAL*8 (A-H,O-$)
196           ALOG(X)=DLOG(X)
197           ATAN(X)=DATAN(X)
198           SQRT(X)=DSQRT(X)
199           F2=X*ALOG(X+SQRT(X**2+1.0))/(X*X+1.0)
200           RETURN
201           END

        $ENTRY
   DCLDH      DCLDPA     DCMDH      DCMDPA
 -238.3341    74.1260    -2.8839    -7.4252

   DCLDHDT    DCLDQ      DCMDHDT    DCMDQ
   -14.9049    4.6785     0.4439    -0.6365

 ABCVE RUN AT XC=     0.40200 ALFBAR=     1.40000



  BTE:          0.300C00000C0000C0D 01    THETA0:       0.00000000E 00
  ALFBAR:            0.14000000432133680 01    RC:          0.4999978E 00    R1:

  I2=           0.2562657958325629D 00    I3=           0.8935115316480926D-01
  M2=           0.3402472884871867D 00    M3=           0.1270643384604157D 00
  DCMDA=          -0.9227058291176051D-02    DCLDA=          0.1360770407624580D 00
  DCMDR0=         -0.3953353772247967D-02    DCLDR0=    UUUUUUUUUUUUUUUUUUUUUUUUUUUUU
  DCMDR1=          0.7445993955771322D-02    DCLDR1=        -0.6389579017692520D-01

THE FOLLOWING ARE NOT THE ACTUAL COEFFICIENTS, BUT RATHER THEY ARE THE CORRESPOND
DCLDHC=        -0.5116840674125913D 01    DCLDQ=          0.1606126276395752D 01
DCLDH=        -0.2383341323638948D 03    DCLDPA=         0.7412600254190446D 02
```

APPENDIX C

FINITE PAD LENGTH EFFECT

As an air cushion vehicle travels over the ground, it encounters a series of surface irregularities which alter the conditions of the air cushion. Since the irregularities occur in all wavelengths, it is likely that some of the irregularities will be of much shorter wavelength than the length of the air cushion. When this is the case, the shape of the ground with respect to the vehicle cannot be described by a single number, as is the case with a point contact suspension, but is instead some function of the pad length, or length of the air cushion. For instance, to a point contact suspension a stairstep is a step change in surface height, but to a pad of finite length it is an obstacle to be climbed, for a step change in surface height implies that all points under the pad change height simultaneously, which is not the present case.

The model in this paper uses attitude and rate terms to describe the effects of vehicle motions on the forces on the body. Because of this fact, the typical surface spectrum will cause the vehicle to have a constant acceleration spectral density high frequency asymptote when constant guideway descriptors are used. This implies infinite rms accelerations which is obviously wrong, and experience shows that very high frequencies are usually severely attenuated. The discrepancy is caused by the model chosen which implies that the relative height and pitch of the vehicle over the guideway may each be described by a single value. In actuality, where irregularity wavelengths on the order of

and shorter than vehicle length are present, the relative height and pitch are necessarily functions of distance along the vehicle.

Including such functions in the model make any kind of analysis extremely tedious if not impossible. Simplification is possible, however. Suppose we assume two-dimensional irregularities such that the surface is constant across the track width at any point and that the average height and pitch of the guideway portion under the vehicle are the most significant descriptors. It then becomes possible to describe the effect of vehicle size on small disturbances as an attenuation by $\left|\frac{\sin \xi}{\xi}\right|$ (Riblich, Captain, and Richardson, 1967).

For ease of description, we assume at $t_o = 0$ the center of the vehicle is at a crest of the guideway and that the guideway itself is expressed as a sum of sinusoids over a continuous frequency domain. Using λ to represent guideway wavelength, the height of the guideway with respect to some mean datum plane is

$$\bar{h}_g = \left|\bar{h}_g(\lambda)\right| \cos\left(\frac{2\pi x}{\lambda} + \frac{2\pi Ut}{\lambda}\right)$$

where x is distance in front of the vehicle center. If we normalize guideway amplitude to one, then the average height of the guideway under the vehicle is

$$\bar{h}_{g_{Avg}} = \frac{1}{L}\int_{-L/2}^{L/2} \cos\left(\frac{2\pi x}{\lambda} + \frac{2\pi U}{\lambda} t\right) dx$$

$$\bar{h}_{g_{Avg}} = \frac{\lambda}{2\pi L}\left[\sin\left(\frac{\pi L}{\lambda} + \frac{2\pi Ut}{\lambda}\right) - \sin\left(\frac{-\pi L}{\lambda} + \frac{2\pi Ut}{\lambda}\right)\right]$$

and by trigonometric identity

$$\bar{h}_{g_{Avg}} = \left(\frac{\lambda}{\pi L} \sin \frac{\pi L}{\lambda}\right) \cos \frac{2\pi Ut}{\lambda} \qquad \text{(C-1)}$$

The term in parentheses in equation (C-1) is the $\frac{\sin \xi}{\xi}$ function for $\xi = \frac{\pi L}{\lambda}$. This function is plotted in Figure C-1 which demonstrates that this function goes to zero for very short wavelengths. This result is not surprising since experience tells us that disturbances with a wavelength of one inch will be of no effect on a large, 150 foot long vehicle.

The rate of guideway height change, $\dot{\bar{h}}$, is found in a similar fashion. Normalized height was expressed by

$$\bar{h}_g = \cos \left(\frac{2\pi x}{\lambda} + \frac{2\pi Ut}{\lambda}\right)$$

so its time derivative is

$$\dot{\bar{h}}_g = \frac{-2\pi U}{\lambda} \sin \left(\frac{2\pi x}{\lambda} + \frac{2\pi Ut}{\lambda}\right)$$

The average value is

$$\dot{\bar{h}}_{g_{Avg}} = \frac{1}{L} \int_{-L/2}^{L/2} \frac{-2\pi U}{\lambda} \sin \left(\frac{2\pi x}{\lambda} + \frac{2\pi Ut}{\lambda}\right) dx$$

$$\dot{\bar{h}}_{g_{Avg}} = \frac{-2\pi U}{\lambda L} \frac{-\lambda}{2\pi} \left[\cos \left(\frac{\pi L}{\lambda} + \frac{2\pi Ut}{\lambda}\right) - \cos \left(\frac{-\pi L}{\lambda} + \frac{2\pi Ut}{\lambda}\right)\right]$$

$$\dot{\bar{h}}_{g_{Avg}} = \frac{-2U}{L} \sin \frac{\pi L}{\lambda} \sin \frac{2\pi Ut}{\lambda}$$

$$\dot{\bar{h}}_{g_{Avg}} = \frac{-2\pi U}{\lambda} \left(\frac{\lambda}{\pi L} \sin \frac{\pi L}{\lambda}\right) \sin \frac{2\pi Ut}{\lambda} \qquad \text{(C-2)}$$

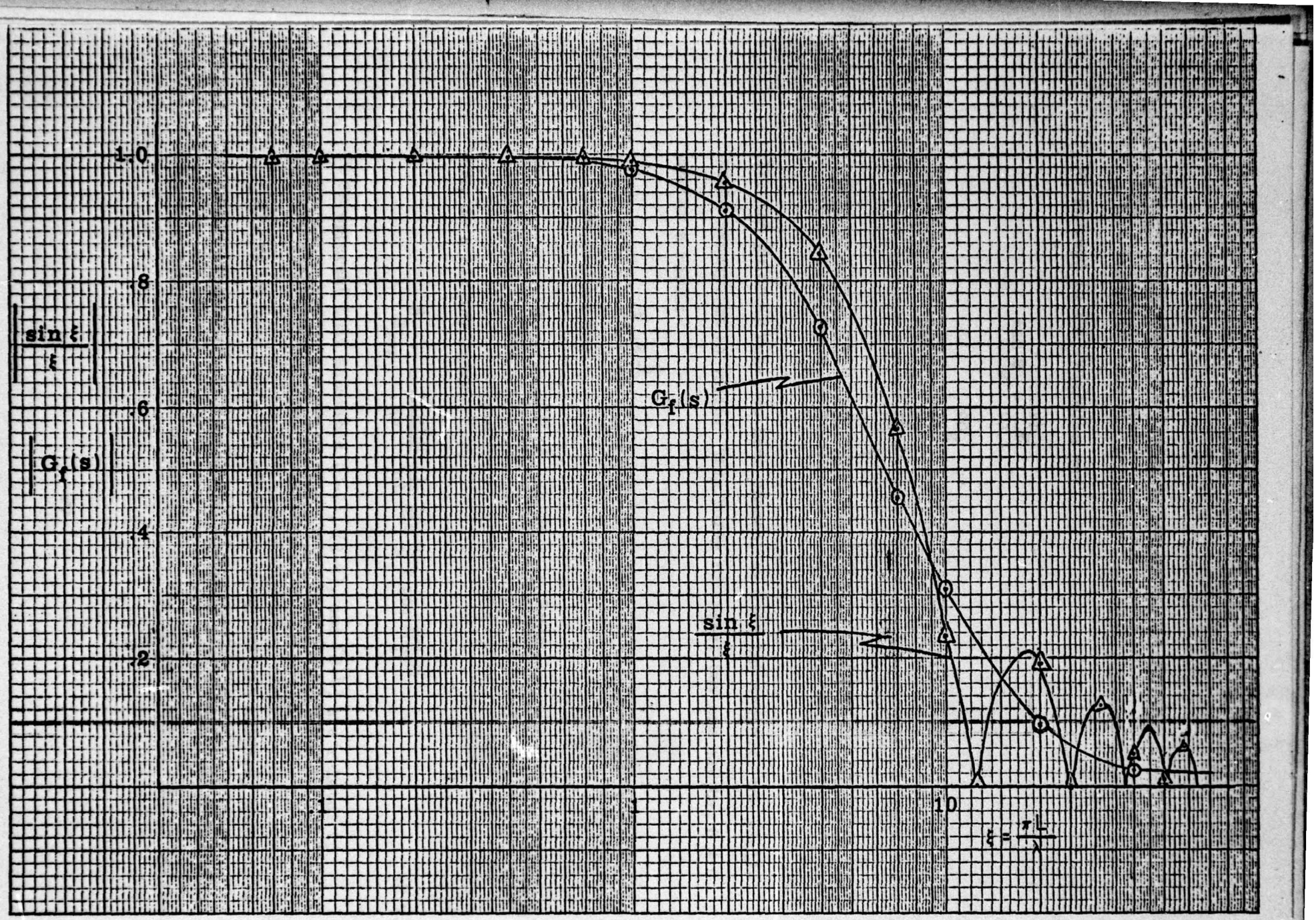

Figure C-1. Approximation of the Finite Pad Length Effect.

This last expression is the time derivative of (C-1).

It turns out that the effect of averaging guideway pitch is similar. We proceed in the following way

$$\tan \theta_g = \frac{dh_g}{dx}$$

$$\tan \theta_g = \frac{\frac{dh_g}{dt}}{\frac{dx}{dt}}$$

$$\tan \theta_g = \frac{\dot{h}}{U}$$

For the guideway model we have chosen, as with the vehicle, the small-angle assumption is valid. This being the case, one can say $\tan \theta \doteq \theta$ and as a result

$$\theta_g \doteq \frac{\dot{h}}{U}$$

It then follows that

$$\theta_{g_{Avg}} = \frac{-2\pi}{\lambda} \left(\frac{\lambda}{\pi L} \sin \frac{\pi L}{\lambda}\right) \sin \frac{2\pi Ut}{\lambda} \qquad \text{(C-3)}$$

and, in a similar manner

$$\dot{\theta}_{g_{Avg}} = \frac{-4\pi^2 U}{\lambda^2} \left(\frac{\lambda}{\pi L} \sin \frac{\pi L}{\lambda}\right) \cos \frac{2\pi Ut}{\lambda} \qquad \text{(C-4)}$$

It is apparent that equations (C-2), (C-3), and (C-4) are related to (C-1) by constants and time derivatives.

If, as we have seen, the effect of using average guideway parameters is to add attenuation to the guideway effects as a function of frequency, then this attenuation must be included in the overall model. It is possible

to approximate the function $\left|\frac{\sin \xi}{\xi}\right|$ with a linear second order filter. Using a linear filter gives us the advantage of freedom in incorporating it anywhere into the model. A second order filter is necessary to be assured that the effect of height and pitch variation in the guideway will diminish with increasing frequency. Figure C-1 shows the actual averaging attenuation function superimposed on the transfer function

$$G(s) = \frac{96}{(s + 8)(s + 12)}$$

Where s is the Laplace operator in non-dimensional time. This illustration depicts the close agreement between the linear approximation and actual function.

As previously stated, the height and pitch spectra of a typical guideway are given as

$$h = \frac{\sqrt{AU}}{s}$$

$$\theta(s) = \sqrt{\frac{A}{U}}$$

The apparent guideway to the vehicle is further attenuated by the size of the vehicle. One may state then that the apparent guideway spectra as the vehicle sees them is given by

$$h_g(s) = \frac{96\sqrt{AU}}{s\,(s + 8)(s + 12)} \qquad \text{(C-5)}$$

$$\theta_g(s) = \frac{96\sqrt{\frac{A}{U}}}{(s + 8)(s + 12)} \qquad \text{(C-6)}$$

Equations (C-5) and (C-6) represent the guideway spectra as they appear to the vehicle. This must be part of the overall model so that the

controller and dynamics analysis may account for it. These two equations represent a close linear approximation to a function which is the result of assuming that the parameters of primary importance are the averages of height and pitch under the vehicle at a given point in time. These can be considered as a filter placed on white noise so that the source of disturbance for control theory purposes is white noise although the guideway itself is not, allowing the controller to account for non-uniform guideway spectra without complicating the analysis.

APPENDIX D

STATE MATRIX FORM

The most convenient way to express the equations of motion is in the state matrix form. From Appendix A we draw (A-5) and (A-6) as the first two equations. This pair represents a fourth-order coupled dynamic system solved explicitly for vertical and pitching accelerations. This pair has a form which is not adaptable to the state variable form directly, so we require the pair:

$$\frac{d}{d\tau}(\bar{h}_r) = \bar{h}_r' - \bar{h}_g'$$

$$\frac{d}{d\tau}(\theta_r) = \theta_r' - \theta_g'$$

which defines the vehicle-guideway relationships.

Appendix C develops the apparent spectra of guideway height and pitch variations. If $\eta(\tau)$ represents the white noise disturbance of unity spectral density (using the non-dimensional time), then the apparent guideway differential equations are:

$$\theta_g'' + 20\,\theta_g' + 96\,\theta_g = 96\sqrt{\frac{A}{U}}\,\eta(\tau)$$

$$\frac{c}{U}\,\bar{h}_g'' = \theta_g'$$

where the prime notation denotes the differential with respect to τ, non-dimensional time.

The guideway relationships sum up to a third order set, and the vehicle

set is fourth order, yielding a seventh order set of equations. This set is necessary for expressing the acceleration equations in state variable form and the state variables are: $\Delta\bar{h}_r'$, $\Delta\theta_r'$, $\Delta\bar{h}_r$, $\Delta\theta_r$, $\Delta\bar{h}_g'$, $\Delta\theta_g'$, $\Delta\theta_g$; the control variables are: $\Delta\delta_{w_1}$, $\Delta\delta_{w_2}$. These equations are expressed in numerical form in Table D-1. This controllable set of equations for the actively suspended vehicle may be considered the rigid case if all elements in the B matrix are set to zero.

Table D-2 shows the generalized form for the passive suspension and lists the substitutions which are not part of the active model. This Table shows the modifications to the equations as discussed in Chapter IV, with $\Delta\delta_{w_1}$ and $\Delta\delta_{w_2}$ now appearing as state variables and the B matrix eliminated. From D-2 one may see the generalized form of the contents of D-1 by striking the last two rows and adding the second term which appears as

$$\begin{bmatrix} C_{L_{\delta_{w_1}}} & C_{L_{\delta_{w_2}}} \\ C_{M_{\delta_{w_1}}} & C_{M_{\delta_{w_2}}} \\ 0 & 0 \\ 0 & 0 \\ 0 & 0 \\ 0 & 0 \\ 0 & 0 \end{bmatrix} \begin{bmatrix} \Delta\delta_{w_1} \\ \Delta\delta_{w_2} \end{bmatrix}$$

TABLE D-1

NUMERIC MATRIX REPRESENTATION OF TRACV STATE EQUATIONS

(ACTIVE CONTROL FORM)

$$\dot{x} = Ax + Bu + Cw$$

$$\begin{bmatrix} \Delta\bar{h}_r'' \\ \Delta\theta_r'' \\ \Delta\bar{h}_r \\ \Delta\theta_r \\ \Delta\bar{h}_g'' \\ \Delta\theta_g'' \\ \Delta\theta_g' \end{bmatrix} = \begin{bmatrix} -5.12 & 1.61 & -192.57 & 62.72 & 5.12 & -1.61 & 0 & \Delta\bar{h}_r' \\ 1.63 & -2.34 & -23.34 & -65.33 & -1.63 & 2.34 & 0 & \Delta\theta_r' \\ 1 & 0 & 0 & 0 & -1 & 0 & 0 & \Delta\bar{h}_r \\ 0 & 1 & 0 & 0 & 0 & -1 & 0 & \Delta\theta_r \\ 0 & 0 & 0 & 0 & 0 & 2 & 0 & \Delta\bar{h}_g' \\ 0 & 0 & 0 & 0 & 0 & -20 & -96 & \Delta\theta_g' \\ 0 & 0 & 0 & 0 & 0 & 1 & 0 & \Delta\theta_g \end{bmatrix} +$$

$$+ \begin{bmatrix} -2.16 & 45.28 \\ -.36 & -56.94 \\ 0 & 0 \\ 0 & 0 \\ 0 & 0 \\ 0 & 0 \\ 0 & 0 \end{bmatrix} \begin{bmatrix} \Delta\delta_{w_1} \\ \Delta\delta_{w_2} \end{bmatrix} + \begin{bmatrix} 0 \\ 0 \\ 0 \\ 0 \\ 0 \\ .0111 \\ 0 \end{bmatrix} [\eta(\tau)]$$

TABLE D-2

GENERAL MATRIX REPRESENTATION OF TRACV STATE EQUATIONS (PASSIVE SUSPENSION)

$$\dot{x} = Ax + Cw$$

$$A = \begin{bmatrix}
\frac{c}{UA} C_{L_{\dot{h}}} & \frac{c}{UA} C_{L_q} & C_{L_h} & C_{L_\theta} & \frac{-c}{UA} C_{L_{\dot{h}}} & \frac{-c}{UA} C_{L_q} & 0 & C_{L_{\delta_{w_1}}} & C_{L_{\delta_{w_2}}} \\
\frac{c}{UA} C_{M_{\dot{h}}} & \frac{c}{UA} C_{M_q} & C_{M_h} & C_{M_\theta} & \frac{-c}{UA} C_{M_{\dot{h}}} & \frac{-c}{UA} C_{M_q} & 0 & C_{M_{\delta_{w_1}}} & C_{M_{\delta_{w_2}}} \\
1 & 0 & 0 & 0 & -1 & 0 & 0 & 0 & 0 \\
0 & 1 & 0 & 0 & 0 & -1 & 0 & 0 & 0 \\
0 & 0 & 0 & 0 & 0 & \frac{u}{c} & 0 & 0 & 0 \\
0 & 0 & 0 & 0 & 0 & -20 & -96 & 0 & 0 \\
0 & 0 & 0 & 0 & 0 & 1 & 0 & 0 & 0 \\
\frac{Pc}{UA\tilde{B}_1} C_{L_{\dot{h}}} & \frac{Pc}{UA\tilde{B}_1} C_{L_q} & \frac{P}{\tilde{B}_1} C_{L_h} & \frac{P}{\tilde{B}_1} C_{L_\theta} & \frac{-Pc}{UA\tilde{B}_1} C_{L_{\dot{h}}} & \frac{-Pc}{UA\tilde{B}_1} C_{L_q} & 0 & \frac{(PC_{L_{\delta_{w_1}}} - K_1)}{\tilde{B}_1} & \frac{P}{\tilde{B}_1} C_{L_{\delta_{w_2}}} \\
\frac{Rc}{UA\tilde{B}_2} C_{M_{\dot{h}}} & \frac{Rc}{UA\tilde{B}_2} C_{M_q} & \frac{R}{\tilde{B}_2} C_{M_h} & \frac{R}{\tilde{B}_2} C_{M_\theta} & \frac{-Rc}{UA\tilde{B}_2} C_{M_{\dot{h}}} & \frac{-Rc}{UA\tilde{B}_2} C_{M_q} & 0 & \frac{R}{\tilde{B}_1} C_{L_{\delta_{w_1}}} & \frac{(RC_{L_{\delta_{w_2}}} - K_2)}{\tilde{B}_2} C_{L_{\delta_{w_2}}}
\end{bmatrix}$$

$$C = \begin{bmatrix} 0 \\ 0 \\ 0 \\ 0 \\ 0 \\ .0111 \\ 0 \\ 0 \\ 0 \end{bmatrix}$$

APPENDIX E

OPTIMIZATION SOLUTION FORMAT

The optimization of the passive and active suspensions was implemented on the digital computer using the interactive language known as APL. The two techniques varied somewhat from one another. Figure E-1 shows the logic flow for the passive case, Figure E-2 depicts the flow for the active case. Following these is a set of listings of the source codes used. The first listing is in FORTRAN and solves the mean squared error integral. The remainder are in APL.

The APL Programs are designed to find the numerators of the various transfer functions of interest and convert them to rms values or sets of poles and zeros for the spectral density routine, which is a modified Bode plot routine.

COSTFN - performs the linear transformation which sets up the performance index in terms of state variables and inputs and converts to standard notation as discussed in Chaper V.

FRAME - converts the A matrix to a vector containing the coefficients of the characteristic polynomial.

GAP - finds the numerator coefficients for the L.E. and T.E. gap transfer functions.

MAKE - generates the A matrix for the passive suspension given the values for the spring and damper constants.

MEANSQ - calculates the mean squared error integral for an eighth order transfer function for the passive solution. Answer given is square root of mean squared value.

NUMB - (and NUM for Passive System) finds the numerator polynomial for any of the state variables.

OPT - performs the four-variable gradient search for the spring and damper constants according to the performance index.

QUAD - finds the rms values of L.E. gap and T.E. gap as well as rms control deflections for the performance index use in OPT.

RIC - solves the matrix-Ricatti equation by reverse-time integration.

ROOTS - finds the roots of a polynomial by calling the Bairstow Method.

SEAT - finds the rms vertical acceleration at a given position in the vehicle, given as the decimal portion of the distance from front to rear.

SET - arranges the numerator polynomials for gap and control variations and calls MEANSQ.

VECTOR - calculates eigenvectors for complex eigenvalues.

WING - finds the rms control deflections.

Particular attention must be given to polynomials having a zero constant term which sometimes do not converge in the Bairstow routine. When this occurs, a convenient method is to drop it and insert the root at the origin later.

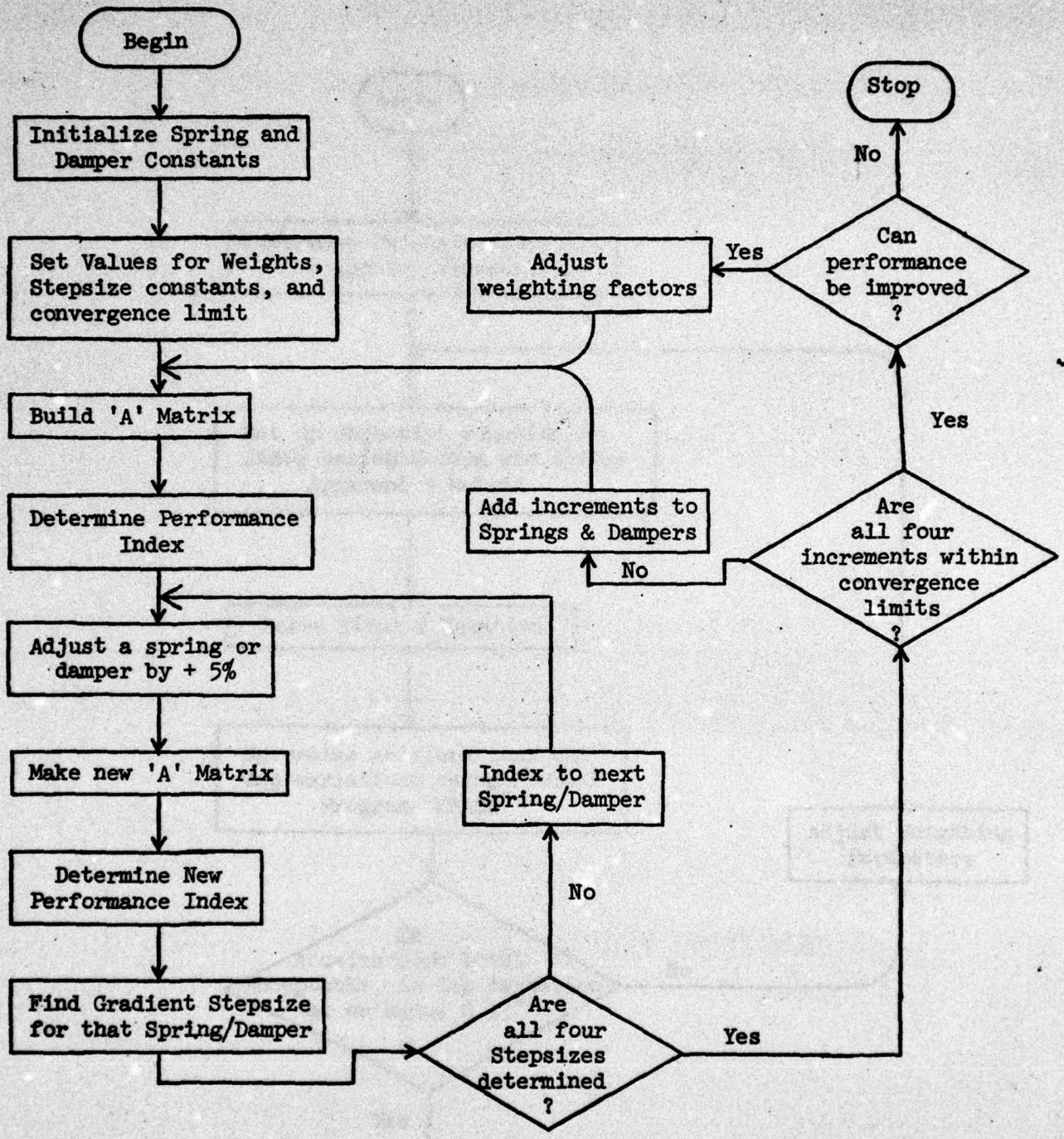

Figure E-1. Passive Suspension Optimization Technique.

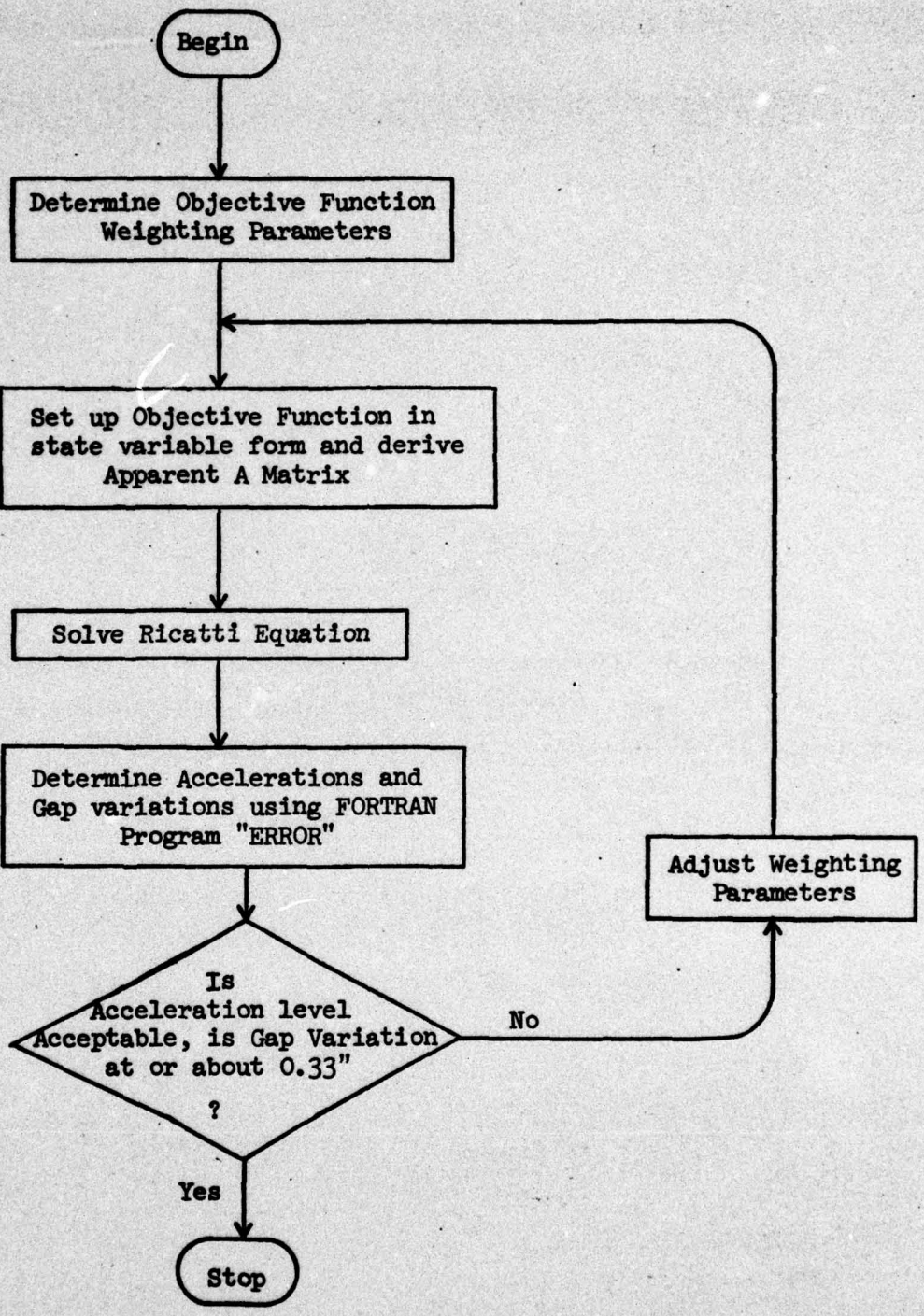

Figure E-2. Active Control Solution Technique.

```
      $JOB          B1002.DOTTRAIN,TIME=20,PAGES=20,BIN=G53
**WARNING**  MIS-PUNCHED JOB OPTION. BIN=G  IS INVALID
      C*****************************************************************
      C**                                                             **
      C**     THIS PROGRAM CALCULATES THE MEAN SQUARED ERROR INTEGRAL **
      C** FOR A TRANSFER FUNCTION WHICH IS OF N ORDER IN THE DENOMINATOR AND**
      C** (N-1) ORDER IN THE NUMERATOR.  THIS INTEGRAL HAS BEEN SOLVED IN **
      C** CLOSED FORM AND IS PRESENTED IN SEVERAL TEXTS ON LINEAR CONTROL **
      C** DESIGN.  THIS PARTICULAR SET OF EQUATIONS WAS TAKEN LITERALLY FROM**
      C** NEWTON,G.C.,L.A.GOULD, AND J.F. KAISER, ANALYTICAL DESIGN OF LINEAR*
      C** FEEDBACK CONTROLS, 1957, PP. 371-377.                       **
      C**     THE INPUT FOR THIS PROGRAM TAKES THE FOLLOWING ORDER:   **
      C** THE FIRST CARD CONTAINS THE NUMBER OF TRIALS TO BE RUN (I2 FORMAT)**
      C** THE SECOND CARD HAS THE TYPE OF SYSTEM (I2,7X) AND A MEMO    **
      C** STARTING AT COLUMN 10 AND CONTAINING SIXTY ALPHABETIC CHARACTERS **
      C** THE NEXT CARD IS THE [illegible]TOR COEFFICIENTS IN DESCENDING ORDER **
      C** IN (N)F10.4 FORMAT A[illegible] AFTER IS THE POLES IN (N+1)F10.4 **
      C**     UP TO EIGHT DATA [illegible]LL FIT ONTO A CATD; IF THERE ARE **
      C** MORE, THEN THE DATA M[illegible]LIT BETWEEN TWO CARDS AS EVENLY AS **
      C** POSSIBLE.  IN THE EVENT [illegible] ODD NUMBER, THE FIRST CARD GETS ONE **
      C** MORE THAN THE SECOND.                                       **
      C**     ANY GAINS TO BE INCLUDED MUST FIRST BE DISTRIBUTED TO ALL THE **
      C** COEFFICIENTS.                                               **
      C**     FORTRAN PROGRAMMING BY R. A. LUHRS.                     **
      C**                                                             **
      C*****************************************************************
    1       IMPLICIT REAL*8 (A-H,M,O-Z)
    2       DIMENSION MEMO(15)
    3       PRINT, '  THE RMS VALUE IS GIVEN FOR EACH INPUT. '
    4       READ(5,201)ICOUNT
    5       DO 999 IJ=1,ICOUNT
    6       READ(5,100)IORDER,(MEMO(NIN),NIN=1,15)
    7  100  FORMAT(I2,7X,15A4)
    8  104  FORMAT(4F10.4)
    9  105  FORMAT(5F10.4)
   10  106  FORMAT(6F10.4)
   11  107  FORMAT(7F10.4)
   12  108  FORMAT(8F10.4)
   13  200  FORMAT(E12.4)
   14  201  FORMAT(I2)
   15  301  FORMAT(1X,'**  NOTE:      ',15A4)
   16       IF (IORDER.EQ.7)GO TO 7
   17       IF (IORDER.EQ.8)GO TO 8
   18       IF (IORDER.EQ.9)GO TO 9
   19  6    CONTINUE
      C*****************************************************************
      C**                                                             **
      C**       THIS SEGMENT PERFORMS THE SIXTH ORDER OPERATION.      **
      C**                                                             **
      C*****************************************************************
   20       READ(5,106)C5,C4,C3,C2,C1,C0
   21       READ(5,107)D6,D5,D4,D3,D2,D1,D0
   22       M1=-D0*D1*D5+D0*D3**2+D1**2*D4-D1*D2*D3
   23       M2=D0*D3*D5+D1**2*D6-D1*D2*D5
   24       M3=D0*D5**2+D1*D3*D6-D1*D4*D5
   25       M4=(D2*M3-D4*M2+D6*M1)/D0
   26       M5=(D2*M4-D4*M3+D6*M2)/D0
   27       M0=(D4*M1-D2*M2+D0*M3)/D6
   28       DEL6=(D1*M5-D3*M4+D5*M3)*D0
   29       ENTGRL=(C5**2*M0+(C4**2-2*C3*C5)*M1+(C3**2-2*C2*C4+2*C1*C5)*M2+
```

```
     1(C2**2-2*C1*C3+2*C0*C4)*M3+(C1**2-2*C0*C2)*M4+C0**2*M5)/(2*DEL6)
30         GO TO 10
31   7     CONTINUE
     C*****************************************************************
     C**                                                             **
     C**       THIS SEGMENT CALCULATES THE SEVENTH ORDER SYSTEM INTEGRAL.  **
     C**                                                             **
     C*****************************************************************
32         READ(5,107)C6,C5,C4,C3,C2,C1,C0
33         READ(5,108)D7,D6,D5,D4,D3,D2,D1,D0
34         M1=-(D1*D4-D0*D5)**2+(D0*D3-D1*D2)*(D0*D7-D1*D6+D2*D5-D3*D4)
35         M2=(D0*D7-D1*D6)*(-D0*D5+D1*D4)+(D0*D3-D1*D2)*(D2*D7-D3*D6)
36         M3=-(D0*D7-D1*D6)**2+(D0*D3-D1*D2)*(D4*D7-D5*D6)
37         M4=(1/D0)*(D2*M3-D4*M2+D6*M1)
38         M5=(1/D0)*(D2*M4-D4*M3+D6*M2)
39         M6=(1/D0)*(D2*M5-D4*M4+D6*M3)
40         M0=(1/D7)*(D5*M1-D3*M2+D1*M3)
41         DEL7=D0*(D1*M6-D3*M5+D5*M4-D7*M3)
42         ENTGRL=(1/(2*DEL7))*(C6**2*M0+(C5**2-2*C4*C6)*M1+(C4**2-2*C5*C3+2*
     1C2*C6)*M2+(C3**2-2*C2*C4+2*C1*C5-2*C0*C6)*M3+(C2**2-2*C1*C3+2*C0*C
     24)*M4+(C1**2-2*C0*C2)*M5+C0**2*M6)
43         GO TO 10
44   8     CONTINUE
     C*****************************************************************
     C**                                                             **
     C**    THIS SEGMENT CALCULATES THE INTEGRAL FOR AN EIGHTH ORDER SYSTEM**
     C**                                                             **
     C*****************************************************************
45         READ(5,108)C7,C6,C5,C4,C3,C2,C1,C0
46         READ(5,105)D8,D7,D6,D5,D4
47         READ(5,104)D3,D2,D1,D0
48         M1=(D0*D7+D2*D5)*(-D0*D1*D7+D0*D3*D5+2*D1**2*D6)+(D3*D7-D5**2)*
     1(D0**2*D5+D1*D2**2)+D1*D3*D8*(D0*D3-D1*D2)-D1**2*D8*(D0*D5-D1*D4)+
     2(-D2*D7+D3*D6-D4*D5)*(D0*D3**2+D1**2*D4)-D1*D6*(D1**2*D6+
     33*D0*D3*D5)-D1*D2*D3*(D3*D6-D4*D5)+2*D0*D1*D4*D5**2
49         M2=(D0*D3-D1*D2)*(D0*D7**2-D1*D5*D8-D1*D6*D7+D2*D5*D7)+
     1(D3*D8-D4*D7)*(-D0*D1*D5+D0*D3**2-D1*D2*D3+D1**2*D4)-
     2D0*D5*D7*(D0*D5-D1*D4)+D1**2*D8*(D0*D7-D1*D6)
50         M3=-D1*(D1*D8-D2*D7)**2+(-D5*D8+D6*D7)*(D0*D1*D5-D0*D3**2+D1*D2*D3
     1-D1**2*D4)+D0*D7**2*(-D0*D5+D1*D4+D2*D3)-(2*D0*D1*D3*D7*D8)
51         M4=(-D5*D8+D6*D7)*(2*D0*D1*D7-D0*D3*D5+D1*D2*D5-D1**2*D6)+
     1(-D3*D8+D4*D7)*(D0*D3*D7-D1*D2*D7+D1**2*D8)-D0**2*D7**3
52         M5=(D2*M4-D4*M3+D6*M2-D8*M1)/D0
53         M6=(D2*M5-D4*M4+D6*M3-D8*M2)/D0
54         M7=(D2*M6-D4*M5+D6*M4-D8*M3)/D0
55         M0=(D6*M1-D4*M2+D2*M3-D0*M4)/D8
56         DEL8=D0*(D1*M7-D3*M6+D5*M5-D7*M4)
57         ENTGRL=(C7**2*M0+(C6**2-2*C5*C7)*M1+(C5**2-2*C4*C6+2*C3*C7)*M2+
     1(C4**2-2*C3*C5+2*C2*C6-2*C1*C7)*M3+(C3**2-2*C2*C4+2*C1*C5-2*C0*C6)
     2*M4+(C2**2-2*C1*C3+2*C0*C4)*M5+(C1**2-2*C0*C2)*M6+C0**2*M7)/(2*DEL
     38)
58         GO TO 10
59   9     CONTINUE
     C*****************************************************************
     C**                                                             **
     C**       THIS SEGMENT CALCULATES THE NINTH ORDER SYSTEM INTEGRAL.   **
     C**                                                             **
     C*****************************************************************
60         READ(5,105)C8,C7,C6,C5,C4
61         READ(5,104)C3,C2,C1,C0
```

```
      READ(5,105) D9,D8,D7,D6,D5
      READ(5,105) D4,D3,D2,D1,D0
      A1=D1*D2-D0*D3
      A2=D1*D4-D0*D5
      A3=D3*D4-D2*D5
      A4=D1*D6-D0*D7
      A5=D3*D6-D2*D7
      A6=D5*D6-D4*D7
      A7=D1*D8-D0*D9
      A8=D3*D8-D2*D9
      A9=D5*D8-D4*D9
      A10=D7*D8-D6*D9
      M1=A1*(A1*A10-A2*A9+A3*A6+A3*A8+2*A4*A6-A5**2-A5*A7-A7**2)+
     1A2*(-A2*A6-A3*A7+A4*A5+2*A4*A7)-A4**3
      M2=A1*(A3*A9+A4*A9-A5*A8+A6*A7-A7*A8)+A2*(-A2*A9+A4*A8+A7**2)-A4**
     12*A7
      M3=A1*(A3*A10+A4*A10+A7*A9-A8**2)+A2*(-A2*A10+A7*A8)-A4*A7**2
      M4=A1*(A5*A10+A7*2*A10-A8*A9)+A2*(A7*A9-A4*A10)-A7**3
      M5=(D2*M4-D4*M3+D6*M2-D8*M1)/D0
      M6=(D2*M5-D4*M4+D6*M3-D8*M2)/D0
      M7=(D2*M6-D4*M5+D6*M4-D8*M3)/D0
      M8=(D2*M7-D4*M6+D6*M5-D8*M4)/D0
      M0=(1/D9)*(D7*M1-D5*M2+D3*M3-D1*M4)
      DEL9=D0*(D1*M8-D3*M7+D5*M6-D7*M5+D9*M4)
      ENTGRL=(C8**2*M0+(C7**2-2*C6*C8)*M1+(C6**2-2*C5*C7+2*C4*C8)*M2+
     1(C5**2-2*C4*C6+2*C3*C7-2*C2*C8)*M3+(C4**2-2*C3*C5+2*C2*C6-
     22*C1*C7+2*C0*C8)*M4+(C3**2-2*C2*C4+2*C1*C5-2*C0*C6)*M5
     3+(C2**2-2*C1*C3+2*C0*C4)*M6+(C1**2-2*C0*C2)*M7+C0**2*M8)/(I*DEL9)
C*******************************************************************
10    CONTINUE
      ENTGRL=ENTGRL*2*3.14159
      ENTGRL=ENTGRL**0.5
      WRITE(6,301) (MEMO(NIN),NIN=1,15)
      WRITE(6,200) ENTGRL
999   CONTINUE
      STOP
      END

      $ENTRY
 THE RMS VALUE IS GIVEN FOR EACH INPUT.
**  NOTE:       OPTIMAL C.G. ACCELERATION, RUN B4
 0.3267D-02
**  NOTE:       TRAILING EDGE RMS VARIATION
 0.2650D 00
**  NOTE:       LEADING  EDGE RMS VARIATION
 0.1780D 00
**  NOTE:       DW1 RMS DEFLECTION
 0.1815D-01
**  NOTE:       DW2 RMS DEFLECTION
 0.8190D-03
**  NOTE:       OPTIMAL C.G. ACCELERATION, RUN B5
 0.2124D-02
**  NOTE:       TRAILING EDGE GAP RMS VARIATION
 0.3266D 00
**  NOTE:       LEADING  EDGE GAP RMS VARIATION
 0.2178D 00
**  NOTE:       DW1 RMS DEFLECTION
 0.2499D-01
**  NOTE:       DW2 RMS DEFLECTION
 0.5505D-03
```

```
      ∇ DT1 RIC L
[1]   A OPTIMAL PROBLEM: A1←AU-BU+.×(⌹P1)+.×(⍉N5)
[2]    N←1↑⍴A1
[3]    Z1←A1,-B1+.×(⌹P1)+.×(⍉B1)
[4]    Z2←-Q1,⍉A1
[5]    Z←Z1,[1]Z2
[6]    THETA←DT1 STM-Z
[7]    THETA11←(N,N)↑THETA
[8]    THETA12←(N,-N)↑THETA
[9]    THETA21←((-N),N)↑THETA
[10]   THETA22←(-N,N)↑THETA
[11]   R←(N,N)⍴0
[12]   I←0
[13] LOOP:ROLD←R
[14]   R←(THETA21+THETA22+.×R)+.×⌹(THETA11+THETA12+.×R)
[15]   R←(R+⍉R)÷2
[16]   ERROR←(+/+/(ROLD-R)*2)*0.5
[17]   I←I+1
[18]   ERROR
[19]   →(ERROR>L)/LOOP
[20]   KT←(⌹P1)+.×((⍉N5)+((⍉B1)+.×R))
[21]   'KT='
[22]   10 ¯3 ⍕KT
[23]   A←AU-BU+.×KT
       ∇
       •
```

```
      ∇ COSTFN
[1]   Z←6⍴0
[2]   'ENTER C1 THRU C6'
[3]   Z←⎕
[4]   Q← 6 6 ⍴0
[5]   Q[1;]←Z
[6]   Q← 0 ¯1 ¯2 ¯3 ¯4 ¯5 ⊖Q
[7]   M← 6 7 ⍴0
[8]   M←TR...
[9]   ALL←(⊖M)∘.×Q∘.×M
[10]  Q5←(7,7)↑ALL
[11]  N5←(7,-2)↑ALL
[12]  P1←(-2,2)↑ALL
[13]  Q1←Q5-(N5+.×(⌹P1)+.×(⊖N5))
[14]  'YOU ARE NOW READY TO RUN RIC'
[15]  A1←AU-BU+.×(⌹P1)+.×(⊖N5)
[16]  B1←BU
      ∇
      ∇WING[⎕]∇
      ∇ WING;Z;I;P
[1]   GAP
[2]   Z←⎕
[3]   ' '
[4]   ' '
[5]   'THE DW1 POLYNOMIAL IS:'
[6]   I←0
[7]   P←P0[;3]
[8]  LOOP:I←I+1
[9]   →((|P[I])≤1E¯6)/LOOP
[10]  I←(⍴P)+1-I
[11]  P←(-I)↑P
[12]  F P
[13]  'THE DW2 POLYNOMIAL IS:'
[14]  I←0
[15]  P←P0[;4]
[16] LOOP2:I←I+1
[17]  →((|P[I])≤1E¯6)/LOOP2
[18]  I←(⍴P)+1-I
[19]  P←(-I)↑P
[20]  F P
      ∇
      •
```

```
      ▽ TRAN
[1]   ⍝THIS ROUTINE CALLS THE OTHERS.
[2]   ⍝GIVEN AN A AND A B MATRIX, THE
[3]   ⍝PROGRAM FINDS THE POLES, ZEROS,
[4]   ⍝AND THE ROOT LOCUS GAIN FOR ANY
[5]   ⍝INPUT-OUTPUT COMBINATION.
[6]    ERASE
[7]    NUMB
[8]    ERASE
[9]    ' '
[10]   ' '
[11]   'THE SYSTEM ZEROS ARE:'
[12]   ' '
[13]   10 ¯3 ⎕FM
[14]   ' '
[15]   'THE SYSTEM POLES ARE:'
[16]   ' '
[17]   M←1E¯7 EIGVAL A
[18]   10 ¯3 ⎕FM
[19]   ' '
[20]   ' '
[21]   'THE TRANSFER FUNCTION ROOT LOCUS GAIN IS:'
[22]   ' '
[23]   GAIN
       ▽
       •
```

```
      ▽ SEAT X0;PA;PB;A1;A2
[1]    A1←A
[2]    A1[;1]←-B
[3]    A2←A1
[4]    A2[1;]←0
[5]    PA←(FRAME A1)-(FRAME A2)
[6]    A1←A
[7]    A1[;2]←-B
[8]    A2←A1
[9]    A2[2;]←0
[10]   PB←(FRAME A1)-(FRAME A2)
[11]   P←PA+((0.402-X0)×PB)
[12]   IK←0
[13] LOOP:IK←IK+1
[14]   →((|P[IK])≤1E¯6)/LOOP
[15]   IK←(⍴P)+1-IK
[16]   P←(-IK)↑P×2.197
[17]   'THE ACCELERATION NUMERATOR FOR THE GIVEN POSITION:'
[18]   10 ¯3 ⎕FM P
[19]   'THE ROOTS ARE:'
[20]   ROOTS P
[21]   10 ¯3 ⎕FM
[22]   'GAIN:'
[23]   GAIN
[24]   'THE MEAN  SQUARED ACCELERATION IS:'
[25]   PN←MEANSQ P
[26]   J←(C[1]×PN)+(C[3]×PL)+(C[4]×PT)+(C[5]×P1)+(C[6]×P2)
[27]   PN
       ▽
```

```
      ∇COSTFN[□]∇
      ∇ COSTFN
[1]   Z←6⍴0
[2]   'ENTER C1 THRU C6'
[3]   Z←□
[4]   Q← 6 6 ⍴0
[5]   Q[1;]←Z
[6]   Q← 0 ¯1 ¯2 ¯3 ¯4 ¯5 ⊖Q
[7]   M← 6 7 ⍴0
[8]   M←TR
[9]   ALL←(⊖M)∘.×Q∘.×M
[10]  Q5←(7,7)↑ALL
[11]  N5←(7,¯2)↑ALL
[12]  P1←(¯2,2)↑ALL
[13]  Q1←Q5-(N5+.×(⌹P1)+.×(⊖N5))
[14]  'YOU ARE NOW READY TO RUN RIC'
[15]  A1←AV-BV+.×(⌹P1)+.×(⊖N5)
[16]  B1←BV
      ∇
      ∘
```

```
      ∇FRAME[□]∇
      ∇ R←FRAME A;I;J;K;N;TR
[1]   N←L/⍴A
[2]   I←(⍳N)∘.=⍳N
[3]   J←I
[4]   K←1
[5]   R←1
[6]   J←A+.×J
[7]   TR←(+/+/I×J)=K
[8]   J←J-TR×I
[9]   R←R,-TR
[10]  →(N≥K←K+1)/5
      ∇
      ∘
```

```
      ∇ NUMB;A1;A2;Z;ZZ;I
[1]   ⍝ THIS IS THE REVISED NUMERATOR ROUTINE.
[2]   A1←A
[3]   'ENTER COL. OF A TO BE REPLACED:'
[4]   Z←□
[5]   'ENTER COL. OF B TO REPLACE IT :'
[6]   ZZ←□
[7]   A1[;Z]←-B[;ZZ]
[8]   A2←A1
[9]   A2[Z;]←0
[10]  P←((FRAME A1)-(FRAME A2))
[11]  I←0
[12] LOOP:I←I+1
[13]  →((|P[I])≤1E¯9)/LOOP
[14]  I←(⍴P)-(I-1)
[15]  P←(-I)↑P
[16]  ROOTS P
      ∇
      ∘
```

```
      ∇COSTFN[□]∇
      ∇ COSTFN
[1]   Z←6⍴0
[2]   'ENTER C1 THRU C6'
[3]   Z←□
[4]   Q← 6 6 ⍴0
[5]   Q[1;]←Z
[6]   Q← 0 ¯1 ¯2 ¯3 ¯4 ¯5 ⌽Q
[7]   M← 6 7 ⍴0
[8]   M←TR
[9]   ALL←(QM)+.×Q+.×M
[10]  Q5←(7,7)↑ALL
[11]  N5←(7,-2)↑ALL
[12]  P1←(-2,2)↑ALL
[13]  Q1←Q5-(N5+.×(⌹P1)+.×(QN5))
[14]  'YOU ARE NOW READY TO RUN RIC'
[15]  A1←AU-BU+.×(⌹P1)+.×(QN5)
[16]  B1←BU
      ∇
      •
```

```
      ∇FRAME[□]∇
      ∇ R←FRAME A;I;J;K;N;TR
[1]   N←L/⍴A
[2]   I←(⍳N)∘.=⍳N
[3]   J←I
[4]   K←1
[5]   R←1
[6]   J←A+.×J
[7]   TR←(+/+/I×J)÷K
[8]   J←J-TR×I
[9]   R←R,-TR
[10]  →(N≥K←K+1)/6
      ∇
      •
```

```
▽GAP[□]▽
      ▽ GAP;CO;P;I;J;K;A1;A2
[1]   ⍝THIS ROUTINE CALCULATES THE
[2]   ⍝L.E. AND T.E. GAP NUMERATORS
[3]   ⍝AND THE WINGLET MOTION
[4]   ⍝NUMERATORS.
[5]   ⍝THESE ARE TO BE USED TO FIND
[6]   ⍝THE RESPECTIVE RMS VALUES.
[7]   ⍝ THIS FUNCTION CALCULATES THE
[8]   ⍝LEADING AND TRAILING EDGE GAP
[9]   ⍝NUMERATOR POLYNOMIALS.
[10]   P← 8 7 ⍴0
[11]   P0← 8 4 ⍴0
[12]   J←1
[13] LOOPA:CO← 8 7 ⍴KT[J;]
[14]   I←1
[15] LOOP:A1←A
[16]   A1[;I]←-B
[17]   A2←A1
[18]   A2[I;]←0
[19]   P[;I]←(-8)↑((FRAME A1)-(FRAME A2))
[20]   I←I+1
[21]   →(I≤7)/LOOP
[22]   K←J+2
[23]   P0[;K]←+/CO×P
[24]   J←J+1
[25]   →(J≤2)/LOOPA
[26]   I←1
[27] LOOPB:A1←A
[28]   K←I+2
[29]   A1[;K]←-B
[30]   A2←A1
[31]   A2[K;]←0
[32]   P0[;I]←(-8)↑((FRAME A1)-(FRAME A2))
[33]   I←I+1
[34]   →(I≤2)/LOOPB
[35]   CO← 8 4 ⍴ 1 ¯0.598 0.0167 ¯0.59
       8
[36]   Q←+/CO×P0
[37]   I←0
[38] LOOPC:I←I+1
[39]   →((|Q[I])≤1E¯7)/LOOPC
[40]   I←(⍴Q)+1-I
[41]   Q←(-I)↑Q
[42]   'THE TRAILING EDGE ZEROS ARE:'
[43]   ' '
[44]   F Q×150×12
[45]   CO← 8 4 ⍴ 1 0.402 0.0167 0.402
[46]   Q←+/CO×P0
[47]   I←0
[48] LOOPD:I←I+1
[49]   →((|Q[I])≤1E¯7)/LOOPD
[50]   I←(⍴Q)+1-I
[51]   Q←(-I)↑Q
[52]   'THE LEADING EDGE ZEROS ARE:'
[53]   ' '
[54]   F Q×150×12
[55]   ' '
```

```
∇MAKE[□]∇
      ∇ MAKE;N;M
[1]   ⍝GENERATES PASSIVE A MATRIX
[2]   ⍝FROM SPRING AND DAMPER CONSTANTS
[3]   ⍝WHICH ARE GLOBAL TO THIS PRGM
[4]    A←AV
[5]    A←A,BV
[6]    N←50123+Z[3]
[7]    M←20081+Z[4]
[8]    A←A,[1](N×A[1;])
[9]    A←A,[1](M×A[2;])
[10]   A[8;8]←A[8;8]-(Z[1]+Z[3])
[11]   A[9;9]←A[9;9]-(Z[2]+Z[4])
       ∇
       •
```

```
      ∇QUAD[□]∇
      ∇ QUAD;H;TH
[1]   ⍝FINDS THE COST FUNCTION VALUE,
[2]   ⍝FOR THE SYSTEM GIVEN.  CALLS
[3]   ⍝FUNCTIONS NUM AND SET TO DO SO.
[4]    PD←(9)↑FRAME A
[5]    P1←NUM 8
[6]    P2←NUM 9
[7]    H←NUM 3
[8]    TH←NUM 4
[9]    PT←H+(0.0167×P1)+(¯0.598×(TH+P2))
       )
[10]   PL←H+(0.0167×P1)+(0.402×(TH+P2))
       )
[11]   PT←(SET PT)×150×12
[12]   PL←(SET PL)×150×12
[13]   P1←SET P1
[14]   P2←SET P2
[15]   '    PT          PL          P1
       P2'
[16]   10 ¯3 ⍕PT,PL,P1,P2
       ∇
       •
```

```
     ▽ OPT;JOLD;Z2;I;ZSTEP;N
[1]  ⍝THIS PROCEDURE PERFORMS A
[2]  ⍝FOUR VARIABLE GRADIENT SEARCH
[3]  ⍝AROUND A FUNCTION OF COST
[4]  ⍝DEFINED IN 'QUAD'.
[5]   F Z
[6]   ' STEP    ZSTEP1   2        3        4        Z1       2        3
 4   '
[7]   I←1↑0
[8]   ZSTEP←Z2←4↑0
[9]  LOOP:I←I[1]+1
[10]  Z2←Z
[11]  N←0
[12] LOOPA:N←N+1
[13]  MAKE
[14]  QUAD
[15]  SEAT 0.4
[16]  JOLD←J
[17]  Z[N]←((0.05×Z[N])+Z[N])
[18]  MAKE
[19]  QUAD
[20]  SEAT 0.4
[21]  ZSTEP[N]←-(EPS[N]×((J-JOLD)÷(Z[N]-Z2[N])))
[22]  Z[N]←Z2[N]
[23]  →(N<4)/LOOPA
[24]  Z←Z2+ZSTEP
[25]  I←I,ZSTEP,Z
[26]  8 2 ⍕I
[27]  →((+/((|ZSTEP)≥(|(CON×Z))))>0)/LOOP
      ▼
      •
```

```
      ∇ VECTOR;BB;YY;UU;DD;FF;N1;K1;J1;P1;Z1;I1;SS;IQ;RE;IM;WE
[1]   RE←0
[2]   IM←0
[3]   P1←0
[4]   N1←0.5×+/⍴A
[5]   I1←⍳N1
[6]   Z1←¯1↓(⍳(1-P1))↑⍳P1
[7]   K1←⍳(N1-P1)
[8]   J1←⍳(N1-1)
[9]   UU←(⍳N1)∘.=(⍳N1)
[10]  YY←IQ←RV←((N1-1),1)↑0
[11]  BB←FF←DD←((N1-1),(N1-1))↑0
[12]  BB[Z1;Z1]←A[Z1;Z1]
[13]  BB[Z1;K1+(P1-1)]←A[Z1;K1+P1]
[14]  BB[K1+(P1-1);Z1]←A[K1+P1;Z1]
[15]  BB[K1+(P1-1);K1+(P1-1)]←A[K1+P1;K1+P1]
[16]  YY[Z1;1]←-A[Z1;P1]
[17]  YY[K1+(P1-1);1]←-A[K1+P1;P1]
[18]  FF[J1;J1]←RE×UU[J1;J1]
[19]  DD[J1;J1]←IM×UU[J1;J1]
[20]  SS←(BB-FF)+.×((⌹DD)+.×(BB-FF))
[21]  IQ←(⌹(SS+DD))+.×YY
[22]  RV←((⌹DD)+.×(BB-FF))+.×IQ
[23]  RV←RV,IQ
[24]  UU←+/UU
[25]  UU[P1]←0
[26]  RV←UU⌿RV
[27]  RV[P1;]← 1 0
[28]  WE←RV
[29]  RV[I1;1]←((RV[I1;1]*2)+(RV[I1;2]*2))*0.5
[30]  RV[I1;2]←((¯3○WE[I1;2])+WE[I1;1])+(WE[I1;1]<0)×○1)×180÷○1
[31]  10 ¯3 ⍕RV
      ∇
      •
```